DISSERTATION

HIGH GROUNDWATER IN IRRIGATED REGIONS: MODEL DEVELOPMENT FOR ASSESSING CAUSES, IDENTIFYING SOLUTIONS, AND EXPLORING SYSTEM DYNAMICS

Submitted by

Chenda Deng

Department of Civil and Environmental Engineering

In partial fulfillment of the requirements

For the Degree of Doctor of Philosophy

Colorado State University

Fort Collins, Colorado

Spring 2021

Doctoral Committee:

Advisor: Ryan T. Bailey

Neil Grigg
Jeffrey Niemann
Keith Paustian

ABSTRACT

HIGH GROUNDWATER IN IRRIGATED REGIONS: MODEL DEVELOPMENT FOR ASSESSING CAUSES, IDENTIFYING SOLUTIONS, AND EXPLORING SYSTEM DYNAMICS

Waterlogging occurs in irrigated areas around the world due to over-irrigation and lack of adequate natural or artificial drainage. This phenomenon can lead to adverse social, physical, economic, and environmental issues, such as: damage to crops and overall land productivity; soil salinization; and damage to homes and building foundations. Solutions to waterlogging include implementation of high-efficient irrigation practices, installation of artificial drainage systems, and increased groundwater pumping to lower the water table. However, in regions governed by strict water law, wherein groundwater pumping is constrained by impact on nearby surface water bodies, these practices can be challenging to implement. In addition, current engineering and modeling approaches used to quantify soil-groundwater and groundwater-surface water interactions are crude, perhaps leading to erroneous results. An accurate representation of groundwater state variables, groundwater sources and sinks, and plant-soil-water interaction is needed at the regional scale to assist with groundwater management issues.

This dissertation enhances understanding of major hydrological processes and trade-offs in waterlogged agricultural areas, through the use of numerical modeling strategies. This is accomplished by developing numerical modeling tools to: (1) analyze and quantify the cause of high groundwater levels in highly managed, irrigated stream-aquifer systems; (2) assess the impact of artificial recharge ponds on groundwater levels, groundwater-surface water interactions, and stream depletions in irrigated stream-aquifer systems; (3) and gain a better

understanding of plant-soil-water dynamics in irrigated areas with high water tables. These objectives use a combination of agroecosystem (DayCent) and groundwater flow (MODFLOW) models, sensitivity analysis, and management scenario analysis.

Each of these sub-objectives is applied to the Gilcrest/LaSalle agricultural region within the South Platte River Basin in northeast Colorado, a region subject to high groundwater levels and associated waterlogging and infrastructure damage in the last 7 years. This region is also subject to strict water law, which constrains groundwater pumping due to the effect on the water rights of the nearby South Platte River. Results indicate that recharge from surface water irrigation, canal seepage, and groundwater pumping have the strongest influence on water table elevation, whereas precipitation recharge and recharge from groundwater irrigation have small influences from 1950 to 2012. Mitigation strategy implementation scenarios show that limiting canal seepage and transitioning > 50% of cultivated fields from surface water irrigation to groundwater irrigation can decrease the water table elevation by 1.5 m to 3 m over a 5-year period. Decreasing seepage from recharge ponds has a similar effect, decreasing water table elevation in local areas by up to 2.3 m. However, these decreases in water table elevation, while solving the problem of high groundwater levels for residential areas and cultivated fields, results in a decrease in groundwater discharge to the South Platte River. As the intent of the recharge ponds is to increase groundwater discharge and thereby offset stream depletions caused by groundwater pumping, mitigating high water table issues in the region can be achieved only by (1) modifying fluxes of sources and sinks of groundwater besides recharge pond seepage, or (2) modifying or relaxing the adjudication of water law, which dictates the need for offsetting pumping-induced stream depletion, in this region. The modeling tools developed in this dissertation, specifically the loose and tight coupling between DayCent and MODFLOW, can be used in the study region

to quantify pumping-induced stream depletion, recharge pond induced stream accretion, and the interplay between them in space and time. In addition, these models can be used in other irrigated stream-aquifer systems to assess baseline conditions and explore possible effects of water management strategies.

ACKNOWLEDGEMENTS

There are many who helped me along the way on this journey. I want to take a moment to thank them.

First, a great and sincere gratitude is served for my advisor, Dr. Ryan T. Bailey. I would not have been able to complete this journey without his support. He is one of the best teachers I have ever met. I am greatly humbled by his kindness and teaching. He always encourages me and appreciates my work and research. The academic freedom he gave to me greatly developed my potential. I really appreciate his help and effort through my entire graduate study. I also would like to acknowledge my other committees, Dr. Neil Grigg, Dr. Jeffrey Niemann, and Dr. Keith Paustian.

Second, I want to thank my sincere friend and co-worker, Dr. André Dozier. He gave me tremendous help on my research and teaching me skills. I greatly appreciate his kindness and humbleness.

Third, I would like to thank Dr. Yao Zhang, Dr. Xiaolu Wei for being amazing friends, roommates, and co-worker. They are not only helping me with research but also all kinds of aspects in my life. I am so grateful I have them in my life. Thanks for the funding from Colorado Water Conservation Board

Finally, I give thanks to my parents and friends who have encouraged and supported me along the way.

TABLE OF CONTENTS

CHAPTER 1. INTRODUCTION AND LITERATURE REVIEW

1.1 THE HIGH GROUNDWATER PROBLEMS

Waterlogging is the action of groundwater rising to the root zone of plants, leading to crop yield decrease, soil salinization and subsequent land degradation, and poor gas exchange and anaerobic conditions (Moore and McFarlane, 1998). High groundwater levels can have severe adverse physical, economic, and environmental consequences in both urban and agricultural areas, including damage to infrastructure, land degradation and salinization through waterlogging, and productivity and health of rivers (Tawhid, 2004a). Damages from groundwater flooding in urban areas include sewage system infiltration, buildings and infrastructure (Kreibich et al., 2009), basements of buildings (Schinke et al., 2012), and road infrastructure (Knott et al., 2017, 2018), whereas damages in agricultural areas include soil salinization and crop yield reductions (Grassini et al., 2007; Milroy et al., 2009; Singh and Panda, 2013; Singh, 2015). Groundwater levels can rise in coastal areas due to sea level rise, leading to soil salinization (Ascott et al., 2017; Oude Essink et al., 2010). Crop losses averaged $360 million/year during 2010-2016 due to waterlogging, an even greater loss than that due to drought in the United States (Ploschuk et al., 2018). Waterlogging can dramatically change the dynamics of carbon and nitrogen in soil. The resulting anaerobic condition decreases the rate of organic matter decomposition (Meurant & Riker, 2014), resulting in an accumulation of soil organic matter that affects nitrogen mineralization and available nitrogen for crop uptake; and also increases denitrification, which can increase methane (CH_4) emission and nitrous oxide (N_2O) emission (Bartlett & Harriss, 1993; Parton et al., 2001), both of which are greenhouse gases.

The cause of shallow water tables can be due to an assortment of natural and anthropogenic causes, including excess rainfall, river flooding and accompanying infiltration, seepage from

earthen irrigation canals, poor drainage or lack of proper artificial drainage, low-permeability soils, presence of shallow impermeable clay or rock layers, improper irrigation management, and rising sea levels adjacent to coastal aquifers (Burkhalter & Gates, 2005; J. Cox & McFarlane, 1990; J. W. Cox & McFarlane, 1995; Oude Essink et al., 2010; Singh et al., 2012; Tawhid, 2004b; Xiuling, 2001). Artificial recharge of groundwater can cause the excessive rise of groundwater mounds as well as when aquifers have low transmissivities (Bouwer et al., 1999). Artificial recharge ponds are often used in semi-arid and arid regions to store water in underlying aquifers (Hossein Hashemi et al., 2015; Ringleb et al., 2016; Scanlon et al., 2006) or to alter the baseline groundwater gradients in an aquifer system. In terms of the former, recharge ponds can be part of an overall approach to manage aquifer recharge, with the benefits of not losing water to evaporation and requiring very little land for regional water storage. As for the latter, recharge ponds can be used to augment streamflow, as a means of offsetting stream depletion caused by groundwater pumping located in the alluvium of river corridors (Warner et al., 1986). This is needed when groundwater is pumped out of priority in water rights systems. For either purpose, water is often diverted from nearby streams, rivers, or canals and deposited into the recharge pond sites, with the water seeping through the pond bed into the underlying aquifer material.

The plant-soil-water system during waterlogging controls the movement of water, nutrients, and greenhouse gases in agricultural landscapes. Understanding this system under a variety of hydrologic conditions is important for food production, land management, water management, and nutrient management. The plant-soil-water system is a complex system consisting of surface water runoff, infiltration, soil water dynamics, crop growth, evapotranspiration, recharge and nutrient leaching, carbon-nitrogen cycling, and consequent hydro-chemical processes such as flow and nutrient transport in aquifers, stream discharge and nutrient loading, and greenhouse

gas emissions. The challenge of simulating water transport and nutrient cycling in such a complex system resides mainly in the interaction between "zones", such as water movement between the soil profile and the saturated zone of the aquifer. As stated by Alley et al. (2002), groundwater recharge is the most difficult groundwater budget to simulate due the spatio-temporal variations of factors such as precipitation, irrigation application, evapotranspiration, land use, crop type, and soil type. A special condition of plant-soil-water interaction is the presence of saturated conditions in the root zone of crops (i.e. "waterlogging"), which can decrease crop yield and damage soil health and structure (Cannell et al., 1980; Cavazza & Pisa, 1988; Houk et al., 2006, 2006; Kaur et al., 2017).

1.2 APPROACHES FOR ASSESSING HIGH GROUNDWATER PORBLEMS

Groundwater levels can rise in coastal areas due to sea level rise, leading to soil salinization (Ascott et al., 2017; Oude Essink et al., 2010). Ascott et al. (2017) provided a methodology to improve the understanding of groundwater flooding at the regional scale due to fluvial flooding in England. They found that controls on the spatio-temporal extent of groundwater flooding are poorly understood, but the main controls in their study region included antecedent soil moisture conditions, rainfall, and catchment hydrogeological properties. Zhang et al. (2019), again studying groundwater flooding, found that controls are rainfall intensity, land surface topography, and distance to surface water. However, controls on water table elevation and waterlogging at the regional scale in agriculture have not been systematically performed. Field surveys and informal interviews can assist in diagnosing the problem (Tawhid, 2004b), as was done in the urban groundwater flooding study of Kreibich et al. (2009) in Dresden, Germany. Field studies of soil profile and landscape, measurement of local climate (J. W. Cox & McFarlane, 1995), water budget analysis, and correlation analysis between groundwater head

and potential causes (Jaber et al., 2006) can provide approximate contribution of system components to water table elevation. However, investigating the controls on water table elevation has not yet been performed in an agricultural setting at the regional scale wherein hydrology is complicated by human influences of irrigation and water conveyance.

There are studies that use models to assess the impact of these different artificial recharge options on groundwater systems. Barber et al. (2009) used MODFLOW to examine the impacts of artificial recharge on stream discharges in Spokane Valley-Rathdrum Prairie aquifer of Idaho and Washington, USA. It simulates hypothetical recharge scenarios by putting injection wells and infiltration basins (spreading method) at different locations. They found that both of the methods can be successful and a significant portion of the recharge returned to the Spokane River. Lacher et al. (2014) found that the near stream recharge can sustain the baseflows to the Upper San Pedro River (Arizona) to compensate the stream depletion by pumping. Three potential sites were selected for simulating hypothetical recharge near the river through MODFLOW modeling. Through water balance method and groundwater modeling, balanced pumping rate can be found not to diminish the artificial recharge gain and efficiently increase the groundwater resources (Hashemi et al., 2015). Mirlas et al. (2015) used MODFLOW hypothetical forecast the artificial recharge from infiltration pools to supply the rural drinking water. The recharge can also create a groundwater mound preventing inflow of contaminated groundwater from irrigated fields. Groundwater recharge due to artificial recharge systems can also be estimated through MODFLOW modeling, separating the recharge from a natural system like a river (Hashemi et al., 2013). However, most of the studies use hypothetical approaches whereas field data are provided in our study.

There are many numerical physically based models that simulate a range of hydrologic and chemical processes in the plant-water-soil system. A subset of these models are agronomic models that simulate hydrologic and crop growth processes in a one-dimensional domain at the soil profile-scale. These include SWAP (Kroes et al., 2009), DSSAT (Jones et al., 2003), and DayCent (Parton et al., 1998; Zhang et al., 2018). They simulate irrigation, runoff, infiltration, and percolation through soil layers, crop ET, and deep percolation from the bottom of the soil profile. However, as they do not simulate groundwater flow in the saturated zone of the underlying aquifer, the fluctuation of the water table and its possible presence in the soil profile and crop root zone is not represented. The Soil & Water Assessment Tool (SWAT) (Arnold et al., 1998) simulates hydrological processes and crop yield at the watershed scale, with a water balance and crop growth simulation occurring at individual hydrologic response units (HRUs) across the watershed landscape. The model accounts for groundwater storage and groundwater discharge to streams but does not simulate water table fluctuation in a physically based manner and hence cannot account for waterlogging effects on root zone processes and crop yield. Even the linked SWAT-MODFLOW model (Bailey et al., 2016) does not account for the condition of shallow groundwater in the root zone – MODFLOW may simulate a water table at the elevation of an HRU's soil profile, but it has no effect on SWAT's HRU soil profile and root zone processes. The linked DSSAT-MODFLOW model (Xiang et al., 2020) also does not account for the effect of shallow groundwater on root zone processes, as the linkage between the models is performed at the annual time scale, and day-to-day DSSAT crop growth and nutrient cycling algorithms are not affected by MODFLOW-simulated water table elevation.

Another subset of models simulates vadose zone hydrologic processes and water table fluctuation, but does not simulate near-surface hydrology, vegetative growth, root zone

processes, and nutrient cycling. These include the hydrologic and hydrogeologic models MODFLOW (Niswonger et al., 2011), HYDRUS (Šimůnek et al., 2012), MODFLOW-SURFACT (Panday & Huyakorn, 2008), STOMP (White & Oostrom, 2003), TOUGH2 (Pruess et al., 1999), VS2DI (Healy, 2008), the VSF package (Thoms et al., 2006), and HydroGeoSphere (Therrien et al., 2010), among many others. There is a general lack of hydro-agronomic models wherein the simulated water table affects root zone processes, and root zone processes, in turn, affect recharge to the water table.

1.3 GOAL AND OBJECTIVES

The overall objective of this dissertation is to enhance understanding of major hydrological processes and trade-offs in waterlogged agricultural areas. A suite of numerical modeling tools is used and developed to accomplish this objective for the LaSalle/Gilcrest region of the South Platte River Basin. This region has experienced high water tables in previous years. The following tasks are carried out and demonstrated in Chapters 2, 3, and 4:

(1) Develop a new method to identify the cause of waterlogging in a highly managed irrigated stream-aquifer system. A MODFLOW model is constructed and applied with detail in terms of geological information, hydrological properties, and groundwater sources or sinks, for the time period 1950-2012. Multiple sensitivity analyses are employed to quantify the impact of water budget components such as irrigation, pumping, canal seepage, recharge and pond seepage on groundwater levels. These results and the model in general can assist with water management issues in the region.

(2) Assess the impact of artificial recharge ponds on groundwater levels and groundwater return flows to the South Platte River. This is accomplished by linking the agroecosystem

model DayCent with the MODFLOW model from (1), for the 2012-2020 time period, during which construction of recharge ponds was significant. The model is also used to determine the ability of recharge ponds to offset the stream depletion caused by groundwater pumping during this time period.

(3) Gain a more complete understanding of interaction between the root zone and saturated groundwater zone in a plant-soil-water system at a regional scale in an irrigated stream-aquifer system. This is accomplished by tightly coupling DayCent and MODFLOW on a daily time step using a novel Message Passing Interface (MPI) (Gropp et al., 1996) method that avoids code modification to DayCent and MODFLOW codes, and therefore can work with updated versions of DayCent and MODFLOW. The model is used to estimate groundwater recharge and evaluate the agronomic impact of waterlogging.

REFERENCES

Alley, W. M., Healy, R. W., LaBaugh, J. W., & Reilly, T. E. (2002). *Flow and Storage in Groundwater Systems*. *296*, 7.

Arnold, J. G., Srinivasan, R., Muttiah, R. S., & Williams, J. R. (1998). Large area hydrologic modeling and assessment part I: Model development 1. *JAWRA Journal of the American Water Resources Association*, *34*(1), 73–89.

Ascott, M. J., Marchant, B. P., Macdonald, D., McKenzie, A. A., & Bloomfield, J. P. (2017). Improved understanding of spatio-temporal controls on regional scale groundwater flooding using hydrograph analysis and impulse response functions. *Hydrological Processes*, *31*(25), 4586–4599. https://doi.org/10.1002/hyp.11380

Bailey, R. T., Wible, T. C., Arabi, M., Records, R. M., & Ditty, J. (2016). Assessing regional-scale spatio-temporal patterns of groundwater–surface water interactions using a coupled SWAT-MODFLOW model. *Hydrological Processes*, *30*(23), 4420–4433.

Barber, M. E., Hossain, A., Covert, J. J., & Gregory, G. J. (2009). Augmentation of seasonal low stream flows by artificial recharge in the Spokane Valley-Rathdrum Prairie aquifer of Idaho and Washington, USA. *Hydrogeology Journal*, *17*(6), 1459–1470. https://doi.org/10.1007/s10040-009-0467-6

Bartlett, K. B., & Harriss, R. C. (1993). Review and assessment of methane emissions from wetlands. *Chemosphere*, *26*(1–4), 261–320.

Bouwer, H., Back, J. T., & Oliver, J. M. (1999). Predicting Infiltration and Ground-Water Mounds for Artificial Recharge. *Journal of Hydrologic Engineering*, *4*(4), 350–357. https://doi.org/10.1061/(ASCE)1084-0699(1999)4:4(350)

Burkhalter, J. P., & Gates, T. K. (2005). Agroecological Impacts from Salinization and Waterlogging in an Irrigated River Valley. *Journal of Irrigation and Drainage Engineering*, *131*(2), 197–209. https://doi.org/10.1061/(ASCE)0733-9437(2005)131:2(197)

Cannell, R. Q., Belford, R. K., Gales, K., Dennis, C. W., & Prew, R. D. (1980). Effects of waterlogging at different stages of development on the growth and yield of winter wheat. *Journal of the Science of Food and Agriculture*, *31*(2), 117–132. https://doi.org/10.1002/jsfa.2740310203

Cavazza, L., & Pisa, P. R. (1988). Effect of watertable depth and waterlogging on crop yield. *Agricultural Water Management*, *14*(1–4), 29–34. https://doi.org/10.1016/0378-3774(88)90057-1

Collaku, A., & Harrison, S. A. (n.d.). Losses in wheat due to waterlogging. *Crop Science*, *42*(2), 444–450.

Cox, J., & McFarlane, D. (1990). *Causes of waterlogging*. *31*, 6.

Cox, J. W., & McFarlane, D. J. (1995). The causes of waterlogging in shallow soils and their drainage in southwestern Australia. *Journal of Hydrology*, *167*(1–4), 175–194. https://doi.org/10.1016/0022-1694(94)02614-H

Grassini, P., Indaco, G. V., Pereira, M. L., Hall, A. J., & Trápani, N. (2007). Responses to short-term waterlogging during grain filling in sunflower. *Field Crops Research*, *101*(3), 352–363. https://doi.org/10.1016/j.fcr.2006.12.009

Gropp, W., Lusk, E., Doss, N., & Skjellum, A. (1996). A high-performance, portable implementation of the MPI message passing interface standard. *Parallel Computing*, *22*(6), 789–828.

Hashemi, H., Berndtsson, R., Kompani-Zare, M., & Persson, M. (2013). Natural vs. Artificial groundwater recharge, quantification through inverse modeling. *Hydrology and Earth System Sciences*, *17*(2), 637–650. https://doi.org/10.5194/hess-17-637-2013

Hashemi, Hossein, Berndtsson, R., & Persson, M. (2015). Artificial recharge by floodwater spreading estimated by water balances and groundwater modelling in arid Iran. *Hydrological Sciences Journal*, *60*(2), 336–350. https://doi.org/10.1080/02626667.2014.881485

Healy, R. W. (2008). Simulating water, solute, and heat transport in the subsurface with the VS2DI software package. *Vadose Zone Journal*, *7*(2), 632–639.

Houk, E., Frasier, M., & Schuck, E. (2006). The agricultural impacts of irrigation induced waterlogging and soil salinity in the Arkansas Basin. *Agricultural Water Management*, 9.

Jaber, F. H., Shukla, S., & Srivastava, S. (2006). Recharge, upflux and water table response for shallow water table conditions in southwest Florida. *Hydrological Processes*, *20*(9), 1895–1907. https://doi.org/10.1002/hyp.5951

Jones, J. W., Hoogenboom, G., Porter, C. H., Boote, K. J., Batchelor, W. D., Hunt, L. A., Wilkens, P. W., Singh, U., Gijsman, A. J., & Ritchie, J. T. (2003). The DSSAT cropping system model. *European Journal of Agronomy*, *18*(3–4), 235–265.

Kaur, G., Zurweller, B. A., Nelson, K. A., Motavalli, P. P., & Dudenhoeffer, C. J. (2017). Soil Waterlogging and Nitrogen Fertilizer Management Effects on Corn and Soybean Yields. *Agronomy Journal*, *109*(1), 97–106. https://doi.org/10.2134/agronj2016.07.0411

Knott, J. F., Daniel, J. S., Jacobs, J. M., & Kirshen, P. (2018). Adaptation Planning to Mitigate Coastal-Road Pavement Damage from Groundwater Rise Caused by Sea-Level Rise.

Transportation Research Record: Journal of the Transportation Research Board, *2672*(2), 11–22. https://doi.org/10.1177/0361198118757441

Knott, J. F., Elshaer, M., Daniel, J. S., Jacobs, J. M., & Kirshen, P. (2017). Assessing the Effects of Rising Groundwater from Sea Level Rise on the Service Life of Pavements in Coastal Road Infrastructure. *Transportation Research Record: Journal of the Transportation Research Board*, *2639*(1), 1–10. https://doi.org/10.3141/2639-01

Kreibich, H., Thieken, A. H., Grunenberg, H., Ullrich, K., & Sommer, T. (2009). Extent, perception and mitigation of damage due to high groundwater levels in the city of Dresden, Germany. *Natural Hazards and Earth System Science*, *9*(4), 1247–1258. https://doi.org/10.5194/nhess-9-1247-2009

Kroes, J. G., Dam, J. C. van, Groenendijk, P., Hendriks, R. F. A., & Jacobs, C. M. J. (2009). *SWAP Version 3.2. Theory description and user manual* (1649(02); p.). Alterra. https://library.wur.nl/WebQuery/wurpubs/400886

Lacher, L., Turner, D., Gungle, B., Bushman, B., & Richter, H. (2014). Application of Hydrologic Tools and Monitoring to Support Managed Aquifer Recharge Decision Making in the Upper San Pedro River, Arizona, USA. *Water*, *6*(11), 3495–3527. https://doi.org/10.3390/w6113495

Meurant, G., & Riker, A. J. (2014). *Flooding and Plant Growth*. Elsevier Science.

Milroy, S. P., Bange, M. P., & Thongbai, P. (2009). Cotton leaf nutrient concentrations in response to waterlogging under field conditions. *Field Crops Research*, *113*(3), 246–255. https://doi.org/10.1016/j.fcr.2009.05.012

Mirlas, V., Antonenko, V., Kulagin, V., & Kuldeeva, E. (2015). Assessing artificial groundwater recharge on irrigated land using the MODFLOW model. *Earth Science Research*, *4*(2), p16. https://doi.org/10.5539/esr.v4n2p16

Niswonger, R. G., Panday, S., & Ibaraki, M. (2011). MODFLOW-NWT, a Newton formulation for MODFLOW-2005. *US Geological Survey Techniques and Methods*, *6*(A37), 44.

Oude Essink, G. H. P., van Baaren, E. S., & de Louw, P. G. B. (2010). Effects of climate change on coastal groundwater systems: A modeling study in the Netherlands. *Water Resources Research*, *46*(10), 2009WR008719. https://doi.org/10.1029/2009WR008719

Panday, S., & Huyakorn, P. S. (2008). MODFLOW SURFACT: A State-of-the-Art Use of Vadose Zone Flow and Transport Equations and Numerical Techniques for Environmental Evaluations. *Vadose Zone Journal*, *7*(2), 610–631. https://doi.org/10.2136/vzj2007.0052

Parton, W. J., Holland, E. A., Del Grosso, S. J., Hartman, M. D., Martin, R. E., Mosier, A. R., Ojima, D. S., & Schimel, D. S. (2001). Generalized model for NO x and N2O emissions from soils. *Journal of Geophysical Research: Atmospheres*, *106*(D15), 17403–17419.

Parton, William J., Hartman, M., Ojima, D., & Schimel, D. (1998). DAYCENT and its land surface submodel: Description and testing. *Global and Planetary Change*, *19*(1–4), 35–48.

Ploschuk, R. A., Danlel Jullo, M., & Timothy David, C. (2018). Waterlogging of Winter Crops at Early and Late Stages: Impacts on Leaf Physiology, Growth and Yield. *Frontiers in Plant Science*, *9*, 15.

Pruess, K., Oldenburg, C. M., & Moridis, G. J. (1999). *TOUGH2 user's guide version 2*. Lawrence Berkeley National Lab.(LBNL), Berkeley, CA (United States).

Ringleb, J., Sallwey, J., & Stefan, C. (2016). Assessment of Managed Aquifer Recharge through Modeling—A Review. *Water*, *8*(12), 579. https://doi.org/10.3390/w8120579

Scanlon, B. R., Keese, K. E., Flint, A. L., Flint, L. E., Gaye, C. B., Edmunds, W. M., & Simmers, I. (2006). Global synthesis of groundwater recharge in semiarid and arid regions. *Hydrological Processes*, *20*(15), 3335–3370. https://doi.org/10.1002/hyp.6335

Schinke, R., Neubert, M., Hennersdorf, J., Stodolny, U., Sommer, T., & Naumann, T. (2012). Damage estimation of subterranean building constructions due to groundwater inundation – the GIS-based model approach GRUWAD. *Natural Hazards and Earth System Sciences*, *12*(9), 2865–2877. https://doi.org/10.5194/nhess-12-2865-2012

Šimůnek, J., Van Genuchten, M. T., & Šejna, M. (2012). The HYDRUS software package for simulating the two-and three-dimensional movement of water, heat, and multiple solutes in variably-saturated porous media. *Technical Manual*.

Singh, A. (2015). Soil salinization and waterlogging: A threat to environment and agricultural sustainability. *Ecological Indicators*, *57*, 128–130. https://doi.org/10.1016/j.ecolind.2015.04.027

Singh, A., Nath Panda, S., Flugel, W.-A., & Krause, P. (2012). WATERLOGGING AND FARMLAND SALINISATION: CAUSES AND REMEDIAL MEASURES IN AN IRRIGATED SEMI-ARID REGION OF INDIA: Waterlogging: Causes and remedial measures in a semi-arid region. *Irrigation and Drainage*, *61*(3), 357–365. https://doi.org/10.1002/ird.651

Singh, A., & Panda, S. N. (2013). Optimization and Simulation Modelling for Managing the Problems of Water Resources. *Water Resources Management*, *27*(9), 3421–3431. https://doi.org/10.1007/s11269-013-0355-7

Tawhid, K. G. (2004a). *Causes and effects of water logging in Dhaka City, Bangladesh*. 75.

Therrien, R., McLaren, R. G., Sudicky, E. A., & Panday, S. M. (2010). HydroGeoSphere: A three-dimensional numerical model describing fully-integrated subsurface and surface flow and solute transport. *Groundwater Simulations Group, University of Waterloo, Waterloo, ON*.

Thoms, R. B., Johnson, R. L., & Healy, R. W. (2006). *User's guide to the variably saturated flow (VSF) process to MODFLOW*.

Warner, J., Sunada, D., & Hartwell, A. (1986). *Recharge as augmentation in the South Platte River basin. Colorado Water Resources Research Institute*. Colorado State University.

White, M. D., & Oostrom, M. (2003). *STOMP subsurface transport over multiple phases version 3.0 User's guide*. Pacific Northwest National Lab., Richland, WA (US).

Xiang, Z., Bailey, R. T., Nozari, S., Husain, Z., Kisekka, I., Sharda, V., & Gowda, P. (2020). DSSAT-MODFLOW: A new modeling framework for exploring groundwater conservation strategies in irrigated areas. *Agricultural Water Management*, *232*, 106033.

Xiuling, F. S. C. (2001). Rationally utilizing water resources to control soil salinity in irrigation districts. *Sustaining the Global Farm, Selected Papers from the 10th International Soil Conservation Organization Meeting*, 1134–1138.

Zhang, M., Migliaccio, K. W., Her, Y. G., & Schaffer, B. (2019). A simulation model for estimating root zone saturation indices of agricultural crops in a shallow aquifer and canal system. *Agricultural Water Management*, *220*, 36–49. https://doi.org/10.1016/j.agwat.2019.03.044

Zhang, Y., Suyker, A., & Paustian, K. (2018). Improved crop canopy and water balance dynamics for agroecosystem modeling using DayCent. *Agronomy Journal*, *110*(2), 511–524.

CHAPTER 2. ASSESSING CAUSES AND IDENTIFYING SOLUTIONS FOR HIGH GROUNDWATER LEVELS IN A HIGHLY MANAGED IRRIGATED REGION[1]

2.1. SUMMARY

High groundwater levels in urban and irrigated areas around the world can lead to infrastructure damage, land degradation, and crop yield reduction. Causes can include groundwater flooding due to fluvial processes, excess rainfall and irrigation, inadequate subsurface drainage, and additional sources such as injection and seepage from earthen canals and recharge ponds. The principal causes of shallow water tables, however, are difficult to quantify due to the interconnectedness of all possible causes. This paper presents a method to analyze and quantify the cause of high groundwater levels in highly managed, irrigated stream-aquifer systems, using a combination of numerical groundwater flow modeling and global sensitivity analysis (GSA) tools. A tested MODFLOW groundwater model and Sobol GSA methods are used to simulate and then quantify the influence of all major groundwater stresses on water table elevation for a region in northern Colorado, USA experiencing high groundwater levels, with results showing that recharge from surface water irrigation, canal seepage, and [1]groundwater pumping has the strongest influence on water table elevation, whereas precipitation recharge and recharge from groundwater irrigation have small influences. Time series sensitivity plots quantify the seasonality of these influences over a decadal period, and spatial sensitivity plots indicate regions that are strongly influenced by individual stresses. Results from best management practice (BMP) implementation indicate that limiting canal seepage and

[1] As published in the Agricultural Water Management. Chenda Deng & Ryan T. Bailey. Agricultural Water Management 2020, 240, 106329

transitioning > 50% of cultivated fields from surface water irrigation to groundwater irrigation can decrease water table elevation by 1.5 m to 3 m over a 5-year period, leading to beneficial conditions for crop growth in the root zone. These methods can be applied to any waterlogged region worldwide. However, proposed management practices to lower the water table may be constrained by local, state, or national water law.

2.2. INTRODUCTION

High groundwater levels can have severe adverse physical, economic, and environmental consequences in both urban and agricultural areas, including damage to infrastructure, land degradation and salinization through waterlogging, and productivity and health of rivers. The cause of shallow water tables can be due to an assortment of natural and anthropogenic causes, including excess rainfall, river flooding and accompanying infiltration, seepage from earthen irrigation canals, poor drainage or lack of proper artificial drainage, low-permeability soils, presence of shallow impermeable clay or rock layers, improper irrigation management, and rising sea levels adjacent to coastal aquifers (Burkhalter and Gates, 2005; Cox and McFarlane, 1990, 1995; Oude Essink et al., 2010; Singh et al., 2012; Tawhid, 2004; Xiuling, 2001).

Damages from groundwater flooding in urban areas include sewage system infiltration, buildings and infrastructure (Kreibich et al., 2009), basements of buildings (Schinke et al., 2012), and road infrastructure (Knott et al., 2018, 2017), whereas damages in agricultural areas include soil salinization and crop yield reductions (Grassini et al., 2007; Milroy et al., 2009; Singh and Panda, 2013; Singh, 2015). Groundwater levels can rise in coastal areas due to sea level rise, leading to soil salinization (Ascott et al., 2017; Oude Essink et al., 2010). Ascott et al., (2017) provided a methodology to improve understanding of groundwater flooding at the regional scale

due to fluvial flooding in England. They found that controls on the spatio-temporal extent of groundwater flooding are poorly understood, but main controls in their study region include antecedent soil moisture conditions, rainfall, and catchment hydrogeological properties. Zhang et al., (2019), again studying groundwater flooding, found that controls are rainfall intensity, land surface topography, and distance to surface water.

Controls on water table elevation and waterlogging at the regional scale in agriculture has not been systematically performed. Field surveys and informal interviews can assist in diagnosing the problem (Tawhid, 2004), as was done in the urban groundwater flooding study of Kreibich et al., (2009) in Dresden, Germany. Field studies of soil profile and landscape, measurement of local climate (Cox and McFarlane, 1995), water budget analysis, and correlation analysis between groundwater head and potential causes (Jaber et al., 2006) can provide approximate contribution of system components to water table elevation. However, investigating the controls on water table elevation has not yet been performed in an agricultural setting at the regional scale wherein hydrology is complicated by human influences of irrigation and water conveyance.

The objective of this paper is to present a method to analyze and quantify the cause of high groundwater levels in a highly managed, irrigated stream-aquifer system. This is performed through numerical groundwater flow modeling and the use of global sensitivity analysis (GSA) to rank and quantify the influence of principal groundwater stresses on water table elevation in space and time. The method is applied to a 246 km^2 agricultural region in northern Colorado, USA, that has recently experienced groundwater flooding of infrastructure (e.g. flooding basements in residential areas; flooding of wastewater treatment ponds) and cultivated fields. Time series and maps of sensitivity for each groundwater stress also are provided, leading to

targeted management practices (canal sealing; conversion from surface water irrigation to groundwater irrigation) that are investigated for decadal impact on water table elevation.

2.3. METHODS

The general method of identifying causes of waterlogging is illustrated for a region within the South Platte River Basin, Colorado, USA. An overview of the study area is provided first, followed by a presentation of the MODFLOW model construction and testing and the application of global sensitivity analysis using the Sobol method. Finally, application of Best Management Practices (BMP) to lower water table elevation in the region are presented.

2.3.1 Study Area

The study area encompasses a 246 km^2 region located 64 km northeast of Denver, Colorado, within the South Platte River Basin (Figure 2.1A) and specifically within the conductive Quaternary alluvium of the basin. The area includes the towns of Gilcrest and LaSalle, with a total population of about 3500. The study area is used mainly for agricultural use. The main crops are corn, alfalfa, grass pasture. The irrigation type is approximately 50% flood irrigation and 50% sprinkler irrigation, with the irrigation season from April through October and irrigation water obtained from four irrigation canals (diverting water from the South Platte River) or from the alluvial aquifer. Figure 2.1B shows the location of Gilcrest and LaSalle, the South Platte River, the four irrigation canals, and the location of the 340 pumping wells (green dots). Many wells have pumping rates higher than 5450 m^3/day (1000 gal/min). Within the appropriation doctrine of Colorado water law, the majority of the pumping wells are junior in water right to users of the South Platte River, and therefore any streamflow depletion induced by pumping must be replaced by other sources of water. This has led to the construction of recharge ponds in

the area (blue dots in Figure 2.1B), with the recharge from these ponds and the resulting rise in groundwater gradient and groundwater discharge to the South Platte River used to offset the pumping-induced streamflow depletion.

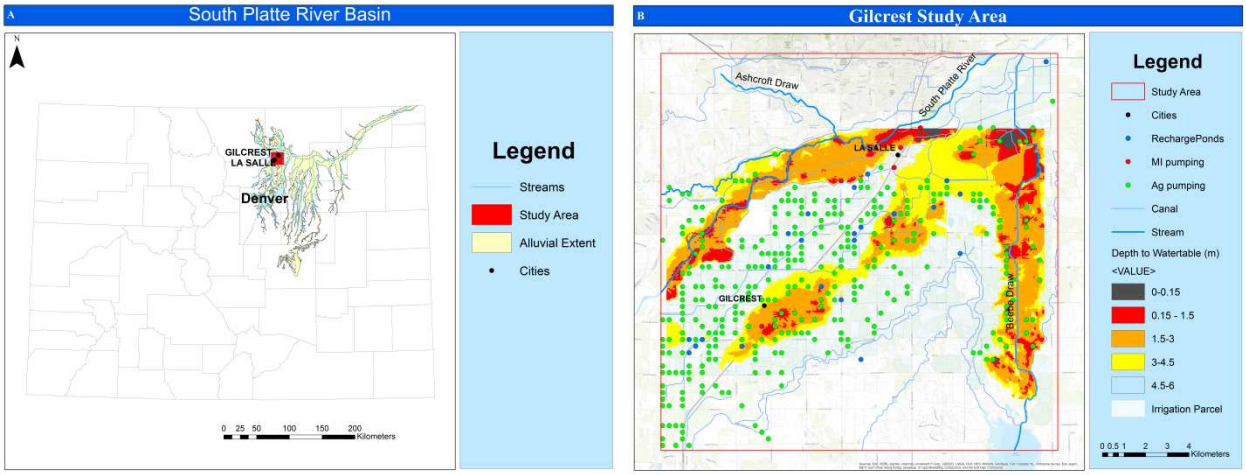

Figure 2.1**:** Figure A shows the South Plate River basin in Colorado. The red area is the Study Area where city of Gilcrest and La Salle located. Figure B shows the location of Gilcrest and LaSalle, the South Platte River, the four irrigation canals, recharge ponds, and the location of the 340 pumping wells (green dots).

Within the past 10-15 years, groundwater levels in the region have risen, leading to flooded basements, waterlogging of cultivated fields, and failure of septic systems. Figure 2.2 shows the estimated depth to the water table (m) during fall 2012, based on water level measurements in the network of 40 monitoring wells (green dots in Figure 2.2). These wells were installed by four organizations: the Central Colorado Water Conservancy District, the Colorado Division of Water Resources, Colorado State University, and the South Platte Decision Support System.

Note that areas in red have extremely shallow water tables (< 1.5 m from ground surface), and areas in orange have water tables between 1.5 and 3 meters below ground surface. Time series of water table depth (m) for three of the wells are shown in Figure 2.2, demonstrating that high groundwater has occurred for decades in some parts of the study area, but others have experienced a dramatic rise in groundwater levels.

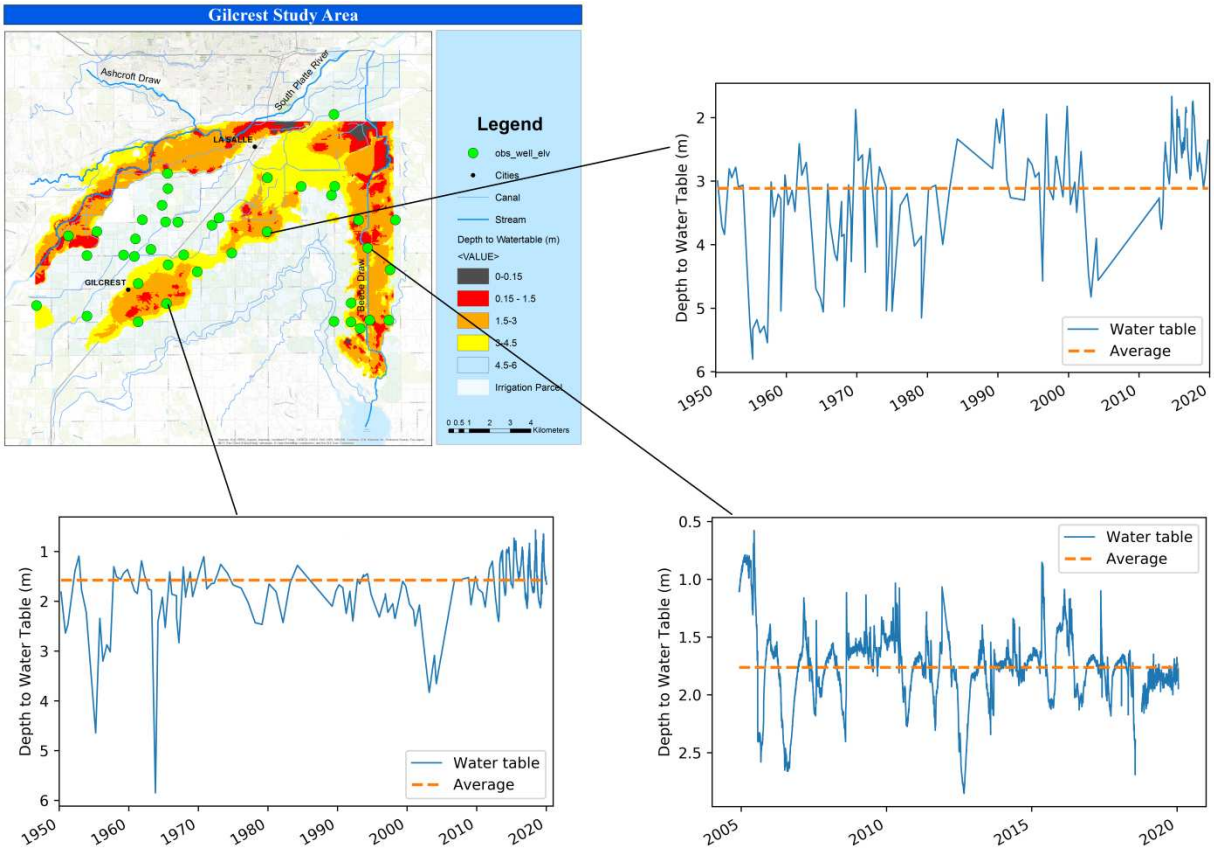

Figure 2.2: The figure displays the depth to the water table of 2012, fall. The red and yellow areas have shallow water tables. The time series plots are depth to water table plots in three locations in the Study Area.

In general, main groundwater inputs include recharge from irrigation events (surface water and groundwater sources), recharge from rainfall events, seepage from earthen irrigation canals, and recharge pond recharge. Groundwater outputs include pumping, evapotranspiration in areas of shallow water table, and discharge to the South Platte River. The volumes of these sources and sinks vary annually based on weather patterns, water rights, and local management decisions.

2.3.2 Geology of the Study Area

In the study area, the South Platte River alluvial aquifer is a heterogeneous geologic unit composed of interbedded gravel, sand, silt and clay underlain by low-permeability bedrock shale. Aquifer thickness varies from 0 to more than 30 m, with most of the area having a thickness of

15-25 m. Shale outcrops occur in several locations along the mid-south boundary of the study area. A digital elevation model (DEM) of the study area is shown in Figure 2.3A. The topography includes a broad fluvial valley along the South Platte River. The land surface has an elevation of 1510 m in the south, lowering to an elevation of 1410 m in the northeast within the South Platte River channel. Highly permeable deposits are found in the central part of the aquifer. Groundwater flow is generally from south to north, following the topography, with groundwater discharging to the South Platte River (Barkmann et al., 2014).

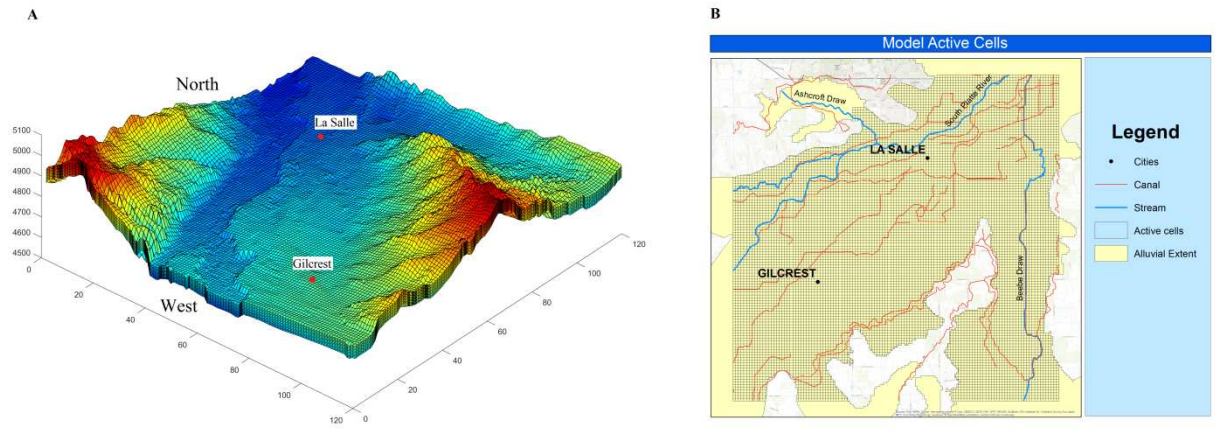

Figure 2.3: Figure A is the digital elevation model (DEM) and gird discretization of the Study Area in MODFLOW model. The topography includes a broad fluvial valley along the South Platte River. The land surface has an elevation of 1510 m in the south. Model active cells are shown in Figure B and represent the extent of the alluvial aquifer.

In a previous study investigating groundwater levels in the region Barkmann et al., 2014), 450 boreholes were drilled to bedrock to explore the three-dimensional material structure of the aquifer (Figure 2.4A, 2.4B). Borehole data are classified as clay, silt, sand, gravel, and mixed types, for 7 material types. In general, the aquifer material is coarser (sand, gravel) near the South Platte River. These borehole data were used in this study to create a three-dimensional (3D) material map, which is then used to obtain a 3D hydraulic conductivity (K) map for the MODFLOW model (see Section 2.3). Ordinary Kriging is employed to interpolate between the

borehole locations. Kriging for the 3D aquifer system is performed using the Stanford Geostatistical Modeling Software (SGeMS) (Remy et al., 2009). A 3D Cartesian grid with 120 x 120 x 50 cells is built in SGeMS to fully represent the aquifer. There are 10 vertical layers evenly distributed between the surface and the bedrock. The thickness of the layers ranges from 1 to 3 m. Each soil type is assigned a *K* value (initial values are shown in Table 1), and a 3D ellipsoid is defined to determine the size of the local neighbors around the estimation points. 3D Kriging is then performed within the ellipsoid of each estimation point to provide each grid cell with an interpolated *K*

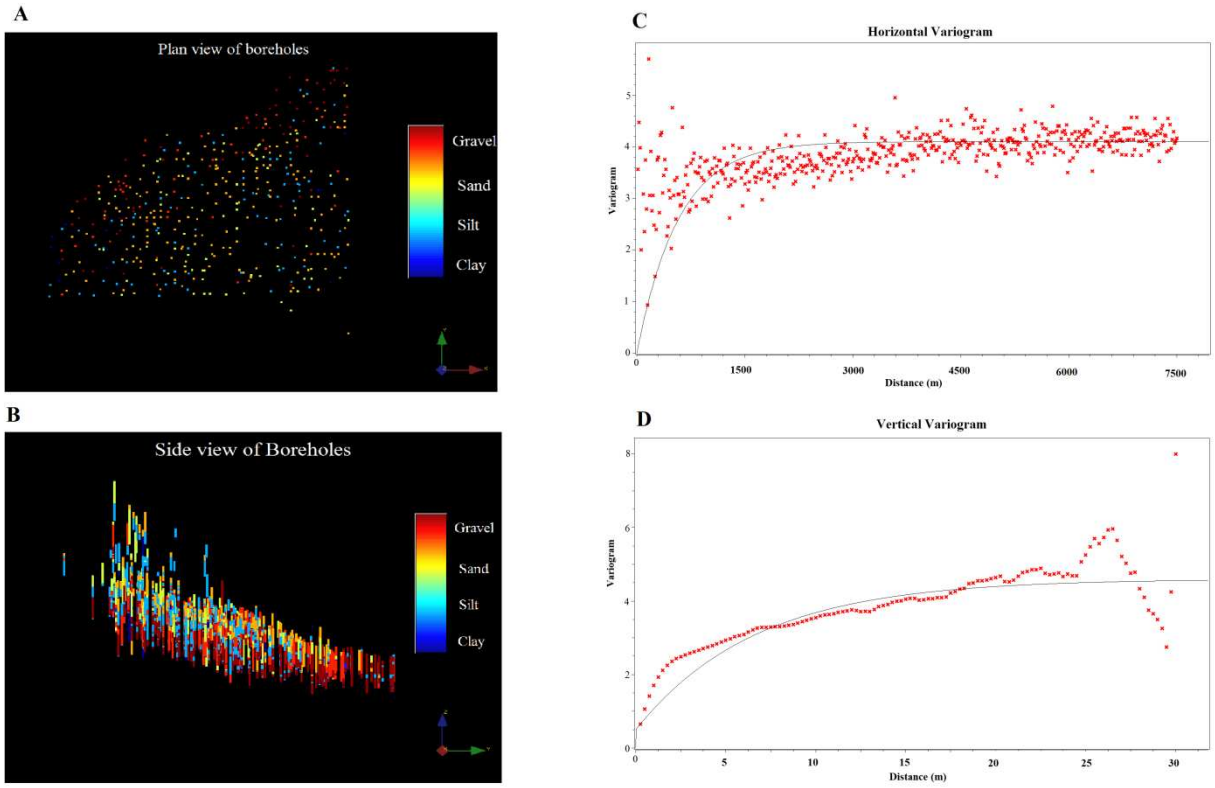

Figure 2.4: Figure A shows the distribution of 450 and their soil types. Figure B is the cross-section view of the boreholes. The horizontal and vertical variograms of *K* of the borehole data are plotted and shown in Figure C and D to show the spatial continuity of the aquifer material data.

Table 2.1: Aquifer properties and corresponding values used in model calibration using PEST. K values are in m/day.

Aquifer Parameter	Material Type	Min Value	Max Value	Initial Value	Calibrated Value
K	Clay	8.63E-07	1.11E-01	5.52E-02	1.11E-01
K	Clay & Silt	4.75E-06	7.59E-01	3.79E-01	6.43E-02
K	Silt	8.63E-06	3.05E+00	1.52E+00	4.63E-01
K	Silt & Sand	2.74E-02	5.79E+01	2.89E+01	5.45E+01
K	Sand	2.74E-01	2.74E+02	1.37E+02	1.75E+02
K	Sand & Gravel	4.33E+00	4.33E+02	2.14E+02	2.56E+02
K	Gravel	2.74E+01	2.74E+04	1.37E+04	3.05E+03
S_y	Clay	8.63E-07	1.83E-02	9.14E-03	5.73E-03
S_y	Clay & Silt	9.14E-03	4.57E-02	1.83E-02	4.57E-02
S_y	Silt	9.14E-03	6.71E-02	2.90E-02	6.71E-02
S_y	Silt & Sand	3.05E-02	1.07E-01	3.81E-02	1.07E-01
S_y	Sand	3.05E-02	1.22E-01	4.57E-02	3.05E-02
S_y	Sand & Gravel	3.35E-02	1.07E-01	3.66E-02	3.72E-02
S_y	Gravel	3.66E-02	1.07E-01	3.51E-02	3.66E-02
K_v:K_h *ratio*	All materials	1.52E-01	1.52E+00	7.62E-01	3.25E-01
S_s	All materials	3.05E-08	3.05E-04	3.05E-06	1.05E-07

The horizontal and vertical variograms of K of the borehole data are plotted and shown in Figure 2.4C and 2.4D to show the spatial continuity of the aquifer material data. The higher the variogram values is, the less similarity between data points. As the distance between data points increases (lag), there are less similarities and reaches a point beyond which there is no more spatial correlation. The lag at this point is called the "Range". Two exponential models are fitted for the horizontal and vertical directions. The vertical range for the borehole data is 30 m, whereas the horizontal range is 1970 m. Figure 2.5 shows the estimated material map for layers near the top, middle, and bottom portions of the aquifer. The aquifer material is more conductive (sand and gravel) near the South Platte River (shown along the north of the study area in black squares). Pockets of clay are present in more abundance in the middle layer, and the bottom of the aquifer has more sand and gravel areas. Figure 2.5 (lower right-hand map) also shows the distribution of clay in the area. Clay layers have accumulated around the mid-south portion and east boundary of the model.

2.3.3 Numerical Groundwater Flow Modeling

2.3.3.1 MODFLOW Model Construction

The MODFLOW flow model constructed for the study region has grid cells of 152.4 m x 152.4 m, resulting in 120 rows and 120 columns. The aquifer is discretized vertically by 10 layers, with the top elevation of the first layer extracted from the DEM (see Figure 2.3A) and the bottom of the lowest layer formed from the base of each borehole (see Figure 2.4B). Model active cells are shown in Figure 2.3B and represent the extent of the alluvial aquifer.

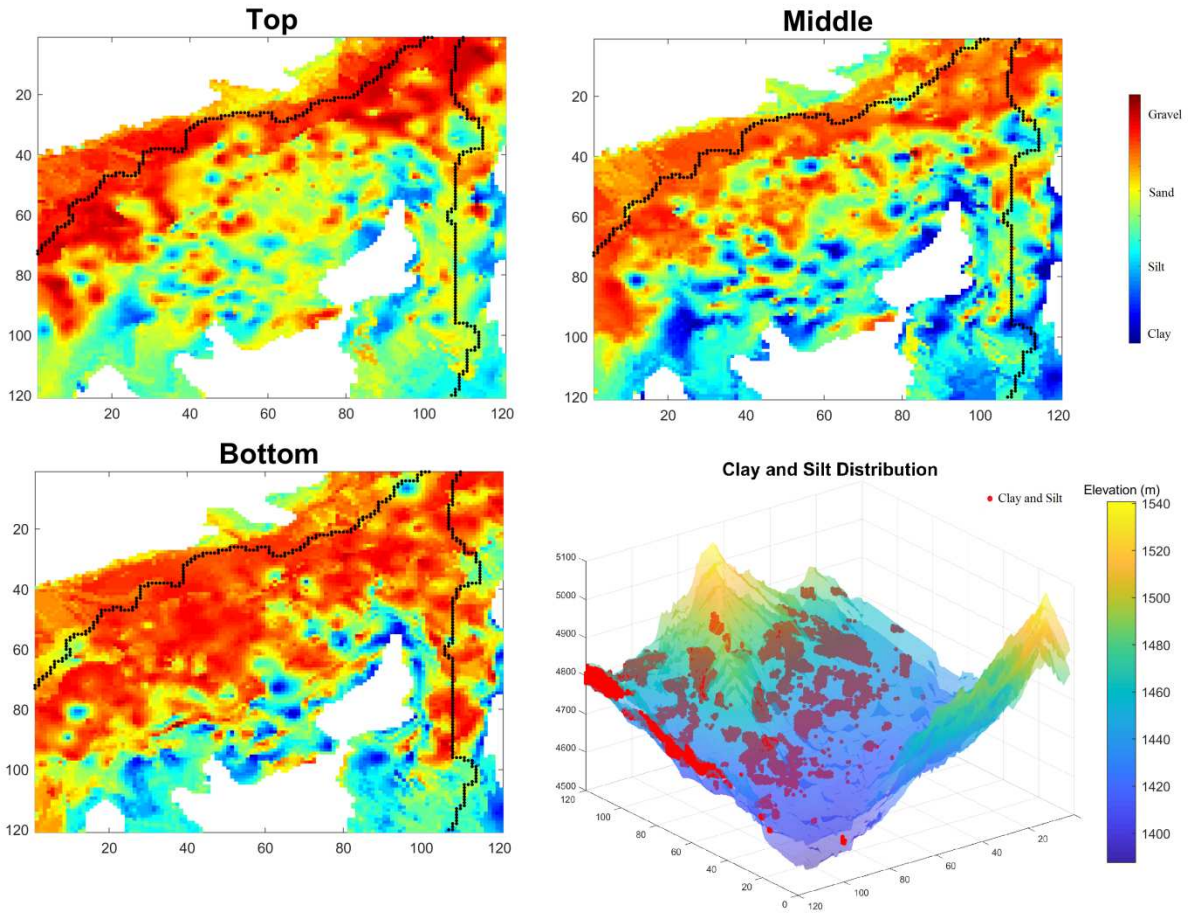

Figure 2.5: Figure A, B, C shows the estimate material map for layers near the top, middle, and bottom portions of the aquifer using 3-D Kriging interpolation. The aquifer material is more conductive (sand and gravel) near the South Platte River (shown along the north of the study area in black squares). Figure D shows the 3-D clay distribution in the aquifer.

All groundwater source and sink data are provided by a MODFLOW flow of the entire South Platte Alluvial Aquifer System (Brown and Caldwell, 2017), constructed in conjunction with the Colorado Division of Water Sources South Platte Decision Support System. These data are obtained from reported and measured flow rates and structure diversions (recharge pond seepage, agricultural pumping, M&I pumping) or are estimated using water balance tools (precipitation recharge, surface water recharge, groundwater recharge, canal seepage, lateral flow from surrounding aquifers, upflow from the underlying bedrock aquifer). Surface water recharge and groundwater recharge are calculated using pre-processing routines, in which recharge is the difference between applied irrigation rates and the resulting surface runoff and crop evapotranspiration (ET). Precipitation recharge, surface water recharge, and groundwater recharge are all applied to the top layer cells for each stress period. Canal seepage is obtained by multiplying river diversion rates by a pre-determined factor (Brown and Caldwell, 2017). The MODFLOW PSB (Partition Stress Boundary) package (Zeiler et al., 2017) was used, in which each groundwater stress can be partitioned into separate inputs. For example, precipitation recharge, surface water recharge, groundwater recharge, canal seepage recharge, and recharge pond seepage are differentiated from general recharge, as is the case with typical MODFLOW codes and models. Using this package, the water balance output by the MODFLOW model also partitions stresses into the separate components, thereby allowing for more detailed analysis of groundwater inputs/outputs.

Hydraulic conductivity and specific yield values for each grid cell were provided initial estimates based on the material maps generated from the borehole data (see Figures 2.4 and 2.5). These initial values were modified during calibration (see Section 2.3.2). Specified head boundary conditions are applied along the north boundary and south boundary of the model. The

head along these boundaries are derived from the historical records of monitoring wells and output from the basin-wide groundwater model (Brown and Caldwell, 2017). The western boundary of the model is the South Platte River. Streamflow in the river is simulated using MODFLOW's StreamFlow Routing (SFR) package. The SFR package uses a stream water budget and Manning's equation to compute the stream flow rate and depth (Prudic et al., 2004). 30 reaches and 516 segments are ordered and numbered based on the flow direction, with each grid cell designated as a river segment. Stream width was set to 45 m. The riverbed conductance [m^2/day] was calculated using the river length in each cell, the hydraulic conductivity of the cell, and the streambed thickness (assumed to be 1.5 m). The SFR package is also used to simulate streamflow in Beebe Draw (see Figure 2.1B), using a stream width of 6 m.

2.3.3.2 Model Simulation and Calibration

The model runs from 1950 to 2012 using monthly stress periods, with 10-time steps per stress period. The calibration and testing periods are 1950 to 2000 and 2000 to 2012, respectively. The initial groundwater head for each grid cell is obtained by interpolating the historical groundwater level from monitoring wells at the beginning of the simulation. The model is run using MODFLOW-NWT (Niswonger et al., 2011). The mass balance error of the simulation is 0.45%.

The model was calibrated using the PEST software (Doherty, 2015, 2007). PEST employs Monte Carlo methodology to select random parameter values, uses a regularization process to attain the uniqueness of calibrated parameters values, and uses nonlinear parameter estimation techniques to minimize the residual between observed and simulated values. The model is run multiple times to obtain the Jacobian Matrix, which contains the set of partial derivatives of all observations with respect to the changes in model parameter values. PEST then uses the

calculated matrix to provide an improved set of parameters. The process continues until residuals are minimized.

In this study, values of aquifer properties are modified by PEST to minimize the residual between simulated and observed groundwater heads. Observed head values are obtained from the network of 40 observation wells in the study region (see Figure 2.2). There are in total 1870 groundwater level measurements during 1950-2012, with 652 observations available in the 1950-2000 calibration period, and 1218 in the 2000-2012 testing period. The sixteen aquifer parameters used by PEST are listed in Table 2.1, along with their maximum value, minimum value, and final calibrated value. Aquifer properties included are horizontal hydraulic conductivity K [m/day], specific yield S_y, vertical anisotropy K_v:K_h *ratio*, and specific storage S_s [1/m]. Each grid cell in the model domain is assigned a material type (clay, clay & silt, silt, silt & sand, sand, sand & gravel, gravel) and an initial K and S_y value based on the results of the 3D Kriging interpolation (see Section 2.2 and Figure 2.5). The set of cells belonging to each material type is assigned as a parameter zone, with values for each zone updated during the PEST calibration process. The PEST "Estimation" model is employed in the calibration, and therefore the solution of the inverse problem is based on the Gauss-Marquardt-Levenberg method (Doherty, 2015). Parallelization was implemented using 10 machines run in parallel to populate the Jacobian Matrix.

2.3.4 Identifying Governing Groundwater Stresses

Once calibrated and tested, the MODFLOW model was used to quantify the influence of groundwater stresses on water table elevation. These stresses are precipitation recharge, surface water recharge, groundwater recharge, groundwater pumping, canal seepage, and recharge pond seepage. These stresses are spatially and temporally distributed within the study area and through

the 1950-2012 simulation period. The quantification is performed using the Sobol method (Sobol, 2001), which provides a quantitative estimate of parameter influence on model output.

The Sobol method is a variance-based global sensitivity analysis (GSA), in which variances of model output are decomposed into fractions attributed to each input (first-order indices) and their interactions (second- or higher-order indices). The sensitivity index *SI* is calculated as:

$$SI_i = \frac{Var[E(y \mid x_i)]}{Var(y)} \quad (1)$$

$$SI_{ij} = \frac{Var[E(y \mid x_i, x_j)] - Var[E(y \mid x_i)] - Var[E(y \mid x_j)]}{Var(y)} \quad (2)$$

$$SI_{Ti} = SI_i + \sum_{j \neq i} SI_{ij} + \sum_{j \neq i} \sum_{k > j} SI_{ijk} \quad (3)$$

where x_i is the i^{th} input and y is the output, SI_i, SI_{ij}, SI_{ijk}, are the first-order, second-order, and third-order indices and SI_{Ti} is the total order index. Sobol's total order sensitivity counts the variances caused by each input variable independently and the interactions with other input variables in all the orders to the output variances. In this study, the total order index SI_{Ti} is used to represent the influence of the 6 groundwater stresses. A total of 224 parameter sets are generated using this method.

As each groundwater stress varies in space (i.e. cell-to-cell variation) and in time (different values for each stress period), each input value is scaled on a percentage basis, from 0 to 150% of the original value. For example, all groundwater pumping rates are multiplied by a percentage value, resulting in a change in model-simulated groundwater head. Simulations are run only for the 2000-2012 period. The sensitivity measure of each groundwater stress is calculated (1) temporally for each simulation stress period and (2) spatially for each MODFLOW grid cell. For

(1), groundwater head is averaged over all grid cells for each stress period, with the change in head related to the change in the groundwater stress value. For (2), the groundwater head in each active grid cell is averaged across all stress periods to provide a single value, thereby yielding a map of spatially-varying sensitivity for each groundwater stress. To our knowledge, this is a new technique that can provide valuable insights into the spatial controls on water table elevation. Maps are generated for periods pre- and post-2006, during which year many irrigation pumping wells were shut off due to potential effects on streamflow in the South Platte River.

2.3.5 Effect of Best Management Practices (BMPs) on Water Table Elevation

Results from the GSA pointed to effective management practices that could lower the water table. The MODFLOW model therefore is also used to explore the effect of these identified best management practices (BMPs). Based on results shown in Section 3.2, these practices are:

(1) Line canals with sealant to prevent canal seepage. As canal seepage is simulated using a recharge source, this is performed in the model by setting these values to 0.

(2) Change the source of irrigation from surface water to groundwater pumping for all fields currently using canal water. This is performed by turning off surface water recharge for these cells, increasing groundwater pumping, and adding the expected groundwater recharge from the enhanced groundwater pumping. For this practice, irrigation efficiency is assumed to be 67%. This scenario assumes that no augmentation is required, i.e. that enhanced streamflow depletion caused by the additional groundwater pumping does not need to be replaced.

(3) Install subsurface drains to lower the water table, particularly in the area around the town of Gilcrest, which has experienced groundwater levels < 1.5 m from the ground surface (see Figure 2.1B). This is performed using MODFLOW's Drain package.

Combinations of these practices also are simulated, for example combining (1) and (2), since canal seepage will not occur if canals are not needed to convey irrigation water to fields. Also, (2) is implemented in increments, from 10% to 100% conversion of surface water irrigation to groundwater irrigation. For all scenarios, head results are compared with results from the original 2000-2012 simulation.

2.4. RESULTS AND DISCUSSIONS

2.4.1 General Model Results

The PEST calibration process improved model accuracy by 15%. The final calibrated values for each of the 16 aquifer properties are listed in Table 1. 1:1 plots of measured groundwater head vs. simulated groundwater head are shown in Figure 2.6 for the calibration period (1950-2000) and the testing period (2000-2012). For the calibration period, the Mean Absolute Error (MAE) is 1.23 m and the Root Mean Square Error (RMSE) is 1.74 m. The histogram of residuals (difference between measured and simulated) also is shown, showing that most of the residuals are < 3 m, with an average residual (mean of errors) of -0.22 m. Plots for the testing (validation) period also are shown, with MAE = 1.34 m, RMSE = 1.65 m, and the average residual = -0.36 m. Knowing that the average aquifer thickness in this region is 18-27 m, generally speaking the residuals between simulated and measured head values indicate that the MODFLOW model simulates the groundwater system in a reasonable manner.

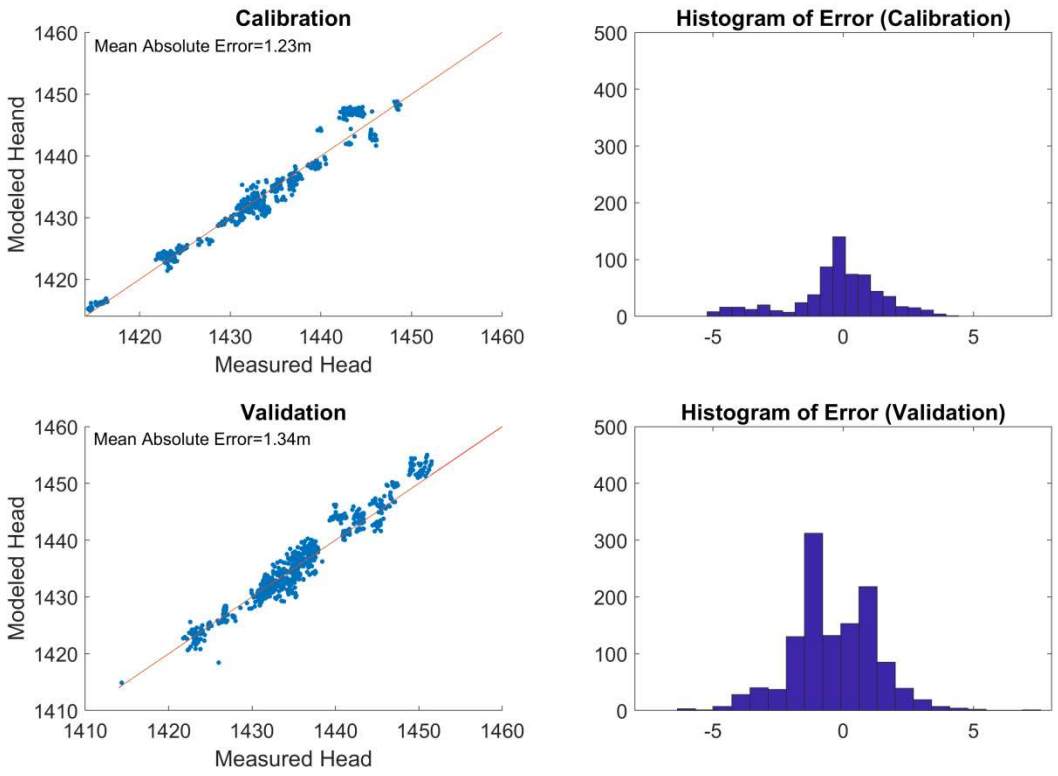

Figure 2.6: 1:1 plots of measured groundwater head vs. simulated groundwater head and histogram of error for the calibration period (1950-2000) and the validation period (2000-2012).

Comparison between simulated and measured groundwater head values is shown spatially in Figure 2.7. Figure 2.7A and 2.7B show the estimated water table contour map for spring 2012 from measurements taken from the 40 observation wells (Barkmann et al., 2014) and the contour map from groundwater values simulated by the tested MODFLOW model. Both maps show the same trend, with groundwater flowing from the south to north to discharge to the South Platte River, and similar values of groundwater hydraulic gradient. Figure 2.7C and 2.7D show the spatial distribution of water table depth for spring 2012 conditions, with the map on the left showing an interpolation from groundwater head at observation wells (Barkmann et al., 2014), and the map on the right showing cell-by-cell results from the MODFLOW model. Red and orange colors indicate areas of shallow (< 3 m) water table. In general, the simulated results

capture the principal patterns in the system, with shallow water table in the areas along the South Platte River, Beebe Draw, near the town of Gilcrest, and in the region to the northeast of Gilcrest and south of La Salle. The MODFLOW model simulates a region of shallow water table to the south of Gilcrest, near the irrigation canals, which is not present in the CGS map. However, as shown in Figure 2.2, there are no observation wells in this area, and hence the actual groundwater levels are not known. However, due to seepage from the two irrigation canals, high groundwater levels likely are present, thus coinciding with the MODFLOW results. In general, simulated spatial distribution of groundwater levels demonstrate model accuracy.

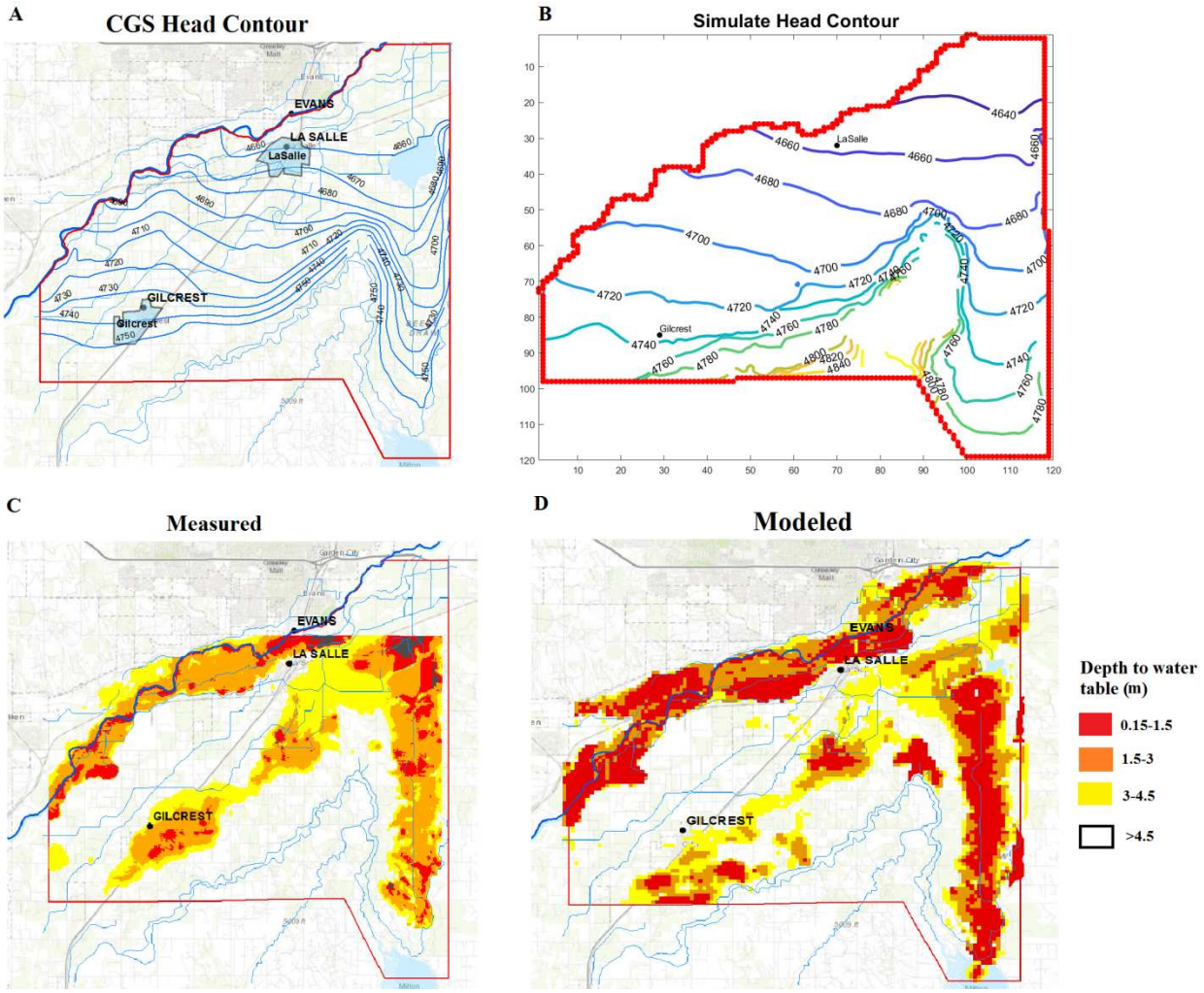

Figure 2.7: Figure A and B show the estimated water table contour map for spring 2012 from measurements taken from the 40 observation wells (Barkmann et al., 2014) and the contour map from groundwater values simulated by the tested MODFLOW model. Figure C and D show the spatial

distribution of water table depth for spring 2012 conditions, with the map on the left showing an interpolation from groundwater head at observation wells (Barkmann et al., 2014), and the map on the right showing cell-by-cell results from the MODFLOW model.

2.4.2 Governing Stresses on Water Table Elevation

The time-dependent measures of S_i for the six groundwater stresses from 2000-2012 using the Sobol method are shown in Figure 2.8. Results are shown for the entire model domain (Figure 2.8A) and for the region around the town of Gilcrest (Figure 2.8B). Results will be discussed for both the 2000-2006 and 2006-2012 time periods, since 2006 marks the transition to lower pumping volumes due to the effect of groundwater pumping on streamflow depletion. For the entire region (Figure 2.8A), the order of influence (S_i) on water table elevation, from highest to lowest, for the 2000-2006 time period is on average 1) canal seepage (0.3), 2) recharge from surface water irrigation (0.28), 3) pumping (0.14), 4) recharge from groundwater irrigation (0.003), 5) recharge from precipitation (0.02), and 6) recharge pond seepage (0.00). After 2006, the impact of pumping decreased due to the overall decrease in groundwater pumping during 2006-2012. For the 2000-2012 period, average S_i of surface water recharge, canal seepage, and groundwater pumping is 0.37, 0.37, and 0.08, respectively. During the 2006-2012 period, the influence of surface water recharge fluctuates with the irrigation season, whereas the seasonal pattern of canal seepage is much more subdued.

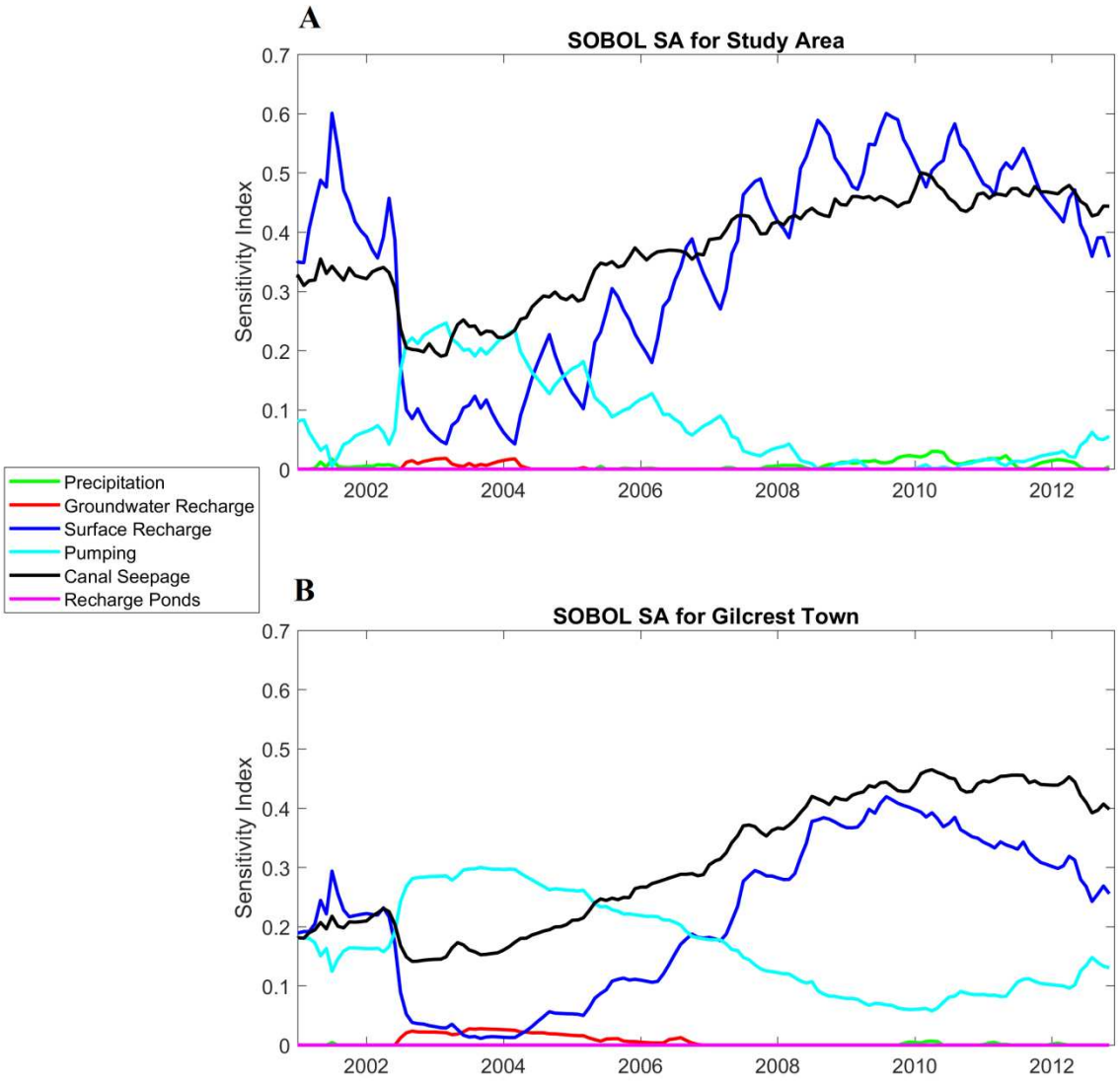

Figure 2.8: The time-dependent measures of S_i for the six groundwater stresses from 2000-2012 using the Sobol method. Results are shown for the entire model domain (Figure A) and for the region around the town of Gilcrest (Figure B).

The influence of pumping is more pronounced for the Gilcrest area. From Figure 2.8B, average S_i of surface water recharge, canal seepage, and groundwater pumping is 0.22, 0.30, and 0.17, respectively, with canal seepage having the strongest influence on water table elevation. However, before 2006 pumping has the strongest control on water table elevation, followed by

canal seepage with surface water recharge having almost no effect; whereas after 2006 surface water recharge has almost as strong an effect on water table elevation as canal seepage, with the influence of pumping decreasing dramatically.

The spatial sensitivity maps are shown in Figure 2.9 for surface water recharge, canal seepage, and groundwater pumping. Maps are shown for both the 2000-2006 (left) and 2006-2012 (right) period. For canal seepage (Figure 2.9A), water table elevation is most influenced by canal seepage along the canals in the southern part of the region. After 2006, the influence of canal seepage increased near the town of Gilcrest (values between 0.21 and 0.30, whereas values are 0 to 0.1 for the 2000-2006 period) (Figure 2.9B), likely due to the decreased influence of groundwater pumping. Not surprisingly, the water table elevation in agricultural regions of the study area are most influenced by surface water recharge (Figure 2.9C, 2.9D). Similar to the influence of canal seepage, the influence of surface water recharge increases after 2006 (Figure 2.9D), due to the decrease in groundwater pumping and increase in surface water irrigation during this time period. Pumping has the strongest influence on water table elevation around the Gilcrest and Beebe Draw areas (Figure 2.9E, F), but this influence decreases after 2006 in the majority of the study region.

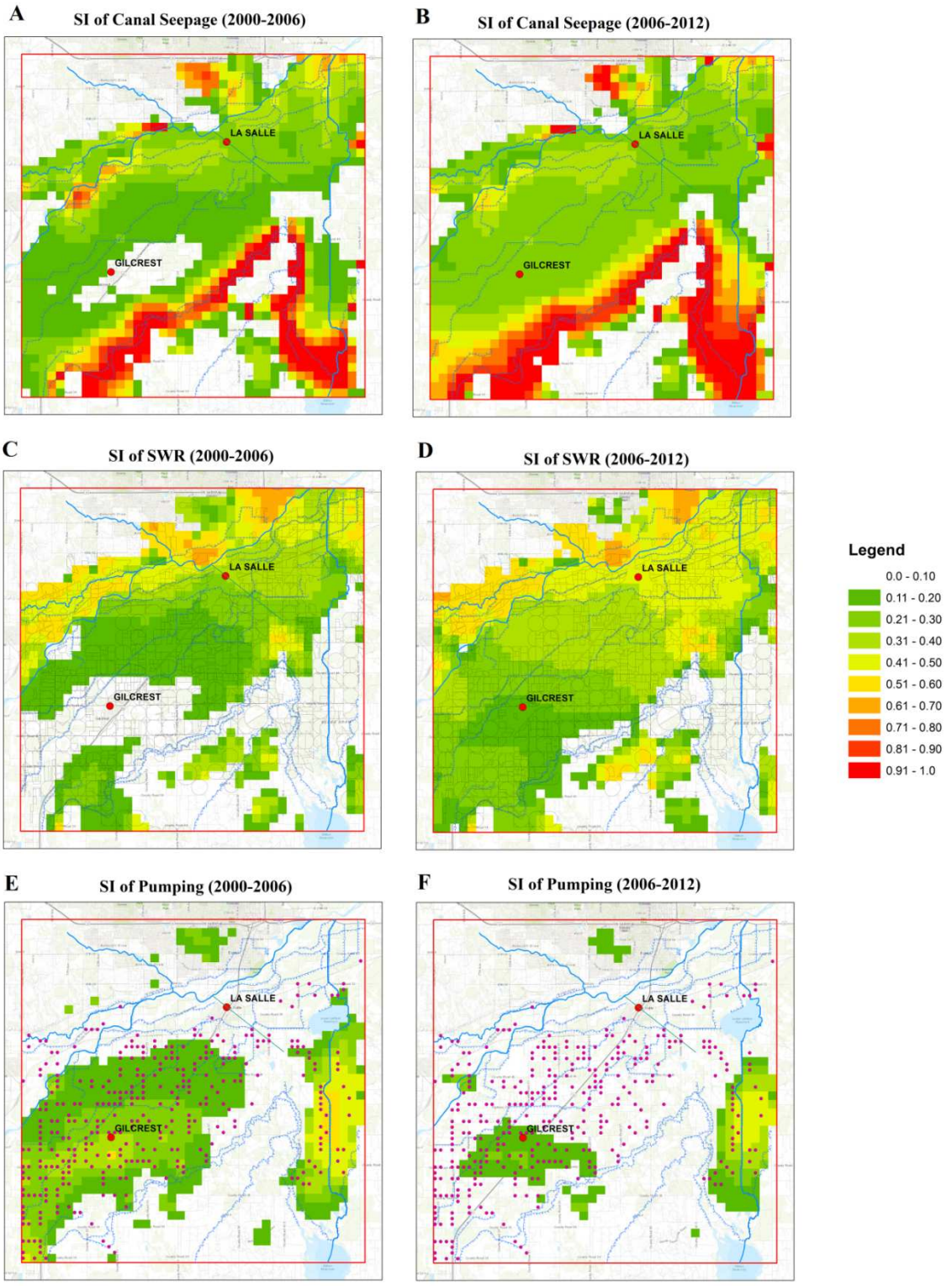

Figure 2.9: The spatial sensitivity maps are shown for surface water recharge, canal seepage, and groundwater pumping. Maps are shown for both the 2000-2006 (left) and 2006-2012 (right) period.

Although similar results could be derived from a spatio-temporal analysis of groundwater source and sink data, the use of the MODFLOW model and the Sobol method allow for more refined temporal and spatial relationships, as the influence of sources and sinks on neighboring areas are quantified using flow rate calculations within the MODFLOW solution. Results indicate that surface water recharge and canal seepage are the primary controls of water table elevation, both generally throughout the model domain (Figure 2.8) and locally (Figure 2.9). Therefore, management practices should focus on limiting these two stresses as much as possible without harming agricultural productivity. As shown from the results in Figure 2.9, these practices could be targeted to local areas or specific stretches of individual irrigation canals.

2.4.3 Effect of Management Practices on Water Table Elevation

The results of applying the BMPs during the 2000-2012 time period are shown in Figures 2.10 and 2.11. Figure 2.10 shows the decrease in groundwater head (water table elevation) for each grid cell in the model domain by 2012 for the scenarios of subsurface drainage in the Gilcrest area (Figure 2.10A), canal sealing (Figure 2.10B), surface water irrigation transition to groundwater irrigation (Figure 2.10C), and the combination of canal sealing and complete surface water irrigation transition to groundwater irrigation. Subsurface drainage near the Gilcrest area (Figure 2.10A) lowers the head by up to 0.6 m and could be a viable solution if implemented generally in the areas of high groundwater levels. Canal sealing (Figure 2.10B) lowers the head generally in the area, with an average decrease of 1.1 m across the study region by the end of 2012 but decreases up to 4-7 m in the areas between the canals. Replacing surface water irrigation with groundwater irrigation (Figure 2.10C) has a strong impact over the cultivated area, lowering the head by an average of 3.6 m with decreases up to 15 m. If irrigation

changes are combined with canal lining (Figure 2.10D), the head is lowered by an average of 4.6 m and maximum decreases of 20 m.

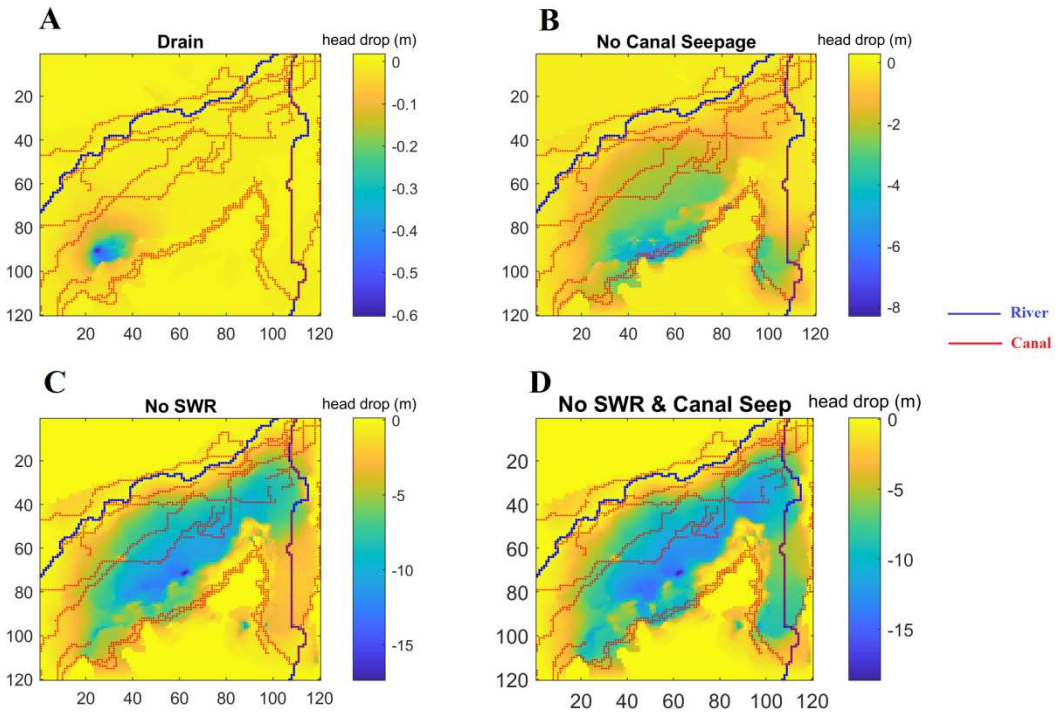

Figure 2.10: This shows the decrease in groundwater head (water table elevation) for each grid cell in the model domain by 2012 for the scenarios of subsurface drainage in the Gilcrest area (A), canal sealing (B), surface water irrigation transition to groundwater irrigation (C). Figure D is the combined effect with irrigation changes and canal lining.

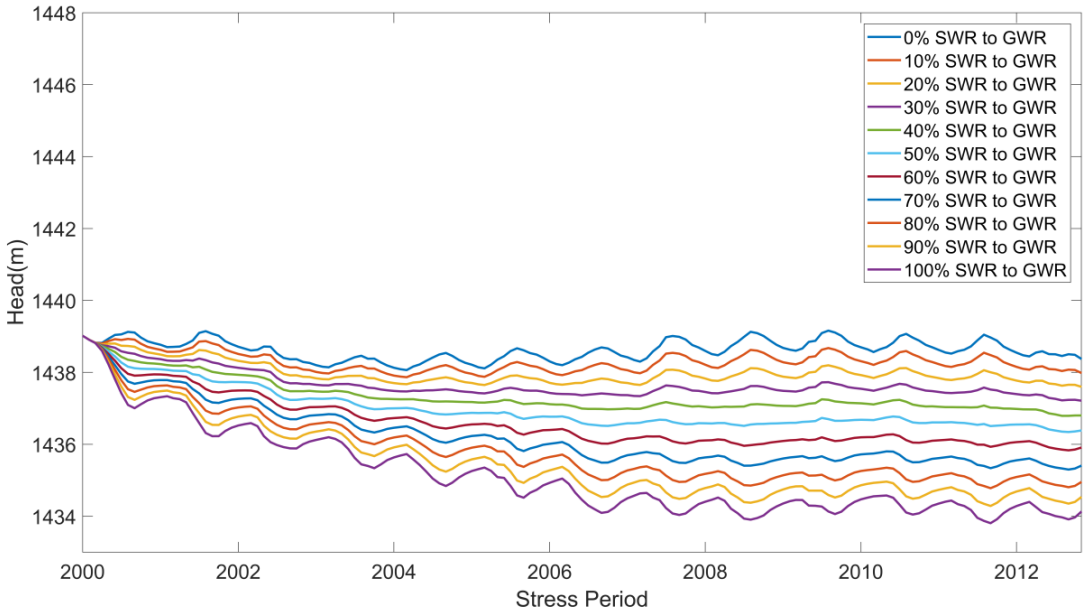

Figure 2.11: Time series of model-wide average groundwater head for percentages (0% to 100%) of conversion from surface water irrigation to groundwater irrigation

As complete conversion from surface water irrigation to groundwater irrigation in the study region is not practicable, additional scenarios were run to investigate the influence of partial conversion. Figure 2.11 shows the time series of model-wide average groundwater head for percentages (0% to 100%) of conversion from surface water irrigation to groundwater irrigation. The 0% scenario represents the baseline, "no change" scenario, showing the seasonal fluctuation of groundwater head throughout the region between 2000 and 2012. Full conversion (100%), as shown by the spatial results in Figure 2.10C, decreases average water table elevation by 4.6 m by 2012, whereas 50% implementation provides a decrease of approximately 2.4 m. However, even a decrease of 1.5 m, resulting from the 30% implementation scenario, would be beneficial to local infrastructure (e.g. house basements, wastewater treatment plant lagoons) and cultivated fields. Therefore, a combination of sealing along selected reaches of individual canals and a 20-30% transition from surface water irrigation to groundwater irrigation could lower the water table adequately to prevent groundwater flooding in residential and cultivated areas. Note that

these transition scenarios as simulated are not currently feasible within the context of Colorado water law, as any increase in groundwater pumping (due to conversion from surface water irrigation to groundwater irrigation) requires a plan to replace estimated streamflow depletion, i.e., increase recharge pond seepage or groundwater injection.

2.5. SUMMARY AND CONCLUSIONS

This study presents a new method to assess the impact of groundwater stresses on water table elevation in waterlogged agricultural areas. First, a numerical groundwater flow model is constructed and used to simulate groundwater head and groundwater flow, with results compared against measured groundwater levels; second, global sensitivity analysis (GSA) methods are applied to rank and quantify temporally and spatially the influence of each groundwater stress on water table elevation; and third, management practices are identified from the GSA results and run with the groundwater flow model to quantify spatio-temporal effects on water table elevation.

For the specified region in northern Colorado, which has experienced significant groundwater flooding in the past 10-15 years, surface water irrigation recharge, groundwater irrigation recharge, precipitation recharge, canal seepage, groundwater pumping, and recharge pond seepage were analyzed for influence on water table elevation during the 2000-2012 time period. Results indicate that surface water recharge, canal seepage, and pumping are the most influential stresses, with surface water recharge and canal seepage being the most impactful from 2006-2012, with the irrigation canal in the southern part of the study region wielding a particularly strong control on water table elevation in the central cultivated areas. Management practices based on GSA results indicate that sealing the canals, or segments of selected canals,

and transitioning 30% of the cultivated fields from surface water irrigation to groundwater irrigation can decrease water table elevation by 1.5 m over a 10-year period. If more immediate changes are required, the degree of implementation should be increased to > 50%.

These methods can be applied to any waterlogged region worldwide. However, proposed management practices to lower the water table may be constrained by local, state, or national water law. For example, in the current study region, groundwater and surface water are managed conjunctively as a single water source in Colorado water law, and hence pumping-induced streamflow depletion must be accompanied by an augmentation plan that replaces the depleted river water, often through seepage from constructed recharge ponds. These recharge ponds increase the local water table gradient, increasing the groundwater discharge to the river and thereby theoretically cancelling the effect of the pumping well on streamflow. The management practices simulated in this study do not include the need for an augmentation plan. Therefore, results show what could happen if Colorado water law were suspended in this region to manage the shallow water table problem.

REFERENCES

Ascott, M.J., Marchant, B.P., Macdonald, D., McKenzie, A.A., Bloomfield, J.P., 2017. Improved understanding of spatio-temporal controls on regional scale groundwater flooding using hydrograph analysis and impulse response functions. Hydrological Processes 31, 4586–4599. https://doi.org/10.1002/hyp.11380

Barkmann, P.E., Horn, A., Moore, A., Pike, J., Curtiss, W., 2014. Gilcrest/LaSalle Pilot Project Hydrogeologic Characterization Report.

Brown and Caldwell, 2017. South Platte Decision Support System Alluvial Groundwater Model Update Documentation, Colorado Water Conservation Board and Division of Water Resources.

Burkhalter, J.P., Gates, T.K., 2005. Agroecological Impacts from Salinization and Waterlogging in an Irrigated River Valley. J. Irrig. Drain Eng. 131, 197–209. https://doi.org/10.1061/(ASCE)0733-9437(2005)131:2(197)

Cox, J., McFarlane, D., 1990. Causes of waterlogging 31, 6.

Cox, J.W., McFarlane, D.J., 1995. The causes of waterlogging in shallow soils and their drainage in southwestern Australia. Journal of Hydrology 167, 175–194. https://doi.org/10.1016/0022-1694(94)02614-H

Doherty, J., 2015. Calibration and uncertainty analysis for complex environmental models. Watermark Numerical Computing.

Doherty, J., 2007. PEST Model-Independent Parameter Estimation User Manual, 5th Edition. 336.

Grassini, P., Indaco, G.V., Pereira, M.L., Hall, A.J., Trápani, N., 2007. Responses to short-term waterlogging during grain filling in sunflower. Field Crops Research 101, 352–363. https://doi.org/10.1016/j.fcr.2006.12.009

Jaber, F.H., Shukla, S., Srivastava, S., 2006. Recharge, upflux and water table response for shallow water table conditions in southwest Florida. Hydrol. Process. 20, 1895–1907. https://doi.org/10.1002/hyp.5951

Knott, J.F., Daniel, J.S., Jacobs, J.M., Kirshen, P., 2018. Adaptation Planning to Mitigate Coastal-Road Pavement Damage from Groundwater Rise Caused by Sea-Level Rise.

Transportation Research Record 2672, 11–22. https://doi.org/10.1177/0361198118757441

Knott, J.F., Elshaer, M., Daniel, J.S., Jacobs, J.M., Kirshen, P., 2017. Assessing the Effects of Rising Groundwater from Sea Level Rise on the Service Life of Pavements in Coastal Road Infrastructure. Transportation Research Record 2639, 1–10. https://doi.org/10.3141/2639-01

Kreibich, H., Thieken, A.H., Grunenberg, H., Ullrich, K., Sommer, T., 2009. Extent, perception and mitigation of damage due to high groundwater levels in the city of Dresden, Germany. Nat. Hazards Earth Syst. Sci. 9, 1247–1258. https://doi.org/10.5194/nhess-9-1247-2009

Milroy, S.P., Bange, M.P., Thongbai, P., 2009. Cotton leaf nutrient concentrations in response to waterlogging under field conditions. Field Crops Research 113, 246–255. https://doi.org/10.1016/j.fcr.2009.05.012

Niswonger, R.G., Panday, S., Ibaraki, M., 2011. MODFLOW-NWT, a Newton formulation for MODFLOW-2005. US Geological Survey Techniques and Methods 6, 44.

Oude Essink, G.H.P., van Baaren, E.S., de Louw, P.G.B., 2010. Effects of climate change on coastal groundwater systems: A modeling study in the Netherlands. Water Resour. Res. 46, 2009WR008719. https://doi.org/10.1029/2009WR008719

Prudic, D.E., Konikow, L.F., Banta, E.R., 2004. A new streamflow-routing (SFR1) package to simulate stream-aquifer interaction with MODFLOW-2000 104.

Remy, N., Boucher, A., Wu, J., 2009. Applied geostatistics with SGeMS: A user's guide. Cambridge University Press.

Schinke, R., Neubert, M., Hennersdorf, J., Stodolny, U., Sommer, T., Naumann, T., 2012. Damage estimation of subterranean building constructions due to groundwater inundation – the GIS-based model approach GRUWAD. Nat. Hazards Earth Syst. Sci. 12, 2865–2877. https://doi.org/10.5194/nhess-12-2865-2012

Singh, A., 2015. Soil salinization and waterlogging: A threat to environment and agricultural sustainability. Ecological Indicators 57, 128–130. https://doi.org/10.1016/j.ecolind.2015.04.027

Singh, A., Nath Panda, S., Flugel, W.-A., Krause, P., 2012. WATERLOGGING AND FARMLAND SALINISATION: CAUSES AND REMEDIAL MEASURES IN AN

IRRIGATED SEMI-ARID REGION OF INDIA: Waterlogging: Causes and remedial measures in a semi-arid region. Irrig. and Drain. 61, 357–365. https://doi.org/10.1002/ird.651

Singh, A., Panda, S.N., 2013. Optimization and Simulation Modelling for Managing the Problems of Water Resources. Water Resour Manage 27, 3421–3431. https://doi.org/10.1007/s11269-013-0355-7

Sobol, I.M., 2001. Global sensitivity indices for nonlinear mathematical models and their Monte Carlo estimates. Mathematics and computers in simulation 55, 271–280.

Tawhid, K.G., 2004. Causes and effects of water logging in Dhaka City, Bangladesh 75.

Xiuling, F.S.C., 2001. Rationally utilizing water resources to control soil salinity in irrigation districts, in: Sustaining the Global Farm, Selected Papers from the 10th International Soil Conservation Organization Meeting. pp. 1134–1138.

Zeiler, K., Weaver, J., Moore, A., Halstead, M., 2017. Application of the Partition Stress Boundary capability with MODFLOW-NWT in a large-scale regional groundwater flow model. In MODFLOW and More 2017: Modeling for Sustainability and Adaptation. Golden, Colorado, USA: Colorado School of Mines.

Zhang, M., Migliaccio, K.W., Her, Y.G., Schaffer, B., 2019. A simulation model for estimating root zone saturation indices of agricultural crops in a shallow aquifer and canal system. Agricultural Water Management 220, 36–49. https://doi.org/10.1016/j.agwat.2019.03.044

CHAPTER 3: ASSESSING THE IMPACT OF ARTIFICIAL RECHARGE PONDS ON HYDROLOGICAL FLUXES IN AN IRRIGATED STREAM-AQUIFER SYSTEM

3.1. SUMMARY

Artificial recharge ponds have been used increasingly in recent years to store water in underlying aquifers and modify baseline groundwater gradients or alter natural hydrologic fluxes and state variables in an aquifer system. The number of constructed ponds, their geographic spacing, and the volume of water diverted to each pond can have a significant impact on baseline system hydrologic fluxes and state variables such as groundwater head, with the latter sometimes rising to cause waterlogging in cultivated areas. This study seeks to quantify the impact of recharge ponds on groundwater state variables (head, saturated thickness) and associated fluxes within an irrigated stream-aquifer system. We use a numerical modeling approach to assess the impact of a set of 40 recharge ponds in a 246 km^2 region of the South Platte River Basin, Colorado on localized groundwater head, regional groundwater flow patterns, and groundwater interactions with the South Platte River. We then use this information to determine the overall influence of recharge ponds on the hydrologic system. A linked agroecosystem-groundwater (DayCent-MODFLOW) modeling system is used to simulate irrigation, crop evapotranspiration, deep percolation to the water table, groundwater pumping, seepage from irrigation canals, seepage from recharge ponds, groundwater flow, and groundwater-surface water interactions. The DayCent model simulates the plant-soil-water dynamics in the root zone and soil profile, while MODFLOW simulates the water balance in the aquifer system. After calibration and testing, the model is used in scenario analysis to quantify the hydrologic impact of recharge ponds. Results indicate that recharge ponds can raise groundwater levels by approximately 2.5 m

in localized areas, but only 15 cm when averaged over the entire study region. Ponds also increase the rate of total groundwater discharge to the South Platte River by approximately 3%, due to an increase in groundwater hydraulic gradient, which generally offsets stream depletion caused by groundwater pumping. These results can assist with groundwater resources management in the study region, and generally provide valuable information for the interplay between pumping wells and recharge ponds and their composite effect on groundwater-surface water interactions. In addition, the developed linked DayCent-MODFLOW modeling system presented herein can be used in any region for which recharge rates should be calculated on a per-field basis.

3.2. INTRODUCTION

Artificial recharge ponds are often used in semi-arid and arid regions to store water in underlying aquifers (Hossein Hashemi et al., 2015; Ringleb et al., 2016; Scanlon et al., 2006) or alter the baseline groundwater gradients in an aquifer system. In terms of the former, recharge ponds can be part of an overall approach to manage aquifer recharge (MAR), with the benefits of not losing water to evaporation and requiring very little land for regional water storage. In terms of the latter, recharge ponds can be used to augment streamflow, as a means of offsetting stream depletion caused by groundwater pumping located in the alluvium of river corridors (Warner et al., 1986). This is needed when groundwater is pumped out of priority in water right systems. For either purpose, water often is diverted from nearby streams or rivers and deposited into the recharge pond sites, with the water seeping through the pond bed into the underlying aquifer material.

There are a wide range of methods that can be used to recharge an aquifer, but five make up the vast majority of MAR techniques, including well, shaft and borehole recharge (57%); spreading methods (29%); in-channel modifications (7%); induced bank filtration (6%); and rainwater and runoff harvesting (Ringleb et al., 2016). MODFLOW is the most commonly used groundwater flow model to simulate the impact of artificial recharge volumes and rates on local and regional groundwater levels and gradients (Ringleb et al., 2016).

Several studies have used a modeling approach to assess the impact of these different artificial recharge options on groundwater system. Barber et al. (2009) used a MODFLOW model to examine the impacts of artificial recharge on stream depletions in the Spokane Valley-Rathdrum Prairie aquifer of Idaho and Washington, USA, based on hypothetical recharge scenarios from potential injection wells and infiltration basins throughout the valley. Both MAR methods were found to be successful in increasing groundwater discharge to the Spokane River. Similarly, Lacher et al. (2014) found that artificial recharge near the Upper San Pedro River (Arizona) can sustain baseflows and offset stream depletion caused by pumping. Mirlas et al. (2015) used MODFLOW to forecast the effect of artificial recharge on regional water supplies for rural drinking water. The volume of recharge can also create a groundwater mound that prevents inflow of contaminated groundwater from irrigated fields. While these studies demonstrate the influence of artificial recharge on a groundwater system and associated fluxes, none quantify the influence of existing recharge ponds using historical recharge pond volumes and pumping rates.

The objective of this study is to quantify the influence of seepage from existing recharge ponds on groundwater system-response variables and fluxes in a highly managed irrigated stream-aquifer system. The study is performed for a 246 km^2 irrigated region located northeast of

Denver, Colorado, wherein artificial recharge ponds are used in conjunction with water right augmentation plans. The impact of recharge ponds on the groundwater system is assessed using a linked agroecosystem-groundwater modeling system, with MODFLOW used to simulate groundwater head, groundwater storage, and the majority of groundwater sources and sinks, and DayCent used to estimate spatio-temporal recharge patterns to the water table. Specifically, the model, once calibrated and tested against field data, is used to explore the impact of recharge ponds on water table elevation and volumetric exchange rates between the aquifer and the South Platte River. The model is also used to determine if the recent implementation of recharge ponds is achieving the intended purpose, i.e. to offset the impact of pumping on streamflow depletion. The methods presented herein can be used to assess the impact of recharge ponds in other agricultural groundwater systems.

3.3. METHODS

3.3.1 Study Area

The study area encompasses a 246 km^2 region located 64 km northeast of Denver, Colorado, within the South Platte River Basin (Figure 3.1A) and specifically within the conductive Quaternary alluvium of the basin. The area includes the towns of Gilcrest and LaSalle, with a total population of about 3500. The study area is used mainly for agriculture. The main crops grown are corn, alfalfa, and grass pasture. The irrigation type is approximately 50% flood irrigation and 50% sprinkler irrigation, with the irrigation season from April through October and irrigation water obtained from four irrigation canals (diverting water from the South Platte River) or from the alluvial aquifer via groundwater pumping wells. Figure 3.1B shows the location of Gilcrest and LaSalle, the South Platte River, the four irrigation canals, and the location of 339

pumping wells (green dots) and 39 monitoring wells, with the latter used to monitor groundwater levels in the region. Many wells have pumping rates higher than 5450 m^3/day (1000 gal/min). The topography includes a broad fluvial valley along the South Platte River. The land surface has an elevation of 1510 m in the south, lowering to an elevation of 1410 m in the northeast within the South Platte River channel. Highly permeable deposits are found in the central part of the aquifer. Groundwater flow is generally from south to north, following the topography, with groundwater discharging to the South Platte River (Barkmann et al., 2014). Within the past 10-15 years, groundwater levels in the region have risen, leading to flooded basements, waterlogging of cultivated fields, and failure of septic systems.

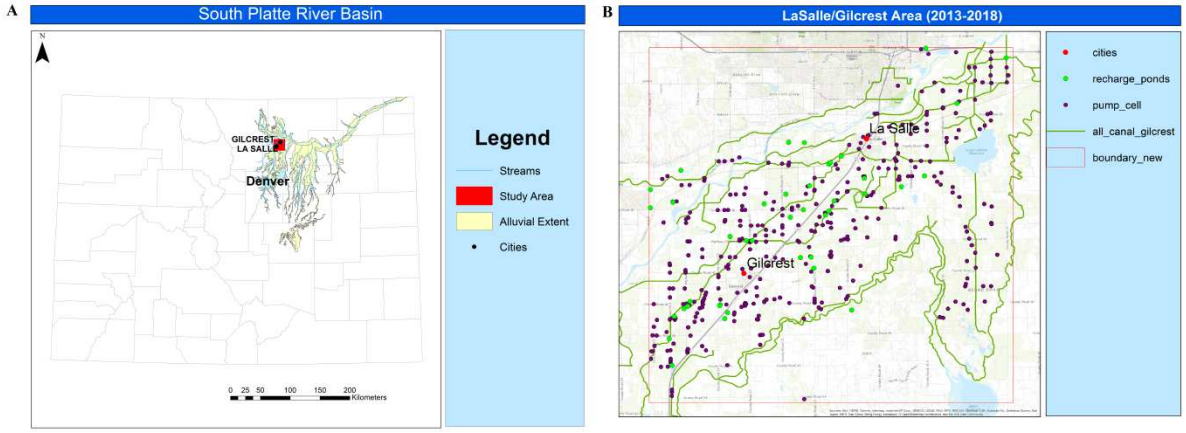

Figure 3.1: Figure A shows the South Platte River basin in Colorado. The red area is the Study Area where the city of Gilcrest and La Salle is located. Figure B shows the location of Gilcrest and LaSalle, the South Platte River, the four irrigation canals, recharge ponds, and the location of the 340 pumping wells (green dots)

Within the appropriation doctrine of Colorado water law, the majority of the 339 pumping wells are junior in water right to water use from the South Platte River, and therefore any streamflow depletion (stream seepage or a decrease in groundwater discharge to the river) induced by pumping must be replaced by other sources of water. This has led to the construction of recharge ponds in the area (blue dots in Figure 3.1B), with the recharge from these ponds and the resulting rise in groundwater gradient and groundwater discharge to the South Platte River

used to offset the pumping-induced streamflow depletion. There are 40 recharge ponds in the study area.

A MODFLOW model of the study area has been constructed and tested against measured groundwater levels from the network of 39 monitoring wells. (Deng & Bailey, 2019). The model is based on water data (pumping, recharge, etc.) from the Colorado Decision Support System, and has been used to assess the causes of high water tables in the region, i.e. the relative influence of irrigation, canal seepage, and pumping on the regional water table (Deng and Bailey, 2019). Modeling results have indicated that recharge from surface water irrigation and canal seepage are the main controls on water table elevation, and therefore may be the cause of the high water table. However, the influence of constructed recharge ponds on water table elevation has not been properly assessed, since the majority of recharge ponds in the LaSalle/Gilcrest area have been constructed since 2013 and the original model only ran through 2012.

3.3.2 Groundwater Numerical Modeling (MODFLOW)

This paper modifies the original MODFLOW model of Deng and Bailey (2019) to extend simulation through 2018. MODFLOW is a FORTRAN-written program that numerically solves the three-dimensional ground-water flow equation, using a finite-difference method (Niswonger et al., 2011). The finite difference method is employed by discretizing the ground-water system spatially into a grid of cells. Each cell represents a volumetric portion of the aquifer and contains uniform hydraulic properties (hydraulic conductivity, specific yield, specific storage). A water balance equation is established for each grid cell, and groundwater storage and associated head is solved at each time step according to groundwater inflows and outflows in three directions and the combined sources or sinks (e.g. pumping, recharge, groundwater-surface water exchange).

The following equation shows the water balance for a cell in an unconfined aquifer ((Bedekar et al., 2012):

$$\frac{\partial}{\partial x}(\mathrm{F}_s K_{xx}\frac{\partial h}{\partial x})+\frac{\partial}{\partial y}(\mathrm{F}_s K_{yy}\frac{\partial h}{\partial y})+\frac{\partial}{\partial z}(\mathrm{f(F)}K_{zz}\frac{\partial h}{\partial z})+W=\varphi\frac{\partial \mathrm{F}_s}{\partial t}+\mathrm{F}_s S_s\frac{\partial h}{\partial t} \qquad (1)$$

where, in equation 1, x, y, z are the three dimensions; h is groundwater head (L); K is hydraulic conductivity (L/T). S_s is specific storage (1/T). φ is porosity taken equal to specific yield S_y; F_s is the fraction of the cell thickness that is saturated; and f(F) is a function of F_s set to 1 for Niswonger et al. (2011).

Inflows or outflows across each cell face is estimated using Darcy's law (equation 2):

$$Q=\frac{-KA(h_2-h_1)}{L} \qquad (2)$$

In Darcy's law equation (equation 2), Q is volumetric flow rate. A is the cross-sectional area perpendicular to the flow. h1- h2 is the head difference across the prism parallel to flow and L is the length of the prism parallel to the flow path.

This study extends the refined LaSalle/Gilcrest MODFLOW model (Deng & Bailey, 2019) to the 2013-2018 time period to assess the influence of the recharge ponds on the high water table in the LaSalle/Gilcrest area. The MODFLOW flow model constructed for the study region has grid cells of 152.4 m x 152.4 m, resulting in 120 rows and 120 columns. The aquifer is discretized vertically by 10 layers, with the top elevation of the first layer extracted from the DEM (see Figure 3.2A) and the bottom of the lowest layer formed from the base of each borehole. Model active cells are shown in Figure 3.2B and represent the extent of the alluvial aquifer.

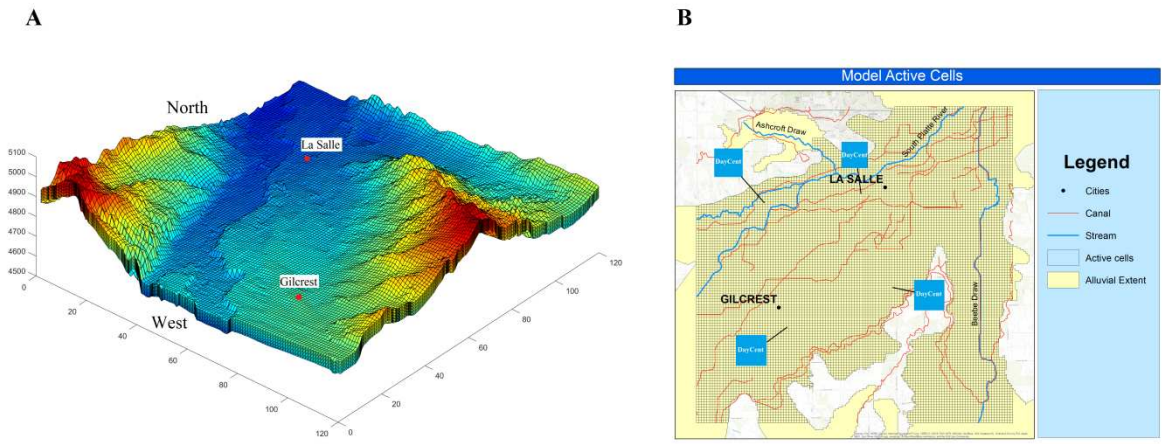

Figure 3.2: Figure A is the digital elevation model (DEM) and gird discretization of the Study Area in MODFLOW model. The topography includes a broad fluvial valley along the South Platte River. The land surface has an elevation of 1510 m in the south. Model active

In the study area, the South Platte River alluvial aquifer is a heterogeneous geologic unit composed of interbedded gravel, sand, silt and clay underlain by low-permeability bedrock shale. Aquifer thickness varies from 0 to more than 30 m, with most of the area having a thickness of 15-25 m. In the previous modeling study, a 3D aquifer material map was developed by interpolating material data from 450 boreholes, using the Kriging method (Deng & Bailey, 2019). Figure 3.3 shows the estimated material map for layers near the top, middle, and bottom portions of the aquifer. The aquifer material is more conductive (sand and gravel) within and near the alluvium corridor of the South Platte River (shown along the north of the study area in black squares). Pockets of clay are present in more abundance in the middle layer, and the bottom of the aquifer has more sand and gravel areas. Figure 3.3D (lower right-hand map) shows the distribution of clay in the area. Clay layers have accumulated around the mid-south portion and east boundary of the model. The values of the aquifer hydraulic properties were estimated in Deng and Bailey (2019).

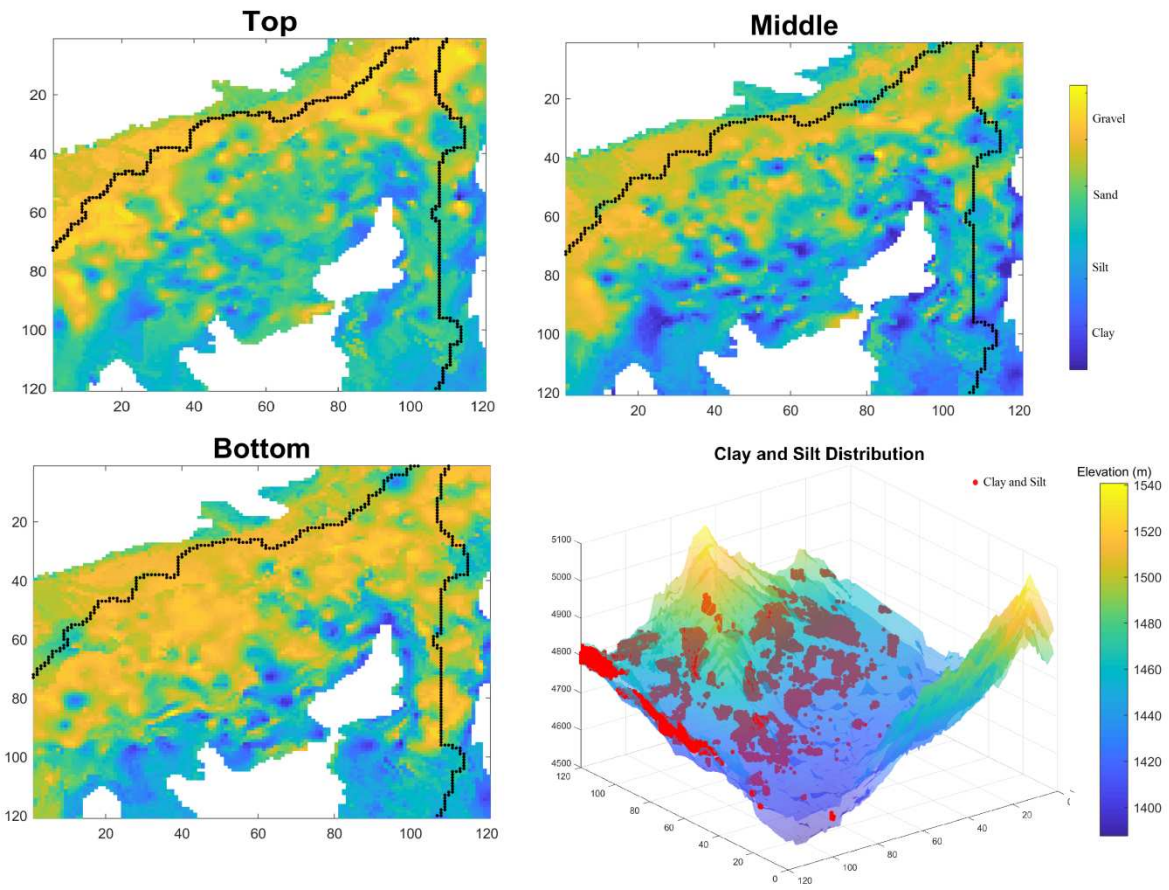

Figure 3.3: Figure A, B, C show the estimated material map for layers near the top, middle, and bottom portions of the aquifer using 3-D Kriging interpolation. The aquifer material is more conductive (sand and gravel) near the South Platte River (shown along the north of the study area in black squares). Figure D shows the 3-D clay distribution in the aquifer.

There are multiple groundwater sources and sinks, including irrigation recharge, precipitation, canal seepage, recharge ponds, and pumping (Figure 3.1B). There are four major irrigation canals in the study area: Union Ditch, Evans No 2, Farmers Independent, and Hewes Cook. The canal seepage is calculated based on South Platte River canal diversion data from the Colorado Division of Water Resources (CDWR) and a specified portion (10%) of the canal water that seeps into the aquifer. The monthly volume of groundwater extraction from each pumping well and the monthly volume of water diverted into each of the 40 recharge ponds also are obtained from the CDWR database. We assume that recharge from the ponds is equal to the

volume diverted to the ponds, minus evaporation from the pond surface. Daily evaporation depths (m/d) are computed using the Penman method (Penman, 1948), and then multiplied by the pond surface area (m^2) to obtain a daily volume of evaporation (m^3). Pumping rates are included in the MODFLOW model using the Well package; recharge from irrigation application, canal seepage, and recharge pond seepage are included using the Recharge package. The calculation of recharge from irrigation application is performed using DayCent, and is described in the next section. Monthly stress periods are used. Time series of monthly rates (m^3/day) for pumping, canal seepage, pond recharge, and groundwater recharge (deep percolation from DayCent) are plotted in Figure 3.4, with average rates of $7.7x10^5$ m^3 /day, $5.1x10^6$ m^3 /day, $7.1x10^5$ m^3 /day, and $4.6x10^6$ m^3 /day (see bottom chart in Figure 3.4). Note the seasonal dependency of rates, as cultivation activities during the growing season (April-October) drive the sources and sinks of the aquifer.

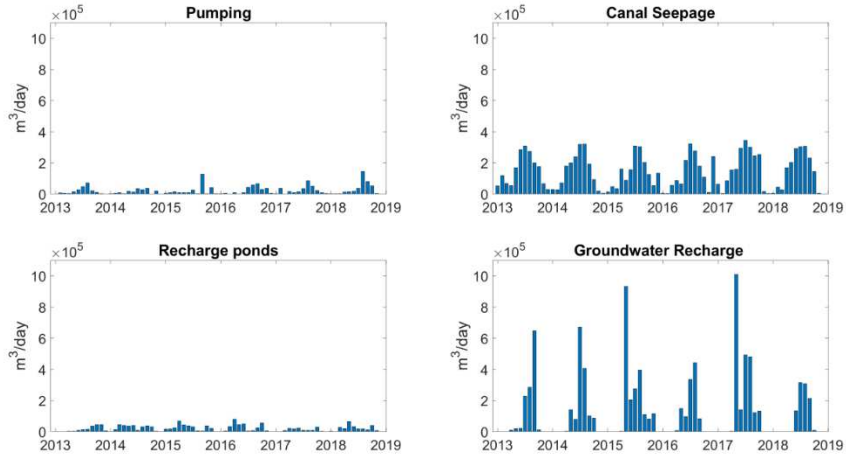

Figure 3.4: Time series plot of pumping, canal seepage, recharge ponds, and groundwater recharge rates from 2013 to 2018.

3.3.3 Agroecosystem Model (DayCent)

The DayCent agroecosystem field-scale model is used to compute the deep percolation (i.e. recharge) to the water table. The DayCent model (Parton et al., 1998; Zhang et al., 2018) is a medium complexity agroecosystem model. The major sub-models of DayCent are plant growth,

soil water flow, soil organic carbon cycling, soil nutrient cycling, and greenhouse gas emission. Major inputs for the model are daily weather, soil physical properties, plant type, and management practices. DayCent has been widely used for carbon and nitrogen simulations in agroecosystems (Del Grosso et al., 2008;. Del Grosso et al., 2006; Robertson et al., 2018; Zhang et al., 2013). The crop growth/production sub-model has been used in simulations of agroecosystem dynamics globally (Cheng et al., 2014; Del Grosso et al., 2008; Gautam et al., 2020; Lee et al., 2012; Stehfest et al., 2007; Zhang, Marx, et al., 2020). Recently, the DayCent modeling code has been improved in simulating crop canopy development, crop growth, and water use (Zhang et al., 2020; Zhang et al., 2018, 2018). This newest version of DayCent is used in this study for linking with MODFLOW. DayCent is written in FORTRAN and C.

The DayCent modeling code includes the main water balance components for a soil profile: infiltration of precipitation and irrigation, surface runoff, deep percolation, evapotranspiration (ET; evaporation and transpiration), and capillary rise of groundwater:

$$\Delta S_i = P + I_{net} - ET_c - RO - DP + GW \quad (3)$$

where ΔS_i is the net change in soil water at the end of day i and i-1. In this equation, P, RO, and DP are precipitation, runoff, and deep percolation on day i, respectively. I_{net} is the net irrigation on day i. GW is the groundwater contribution if a shallow water table is present. ET_c is the actual evapotranspiration on day i. All units are in cm day-1. The soil profile is defined by users which is usually less than three meters in depth. The input soil parameters include soil texture, bulk density, and field capacity, wilting point, and saturated hydraulic conductivity.

Precipitation and irrigation application are the source of surface water. A portion runs off the field, and the remainder infiltrates into the soil. As water flows in the root zone, a portion is removed by evapotranspiration (ET), and the remainder percolates to the water table. Reference ET is simulated in the model using either the standardized Penman-Monteith method (Allen et

al., 1998) or the Hargreave's method (Hargreaves & Allen, 2003), with the latter used when only air temperature is available. Crop coefficients are used in conjunction with reference ET to estimate potential ET for each crop type. The ET is partitioned into potential evaporation and potential transpiration as a function of the green canopy coverage and residue coverage. The green canopy coverage (CC) is calculated from Beer's law (Monsi & Saeki, 1953; Sellers, 1985):

$$CC = 1 - \exp(-k \times GLAI) \qquad (4)$$

where k (dimensionless) is the light extinction coefficient of the vegetation, and GLAI is green leaf area index (m m-1). The GLAI and CC approach was recently added to DayCent (Zhang et al., 2018). Water uptake by crop roots is limited by soil available water.

In this study, DayCent is run for each of the active grid cells (11,372 total, see Figure 3.2B) in the top layer of the MODFLOW model, to facilitate linkage between DayCent deep percolation and MODFLOW's recharge package. For each DayCent model, the root zone is divided uniformly into 14 layers for a total thickness of 210 cm. The main inputs for DayCent include daily weather data, soil data, and crop type. The weather data (precipitation and temperature) are obtained from the Peckham station, part of CoAgMet (Colorado Agricultural Meteorological Network). The soil physical property data for the top soil containing the fraction of gravel, silt, and clay are collected from SSURGO (Soil Survey Geographic Database). The main crops are alfalfa, corn, grass pasture, wheat, sugar beets. Crop schedule files are created for each crop including tillage and irrigation schedule information. Yearly crop rotation data are collected from satellite images from National Agricultural Statistics Service (NASS) (Figure 3.5) and mapped to the DayCent models based on the geological locations.

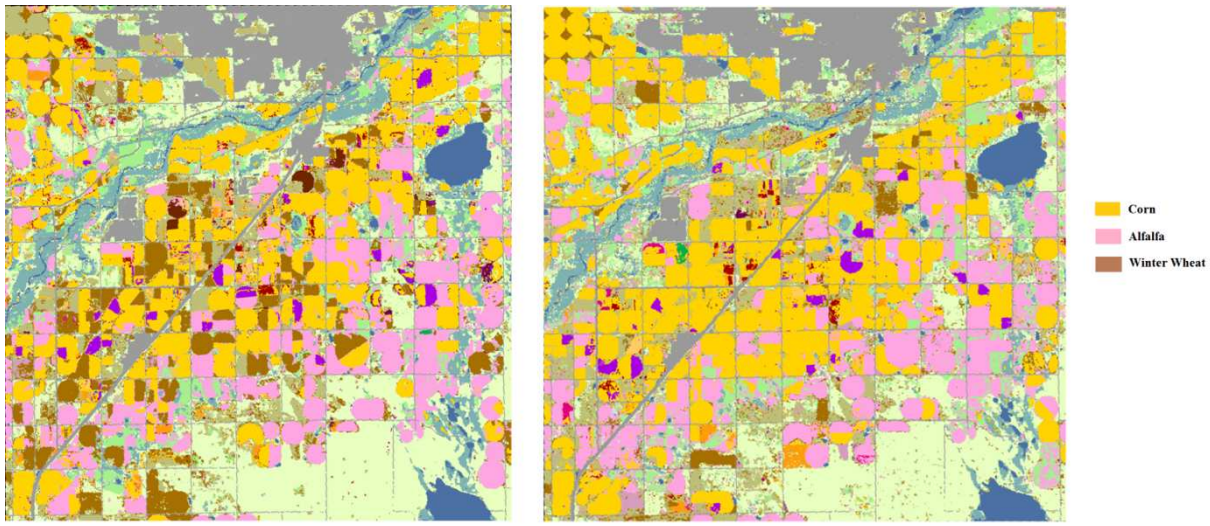

Figure 3.5: Crop type distribution in the Study Area from NASS satellite. The left figure is the crop map in 2013 and the right one is in 2018.

3.3.4 Model Simulation, Calibration and Testing

The simulation period was 2012-2020. The MODFLOW model is loosely coupled with the DayCent model. The DayCent model runs the entire simulation first and generates deep percolation amounts in the output files. Then, the deep percolation is mapped directly to the corresponding MODFLOW grid cell, to be included in the Recharge package. The model is tested by comparing simulated and measured groundwater heads, with simulated values from grid cells that correspond to locations of monitoring wells (see Figure 3.1). In DayCent, one of the largest model factors impacting deep percolation is irrigation efficiency (i.e. the fraction of applied irrigation water that is used by the crops). Irrigation efficiency varies with irrigation type, weather, and irrigation management practices. In this study, irrigation efficiency is treated as an uncertain parameter that requires estimation. A range of irrigation efficiency values (25% to 100%) are tested in the DayCent-MODFLOW simulation, to determine which value provides the best fit between simulated and observed groundwater head.

3.3.5 Estimating the Impact of Recharge Ponds on System Hydrologic Fluxes

After the model is built, calibrated, and tested, the impact of the recharge ponds on groundwater state variables and associated fluxes is quantified. This is accomplished using two sets of simulations:

(1) Decreasing seepage from ponds by varying degrees (10% to 100%), uniformly for all 40 ponds (10 simulations).

(2) Removing each recharge pond from the system one-at-a-time (40 simulations).

For both experiments, output groundwater heads are compared with original head values to quantify the extent and magnitude of recharge pond impact on localized and regional groundwater levels. In addition, exchange rates between the aquifer and the South Platte River are compared with original exchange rates, to determine the impact on groundwater return flows to the river.

A third set of simulations are run to determine the interplay between pumping wells and recharge ponds. The intent of constructing the recharge ponds is to offset stream depletions caused by groundwater wells pumping out of priority, to enable growers to still use groundwater for irrigation when they are junior in the Colorado water right system. The first simulation of this set runs the model without either groundwater pumping or recharge ponds, to determine pre-pumping patterns and rates of groundwater discharge to the South Platte River. A second simulation runs the model with groundwater pumping but no recharge ponds, to determine the amount of stream depletion caused by the use of the pumps. A third simulation runs the model with both groundwater pumping and recharge ponds (i.e. the baseline simulation), to determine if the pre-pumping rates of groundwater discharge are achieved, i.e. if the inclusion of the recharge ponds offsets the effect of the pumping wells on stream depletion. Whereas the first two

simulation sets provide general insights into the impact of recharge ponds on hydrologic fluxes in the irrigated stream-aquifer system, the third simulation set determines if the recharge ponds are effective in the overall water management of the system.

3.4. RESULTS AND DISCUSSION

3.4.1 Groundwater Simulation Results

Figure 3.6A shows the Root Mean Square Error (RMSE) of comparing the simulated groundwater head and observed head with different irrigation efficiencies. The lowest RMSE is 1.41 m with 50% irrigation efficiency, and therefore this irrigation efficiency % was used for all scenario simulations. This level of irrigation efficiency is indicative of a mixture of flood irrigation and sprinkler center-pivot irrigation systems. The ME and MAE are 0.6 m and 1.3 m. Figure 3.6B is the 1:1 plot of modeling head vs. observed head from more than 30,000 observations. Time series of comparison of modeled and observed head are plotted as well for several monitoring well locations (Figure 3.6C and 3.6D). The modeling results successfully catch the seasonal fluctuation of groundwater level Figure 3.7 displays the total volumes (millions of m3) associated with each groundwater source and sink during the 2012-2020 simulation period, for the baseline simulation. Among these, groundwater recharge, recharge, and canal seepage are the biggest components in water balance, corresponding to 749, 383, 345 million m^3 for the entire simulation period. Of the outputs (pumping and groundwater discharge), groundwater discharge to the South Platte River accounts for 94%. Of the inputs, groundwater recharge and canal seepage account for 46% and 38%, respectively. Note that a portion of groundwater pumping returns to the aquifer as irrigation recharge.

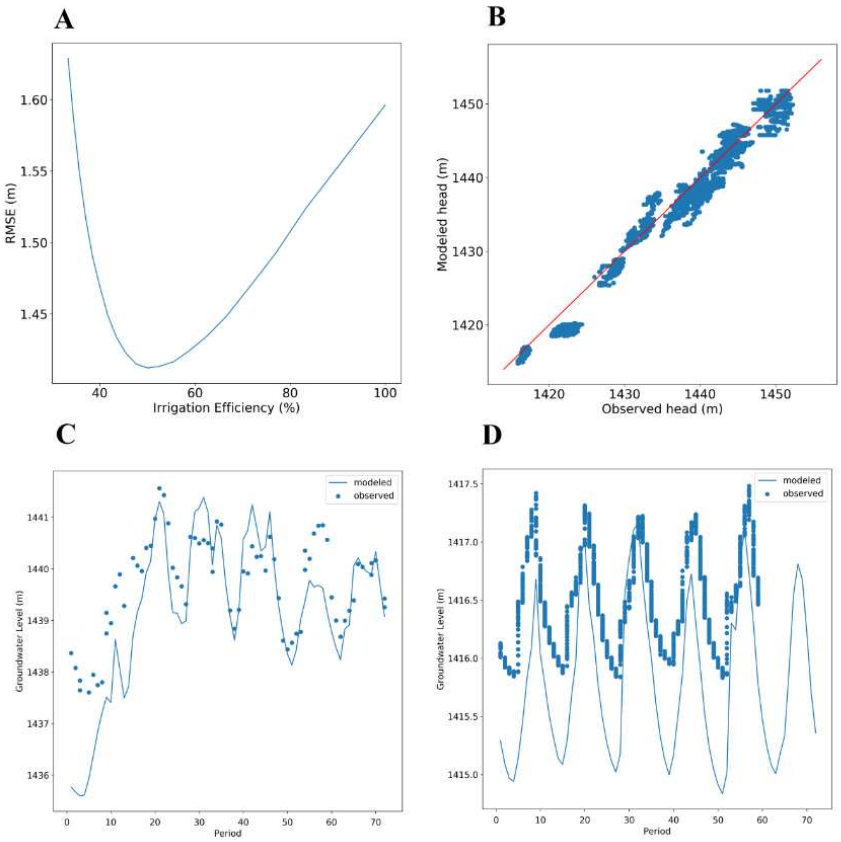

Figure 3.6: Figure A shows the Root Mean Square Error (RMSE) of comparing the modeling head and observations with different efficiencies. Figure B is the 1:1 plot of modeling head vs. observed head. Figure C and D are the time series of comparison of modeled and observed head in different locations of the Study Area.

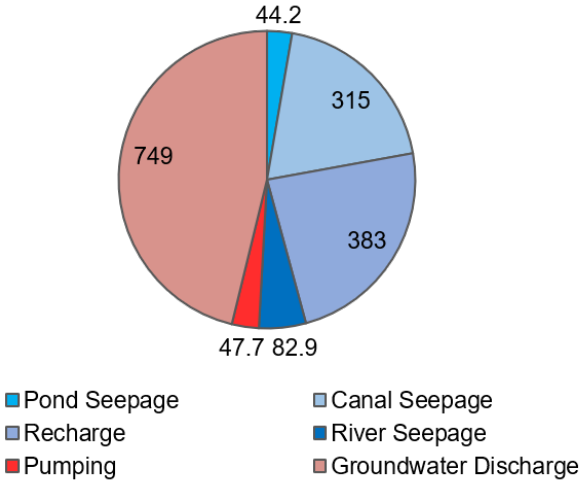

Figure 3.7: Baseline groundwater balance components for the simulation period. Values are in millions of m^3. Red colors indicate system outflows (pumping, groundwater discharge); blue colors indicate system inflows (recharge pond seepage, recharge, canal seepage, seepage from the South Platte River).

3.4.2 Recharge Pond Impact on Groundwater Head and Groundwater Discharge

Figure 3.8 shows the decrease in groundwater head with applying 0% (i.e. baseline simulation) to 80% of current recharge pond seepage rates. The groundwater head can drop as low as 2.3 m in some areas and 0.15 m over the entire Study Area when no recharge ponds are applied. The average head decrease ranges from 0.14 to 0.67 m for the Gilcrest town area, a location where high groundwater levels have caused significant infrastructure damage. Figure 3.9 shows the change in hydrologic fluxes for each of these scenarios. The recharge pond seepage volume (red bars) increases form 0 percent to 100 percent, with the absence of recharge ponds (0% scenario) resulting in the largest decrease (2.8%) in groundwater discharge to the river is 2.8%. Eliminating recharge pond seepage decreases the regional groundwater gradient, decreasing the amount of groundwater flowing towards and discharging to the South Platte River. In general, decreasing recharge pond seepage can have a significant effect on local groundwater levels, lowering the water table sufficiently to decrease impact on building foundations, residential basements, and wastewater treatment pond lining. However, the decrease in pond seepage results in an overall decrease in groundwater discharge to the South Platte River, which impacts water rights of the river. Figure 3.10 shows a time series of percent decrease in groundwater discharge to the South Platte River, for each of the recharge pond seepage scenarios. The average decrease ranges from 0.37% to 3.6%. The decrease can be as high as 10%, around the summer months of 2016. The scenario with no recharge pond seepage (0% pond recharge) shows the largest decrease in groundwater discharge, corresponding to the result shown in Figure 3.9.

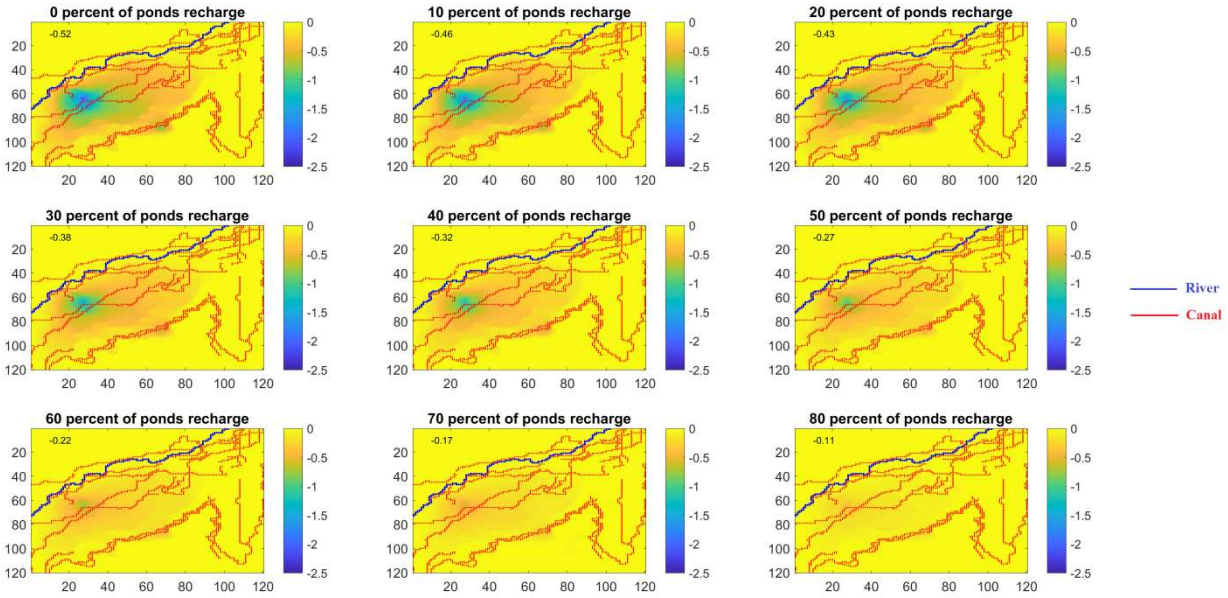

Figure 3.8: The head drop with applying 0% to 80% with current recharge ponds leak rate across the entire Study Area. The average decrease in groundwater head (m) is shown in the upper left corner of each subplot.

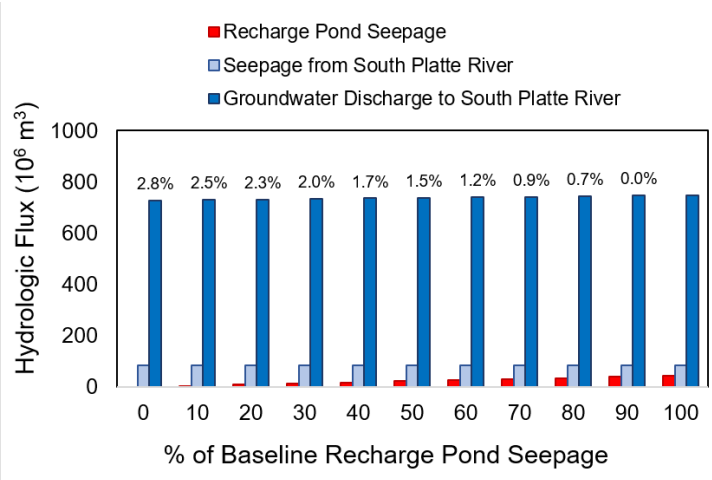

Figure 3.9: The interaction between the aquifer and the South Platte River corresponds to these different scenarios. X-axis is the percent of baseline recharge pond seepage. The percent values above the bars are percent decrease in groundwater discharge from the baseline simulation.

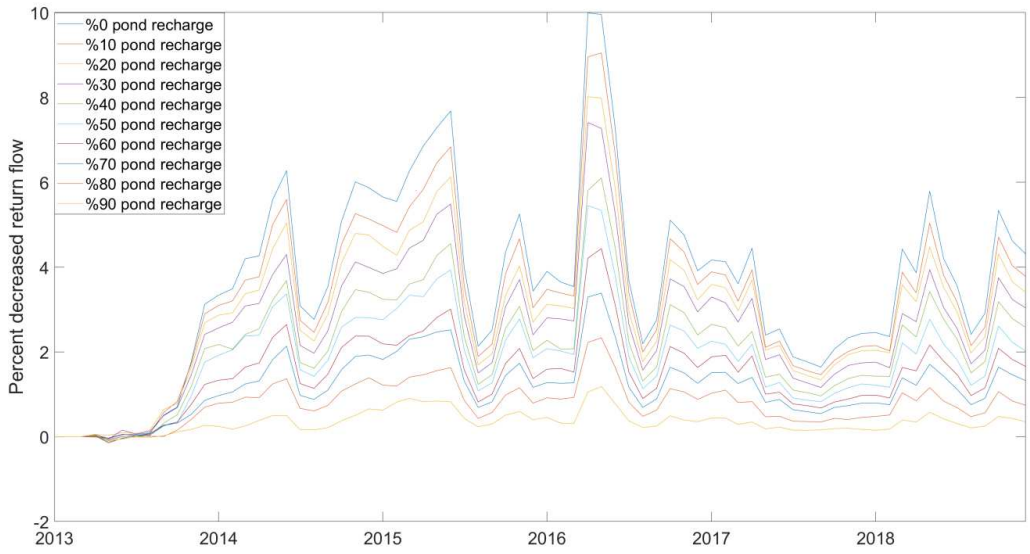

Figure 3.10: Time series of percent of return flow decreased corresponding the % decrease in recharge pond seepage in the model domain.

The impact of each individual recharge pond is also assessed. Figure 3.11A shows the average head decrease over the study region as each recharge pond is removed from the system. Pond #28 has by far the largest impact on groundwater head. Figure 3.11B shows the head drop map corresponding to a removal of Pond #28 from the groundwater system. The groundwater head decreases by 2 m in the localized area around the recharge pond. Figure 12 shows the impact of each individual recharge pond on groundwater discharge to the South Platte River. Pond #28 has the largest impact on groundwater discharge, with a daily average decrease of 6674 m^3/day when this pond is removed from the system.

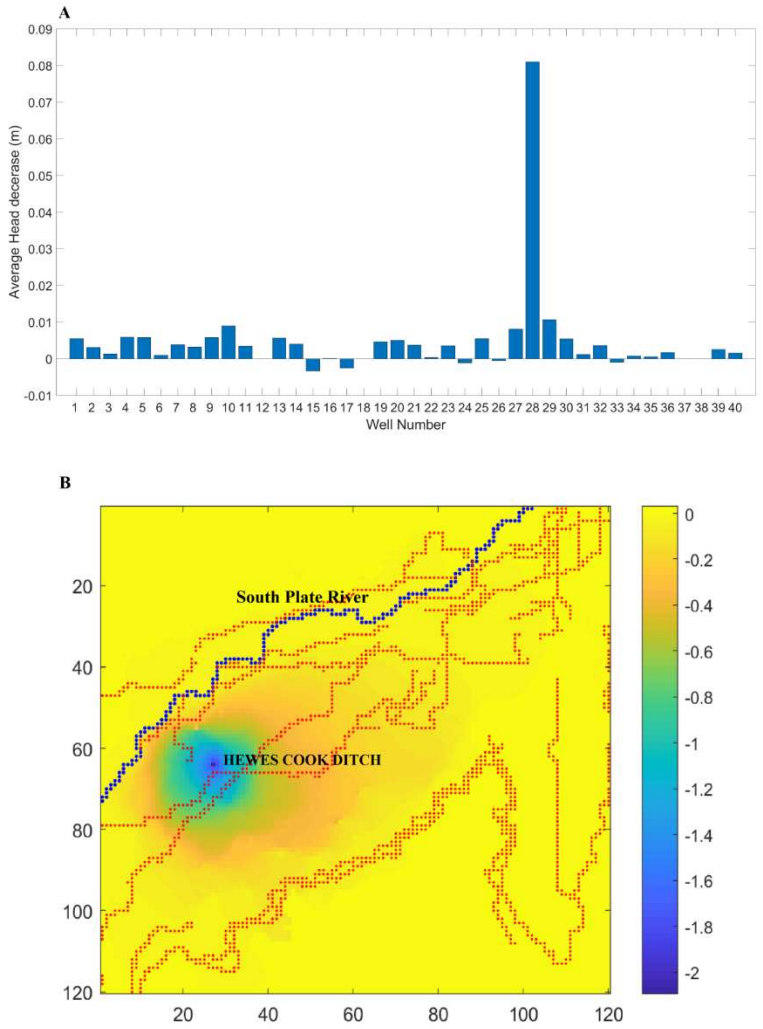

Figure 3.11: Figure A is the average head decrease (m) as each recharge pond is removed from the simulation. Figure B is the head drop (m) map corresponding to Recharge Pond #28.

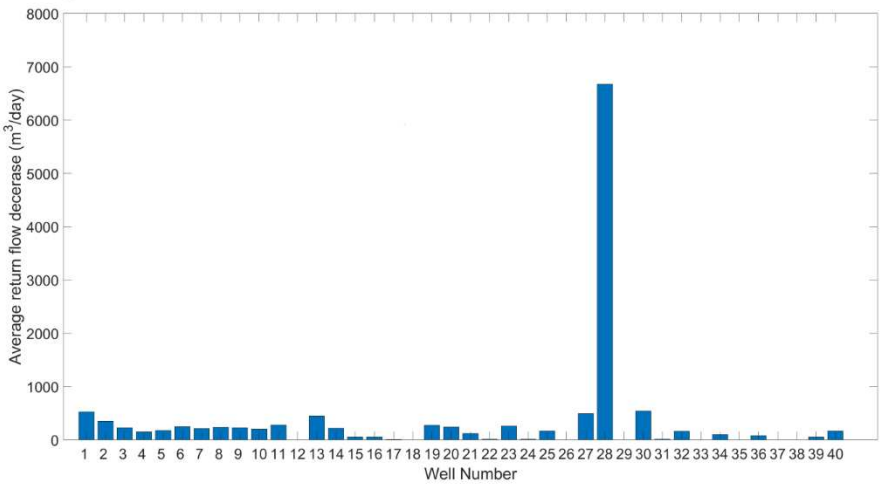

Figure 3.12: Average daily decrease in groundwater discharge to the South Platte River, based on each recharge pond being removed from the system.

Figure 3.13 summarizes the results from the third set of simulations, to quantify the interplay between pumping wells and recharge ponds. The diagram shows a cross-section of the model domain, from the high-elevation bluffs on the east to the South Platte River on the west, with the groundwater sloping from west to east and groundwater discharging to the South Platte River. Arrows and values indicate the water balance of the region under the baseline 2012-2020 simulation period, with gray arrows representing relative amounts of groundwater flux and black text indicating fluxes in millions of m^3. Under the scenario of no pumping and no recharge ponds, net groundwater discharge is 663 x 10^6 m^3. When pumping is included, the discharge rate decreases by 2.9%, to 644 x 10^6 m^3. Including recharge ponds with pumping results in a net discharge of 666 x 10^6 m^3, or a 0.5% increase in discharge compared to the no pumping scenario. These results indicate that the recharge ponds indeed offset the stream depletion caused by pumping, and even increase the discharge by 3 x 10^6 m^3.

A

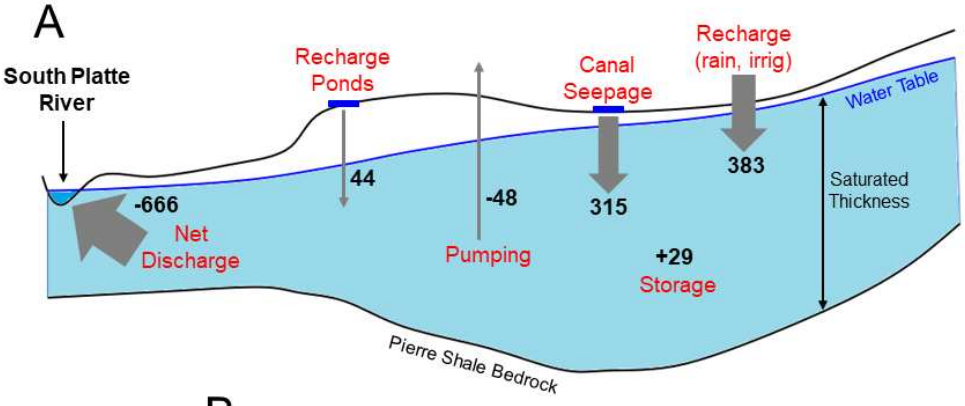

B

Condition	River Seepage	GW Discharge	Net Discharge	% Change in Net Discharge
No Pumping	84	-747	663	-
Pumping	85	-728	644	-2.9%
Pumping + Ponds	83	-749	666	0.5%

Figure 3.13: (A) cross-section schematic of the model region, showing flux magnitudes for groundwater sources and sinks; (B) table showing net discharge for the three scenarios.

3.5. SUMMARY AND CONCLUSIONS

In this study, the impact of recharge ponds on the groundwater system of the Gilcrest/La Salle area in the South Platte River Basin is assessed. This is achieved by introducing a new loosely coupled model that links the MODFLOW groundwater flow model and the DayCent agronomic hydrologic model. Daily deep percolation simulated by field-scale DayCent models is mapped to the MODFLOW grid cells, for use in the Recharge package.

The model is used to quantify the influence of 40 artificial recharge ponds on groundwater head and groundwater-surface water interactions during the 2012-2020 historical period. Several sets of simulations are run to quantify the effect, collectively and individually, of recharge pond seepage on local and regional groundwater levels and groundwater discharge to the South Platte River. Results show that groundwater levels can be decreased by up to 2.3 m in some areas of the study region, which can have a significant effect on historical groundwater flooding. Damage to building foundations, residential basements, and wastewater treatment plant bottom liners, all of which have been impacted by high water tables in recent years, could be mitigated by a decrease in groundwater head of this magnitude.

However, this decrease in groundwater levels results in a decrease in groundwater discharge to the South Platte River by approximately 3%. As the intent of the recharge ponds is to increase groundwater discharge and thereby offset stream depletions caused by groundwater pumping, and simulation results do indicate that pond seepage offset but do not over-offset depletions during the 2012-2020 time period, mitigating high water table issues in the region can be achieved only by (1) modifying fluxes of other sources and sinks of groundwater, or (2) modifying or relaxing the adjudication of water law, which dictates the need for offsetting pumping-induced stream depletion, in this region.

REFERENCES

Allen, R. G., Pereira, L. S., Raes, D., & Smith, M. (Eds.). (1998). *Crop evapotranspiration: Guidelines for computing crop water requirements*. Food and Agriculture Organization of the United Nations.

Barber, M. E., Hossain, A., Covert, J. J., & Gregory, G. J. (2009). Augmentation of seasonal low stream flows by artificial recharge in the Spokane Valley-Rathdrum Prairie aquifer of Idaho and Washington, USA. *Hydrogeology Journal*, *17*(6), 1459–1470. https://doi.org/10.1007/s10040-009-0467-6

Barkmann, P. E., Horn, A., Moore, A., Pike, J., & Curtiss, W. (2014). *Gilcrest/LaSalle Pilot Project Hydrogeologic Characterization Report*.

Bedekar, V., Niswonger, R. G., Kipp, K., Panday, S., & Tonkin, M. (2012). Approaches to the Simulation of Unconfined Flow and Perched Groundwater Flow in MODFLOW. *Ground Water*, *50*(2), 187–198. https://doi.org/10.1111/j.1745-6584.2011.00829.x

Cheng, K., Ogle, S. M., Parton, W. J., & Pan, G. (2014). Simulating greenhouse gas mitigation potentials for Chinese Croplands using the DAYCENT ecosystem model. *Global Change Biology*, *20*(3), 948–962.

Del Grosso, S. J., Halvorson, A. D., & Parton, W. J. (2008). Testing DAYCENT model simulations of corn yields and nitrous oxide emissions in irrigated tillage systems in Colorado. *Journal of Environmental Quality*, *37*(4), 1383–1389.

Del Grosso, Stephen J., Parton, W. J., Mosier, A. R., Walsh, M. K., Ojima, D. S., & Thornton, P. E. (2006). DAYCENT national-scale simulations of nitrous oxide emissions from cropped soils in the United States. *Journal of Environmental Quality*, *35*(4), 1451–1460.

Deng, C., & Bailey, R. (2019). A Modeling Approach for Assessing Groundwater Resources of a Large Coral Island under Future Climate and Population Conditions: Gan Island, Maldives. *Water*, *11*(10), 1963. https://doi.org/10.3390/w11101963

Gautam, S., Mishra, U., Scown, C. D., & Zhang, Y. (2020). Sorghum biomass production in the continental United States and its potential impacts on soil organic carbon and nitrous oxide emissions. *GCB Bioenergy*, *12*(10), 878–890.

Hargreaves, G. H., & Allen, R. G. (2003). History and Evaluation of Hargreaves Evapotranspiration Equation. *Journal of Irrigation and Drainage Engineering*, *129*(1), 53–63. https://doi.org/10.1061/(ASCE)0733-9437(2003)129:1(53)

Hashemi, H., Berndtsson, R., Kompani-Zare, M., & Persson, M. (2013). Natural vs. Artificial groundwater recharge, quantification through inverse modeling. *Hydrology and Earth System Sciences*, *17*(2), 637–650. https://doi.org/10.5194/hess-17-637-2013

Hashemi, Hossein, Berndtsson, R., & Persson, M. (2015). Artificial recharge by floodwater spreading estimated by water balances and groundwater modelling in arid Iran. *Hydrological Sciences Journal*, *60*(2), 336–350. https://doi.org/10.1080/02626667.2014.881485

Lacher, L., Turner, D., Gungle, B., Bushman, B., & Richter, H. (2014). Application of Hydrologic Tools and Monitoring to Support Managed Aquifer Recharge Decision Making in the Upper San Pedro River, Arizona, USA. *Water*, *6*(11), 3495–3527. https://doi.org/10.3390/w6113495

Lee, J., Pedroso, G., Linquist, B. A., Putnam, D., Kessel, C. van, & Six, J. (2012). Simulating switchgrass biomass production across ecoregions using the DAYCENT model. *GCB Bioenergy*, *4*(5), 521–533. https://doi.org/10.1111/j.1757-1707.2011.01140.x

McDonald, M. G., & Harbaugh, A. W. (1988). *A modular three-dimensional finite-difference ground-water flow model*. US Geological Survey.

Mirlas, V., Antonenko, V., Kulagin, V., & Kuldeeva, E. (2015). Assessing artificial groundwater recharge on irrigated land using the MODFLOW model. *Earth Science Research*, *4*(2), p16. https://doi.org/10.5539/esr.v4n2p16

Monsi, M., & Saeki, T. (1953). The light factor in plant communities and its significance for dry matter production. *Japanese Journal of Botany*, *14*(1), 22–52.

Niswonger, R. G., Panday, S., & Ibaraki, M. (2011). MODFLOW-NWT, a Newton formulation for MODFLOW-2005. *US Geological Survey Techniques and Methods*, *6*(A37), 44.

Parton, W. J., Hartman, M., Ojima, D., & Schimel, D. (1998). DAYCENT and its land surface submodel: Description and testing. *Global and Planetary Change*, *19*(1–4), 35–48.

Penman, H. L. (1948). Natural evaporation from open water, bare soil and grass. *Proceedings of the Royal Society of London. Series A. Mathematical and Physical Sciences*, *193*(1032), 120–145.

Ringleb, J., Sallwey, J., & Stefan, C. (2016). Assessment of Managed Aquifer Recharge through Modeling—A Review. *Water*, *8*(12), 579. https://doi.org/10.3390/w8120579

Robertson, A. D., Zhang, Y., Sherrod, L. A., Rosenzweig, S. T., Ma, L., Ahuja, L., & Schipanski, M. E. (2018). Climate change impacts on yields and soil carbon in row crop dryland agriculture. *Journal of Environmental Quality*, *47*(4), 684–694.

Scanlon, B. R., Keese, K. E., Flint, A. L., Flint, L. E., Gaye, C. B., Edmunds, W. M., & Simmers, I. (2006). Global synthesis of groundwater recharge in semiarid and arid regions. *Hydrological Processes*, *20*(15), 3335–3370. https://doi.org/10.1002/hyp.6335

SELLERS, P. J. (1985). Canopy reflectance, photosynthesis and transpiration. *International Journal of Remote Sensing*, *6*(8), 1335–1372. https://doi.org/10.1080/01431168508948283

Stehfest, E., Heistermann, M., Priess, J. A., Ojima, D. S., & Alcamo, J. (2007). Simulation of global crop production with the ecosystem model DayCent. *Ecological Modelling*, *209*(2), 203–219. https://doi.org/10.1016/j.ecolmodel.2007.06.028

United Nations, U. N. F. C. on C. C. (1992). *United Nations framework convention on climate change*. UNFCCC.

USEPA. (2016). *Inventory of US greenhouse gas emissions and sinks: 1990-2014.(No. EPA 430-R-16-002)*. US Environmental Protection Agency Washington, DC.

Warner, J., Sunada, D., & Hartwell, A. (1986). *Recharge as augmentation in the South Platte River basin. Colorado Water Resources Research Institute*. Colorado State University.

Zhang, Y., Arabi, M., & Paustian, K. (2020). Analysis of parameter uncertainty in model simulations of irrigated and rainfed agroecosystems. *Environmental Modelling & Software*, *126*, 104642. https://doi.org/10.1016/j.envsoft.2020.104642

Zhang, Y., Marx, E., Williams, S., Gurung, R., Ogle, S., Horton, R., Bader, D., & Paustian, K. (2020). Adaptation in U.S. Corn Belt increases resistance to soil carbon loss with climate change. *Scientific Reports*, *10*(1), 13799. https://doi.org/10.1038/s41598-020-70819-z

Zhang, Y., Qian, Y., Bremer, D. J., & Kaye, J. P. (2013). Simulation of nitrous oxide emissions and estimation of global warming potential in turfgrass systems using the DAYCENT model. *Journal of Environmental Quality*, *42*(4), 1100–1108.

Zhang, Y., Suyker, A., & Paustian, K. (2018). Improved crop canopy and water balance dynamics for agroecosystem modeling using DayCent. *Agronomy Journal*, *110*(2), 511–524.

CHAPTER 4: EVALUATING CROP-SOIL-WATER DYNAMICS IN WATERLOGGED AREAS USING A COUPLED GROUNDWATER-AGRONOMIC MODEL

4.1. SUMMARY

Waterlogging on croplands has been a known problem for a long time, leading to adverse social, physical, economic and environmental issues. To better solve the problem, the complicated plant-soil-water dynamics system needs to be better understood. The challenge is to simulate the interactions between the components in the systems. There are models that simulate a plant-soil-water system but either run the processes independently leading to inaccuracy or have high invasiveness of using integrated models. This paper presents a tightly coupled model, DayCent-MODFLOW, that links a 3D ground-water flow (MODFLOW) model and a 1D agroecosystem model (DayCent). DayCent is responsible for plant-soil-water dynamics in the root zone, whereas MODFLOW simulates head and groundwater flow in the saturated zone of the aquifer. DayCent passes deep percolation from the soil profile to the water and, under conditions of waterlogging in which the water table is within the soil profile, DayCent soil hydrologic processes are constrained by the presence of the water table simulated by MODFLOW. The coupling is achieved by adopting a parallel inter-process communication technique MPI (Message Passing Interface). The model is applied to a waterlogged agricultural area (22 km^2) in northern Colorado, USA and tested against groundwater head and rates of evapotranspiration (ET). The model runs in parallel with about 800 processes for each time step in an AWS Linux server of 96 CPUs. Groundwater heads match measured heads to a reasonable degree, and ET rates match reference ET and are highly correlated with crop type. Results show the strong hydrologic interaction between the two models. Greenhouse gas emissions from soil

(N_2O and CH_4) were also estimated by the model under the waterlogged conditions. Although the model can be used to simulate any plant-soil-aquifer system, no matter the depth of the water table, results from this study show that the model can be used to assess crop productivity, recharge, ET, and greenhouse gas emissions in areas of shallow groundwater.

4.2. INTRODUCTION

The plant-soil-water system controls the movement of water, nutrients, and greenhouse gases in agricultural landscapes. Understanding this system under a variety of hydrologic conditions is important for food production, land management, water management, and nutrient management. The plant-soil-water system is a complex system consisting of surface water runoff, infiltration, soil water dynamics, crop growth, evapotranspiration, recharge and nutrient leaching, carbon-nitrogen cycling, and consequent hydro-chemical processes such as flow and nutrient transport in aquifers, stream discharge and nutrient loading, and greenhouse gas emissions.

The challenge of simulating water transport and nutrient cycling in such a complex system resides mainly in the interaction between "zones", such as water movement between the soil profile and the saturated zone of the aquifer. As stated by Alley (Alley et al., 2002), groundwater recharge is the most difficult groundwater budget to simulate due to factors such as precipitation, irrigation application, evapotranspiration, land use, crop type, and soil type. A special condition of plant-soil-water interaction is the presence of saturated conditions in the root zone of crops (i.e. "waterlogging"), which can decrease crop yield and damage soil health and structure (Cannell et al., 1980; Cavazza & Pisa, 1988; Collaku & Harrison, n.d.; Houk et al., 2006, 2006; Kaur et al., 2017). $360 million loss of crop production every year during 2010-2016 is due to waterlogging and even greater loss than drought in the United States (Ploschuk et al., 2018).

Waterlogging can dramatically change the dynamics of carbon and nitrogen in soil. The resulting anaerobic condition decreases the rate of organic matter decomposition (Meurant & Riker, 2014), resulting in an accumulation of soil organic matter that affects nitrogen mineralization and available nitrogen for crop uptake; and also increases denitrification, which can increase methane (CH_4) emission and nitrous oxide (N_2O) emission (Bartlett & Harriss, 1993; Parton et al., 2001), both of which are greenhouse gases.

There are many numerical physically based models that simulate a range of hydrologic and chemical processes in the plant-water-soil system. A subset of these models are agronomic models that simulate hydrologic and crop growth processes in a one-dimensional domain at the soil profile-scale. These include SWAP (Kroes et al., 2009), DSSAT (Jones et al., 2003), and DayCent (Parton et al., 1998; Zhang et al., 2018). They simulate irrigation, runoff, infiltration, and percolation through soil layers, crop ET, and deep percolation from the bottom of the soil profile. However, as they do not simulate groundwater flow in the saturated zone of the underlying aquifer, the fluctuation of the water table and its possible presence in the soil profile and crop root zone is not represented. The Soil & Water Assessment Tool (SWAT) (Arnold et al., 1998) simulates hydrological processes and crop yield at the watershed scale, with a water balance and crop growth simulation occurring at individual hydrologic response units (HRUs) across the watershed landscape. The model accounts for groundwater storage and groundwater discharge to streams but does not simulate water table fluctuation in a physically based manner and hence cannot account for waterlogging effects on root zone processes and crop yield. Even the linked SWAT-MODFLOW model (Bailey et al., 2016) does not account for the condition of shallow groundwater in the root zone – MODFLOW may simulate a water table at the elevation of an HRU's soil profile, but it has no effect on SWAT's HRU soil profile and root zone

processes. The linked DSSAT-MODFLOW model (Xiang et al., 2020) also does not account for the effect of shallow groundwater on root zone processes, as the linkage between the models is performed at the annual time scale, and day-to-day DSSAT crop growth and nutrient cycling algorithms are not affected by MODFLOW-simulated water table elevation.

Another subset of models simulates vadose zone hydrologic processes and water table fluctuation, but does not simulate near-surface hydrology, vegetative growth, root zone processes, and nutrient cycling. These include the hydrologic and hydrogeologic models MODFLOW (Niswonger et al., 2011), HYDRUS (Šimůnek et al., 2012), MODFLOW-SURFACT (Panday & Huyakorn, 2008), STOMP (White & Oostrom, 2003), TOUGH2 (Pruess et al., 1999), VS2DI (Healy, 2008), the VSF package (Thoms et al., 2006), and HydroGeoSphere (Therrien et al., 2010), among many others. There is a general lack of hydro-agronomic models wherein the simulated water table affects root zone processes, and root zone processes in turn affect recharge to the water table.

The objective of this paper is to present a coupled agroecosystem-groundwater modeling system that can simulate water movement and crop growth under waterlogged conditions. The DayCent and MODFLOW codes are chosen as the agroecosystem and groundwater models, respectively. DayCent was selected as it includes carbon and nitrogen dynamics in agroecosystems, and thus is more versatile in applications. MODFLOW is chosen as it is the most widely used groundwater flow model worldwide. The models are tightly coupled, with system data passed between them on a daily time step, using a novel Message Passing Interface (MPI) (Gropp et al., 1996) that avoids code modification to DayCent and MODFLOW codes and therefore can work with updated versions of DayCent and MODFLOW. DayCent improves recharge calculations to MODFLOW, and MODFLOW improves accuracy of crop yield and

nutrient cycling of DayCent in the presence of a shallow water table. Although the DayCent-MODFLOW linked system can be applied to any plant-soil-water system, an application to an irrigated area with shallow groundwater in northern Colorado, USA, will be shown to demonstrate its capability in waterlogged conditions. The impact of waterlogged conditions on greenhouse gases will also be briefly described in the model application.

4.3. METHODS

This section provides information about the DayCent and MODFLOW models and a description of how they are tightly coupled using the MPI method.

4.3.1 Introduction to MODFLOW: Groundwater Flow Model

MODFLOW is a Fortran-written program that numerically solves the three-dimensional ground-water flow equation by using a finite-difference method (McDonald & Harbaugh, 1988; Niswonger et al., 2011). MODFLOW is the most widely used groundwater flow model in the world. Versions include MODFLOW-88 (McDonald & Harbaugh, 1988), MODFLOW-96 (Harbaugh & McDonald, 1996), MODFLOW-2000 (Harbaugh et al., 2000), MODFLOW-NWT (Niswonger et al., 2011) and MODFLOW-6 (Langevin et al., 2017). In this study, the MODFLOW-NWT version is used to couple with DayCent.

MODFLOW-NWT simulates groundwater head throughout an aquifer system by solving the groundwater flow equation for a porous medium. The flow equation for an unconfined aquifer (Bedekar et al., 2012) is:

$$\frac{\partial}{\partial x}(\mathrm{F}_s K_{xx}\frac{\partial h}{\partial x})+\frac{\partial}{\partial y}(\mathrm{F}_s K_{yy}\frac{\partial h}{\partial y})+\frac{\partial}{\partial z}(\mathrm{f(F)}K_{zz}\frac{\partial h}{\partial z})+W=\varphi\frac{\partial \mathrm{F}_s}{\partial t}+\mathrm{F}_s S_s\frac{\partial h}{\partial t} \qquad (1)$$

where x, y, z are the three dimensions; h is groundwater head (L); K is hydraulic conductivity (L/T). S_s is specific storage (1/T). φ is porosity taken equal to specific yield S_y; F_s is the fraction of the cell thickness that is saturated; and f(F) is a function of F_s set to 1 for Niswonger et al. (2011).

MODFLOW also solves the equation for confined aquifers, but this study is concerned with water table interaction in soil zones, and hence Equation 1 is presented. The finite difference method is used to solve Equation 1 by discretizing the groundwater system spatially into a grid of cells and the simulation time period into time steps. Each cell is interpreted as a small volume of aquifer material with the same hydraulic properties. The equation describes the volumetric water balance within each of the cell, with groundwater inputs including groundwater flow from adjacent cells and other groundwater sources (e.g. recharge, seepage) and groundwater outputs including flow to adjacent cells and other groundwater sinks (e.g. ET, pumping, discharge). The aquifer hydraulic properties include hydraulic conductivity K, specific yield S_y, and specific storage S_s. Although the primary variable of solution is groundwater head h, flow rates using h can be calculated at each time step.

4.3.2 Introduction to DayCent: Agroecosystem Model

The DayCent model (Parton et al., 1998; Zhang, Suyker, et al., 2018) is a medium complexity agroecosystem model. The major sub-models of DayCent are plant growth, soil water, soil organic carbon, soil nitrogen and greenhouse gas emission. Major inputs for the model are daily weather, soil physical properties, plant type, and management practices. DayCent has been widely used for carbon and nitrogen simulations in agroecosystems (Del Grosso et al., 2008; Del Grosso et al., 2006; Robertson et al., 2018; Zhang et al., 2013). The model was selected to estimate soil CO_2 and N_2O emissions/removals for the US national greenhouse gas inventory (USEPA, 2016) which is annually submitted to the UN Framework

Convention on Climate Change (United Nations, 1992). The crop growth/production sub-model has been used in simulations of agroecosystem dynamics not only in the U.S. but also globally (Cheng et al., 2014; Del Grosso et al., 2008; Gautam et al., 2020, 2020; Lee et al., 2012; Stehfest et al., 2007; Zhang, Marx, et al., 2020). Recently, the DayCent model has been improved in simulations of crop canopy development, growth, and water use (Zhang, Arabi, et al., 2020; Zhang, Hansen, et al., 2018; Zhang, Suyker, et al., 2018). This new version of DayCent is used in this study for coupling with MODFLOW. DayCent is written in Fortran and C.

The DayCent modeling code includes the main water balance components for a soil profile: infiltration of precipitation and irrigation, surface runoff, deep percolation from the bottom of the soil profile, evapotranspiration (ET; evaporation and transpiration), and capillary rise of groundwater:

$$\Delta S_i = P + I_{net} - ET_c - RO - DP + GW \qquad (3)$$

where ΔS_i is the net change in soil water at the end of day i and $i-1$. In this equation, P, RO, and DP are precipitation, runoff, and deep percolation on day i, respectively. I_{net} is the net irrigation on day i. GW is the groundwater contribution if a shallow water table is present. ET_c is the actual evapotranspiration on day i. All units are in cm day-1. The soil profile is defined by users which is usually less than three meters in depth. The input soil parameters include soil texture, bulk density, and field capacity, wilting point, and saturated hydraulic conductivity.

Reference ET is simulated using either the standardized Penman-Monteith method (Allen et al., 1998) or the Hargreave's method (Hargreaves & Allen, 2003), with the latter used when only air temperature is available. Crop coefficients are used in conjunction with reference ET to estimate potential ET for each crop type. The ET is partitioned into potential evaporation and potential transpiration as a function of the green canopy coverage and residue coverage. The green canopy coverage (CC) is calculated from Beer's law (Monsi & Saeki, 1953; SELLERS, 1985):

$$CC = 1 - \exp(-k \times GLAI) \quad (4)$$

where k (dimensionless) is the light extinction coefficient of the vegetation, and GLAI is green leaf area index (m m-1). The GLAI and CC approach was recently added to DayCent and the detailed description can be found in Zhang et al. (2018). Water uptake by root is limited by soil available water. Regarding potential soil evaporation, it can be reduced by the amount of standing dead biomass and litter on the soil surface. In DayCent, actual evaporation is also limited by the soil water potential of the topsoil layer and the upward fluxes from underlying layers(Parton et al., 1998).

DayCent simulates 1D water flows using a combined method: a modified tipping-bucket approach for water flow above field capacity and a Richards' approach (Richards, 1931) for water redistribution below field capacity (Parton et al., 1998). Water table is simply simulated by turning off the drainage of water at the last soil layer for a user-specified period. When water table is present, the water infiltrated from the soil surface starts to saturate soil from the bottom. In the linked DayCent-MODFLOW, the presence of water table in DayCent simulation is controlled by the water table elevation in MODFLOW (Section 2.3).

Greenhouse gas (N_2O, CH_4) emission is simulated in DayCent model using the mass balance of nitrogen in soil:

$$\Delta N = N_{littter} + N_{fert} + N_{deposit} - N_{gas} - N_{erosion} - N_{DP} - N_{Root} \quad (5)$$

where N_{litter} is nitrogen added from plant litter; N_{fert} includes both organic and inorganic fertilizer; $N_{deposit}$ is atmospheric nitrogen deposition; N_{gas} is gas removed via nitrification and denitrification and includes N_2, N_2O, and NO_x gases; $N_{erosion}$ is the loss due to soil erosion; N_{DP} is the removal from the soil profile via deep percolation (both inorganic and organic forms); and N_{Root} is plant root uptake.

The emission of CH_4 is produced in soil under anaerobic conditions by methanogens. In DayCent, the rate is primarily determined by the availability of carbon substrate (derived from decomposition and root rhizo-deposition) for methanogens and the impact of environmental variables including soil texture (redox potential, pH, and soil temperature), climate, and

agricultural practices (Hartman et al., 2020). DayCent simulates soil N_2O and NO_x emissions from nitrification and denitrification (Parton et al., 2001). Nitrification is calculated as a function of soil ammonium (NH_4) concentration, soil moisture, soil temperature, pH, and bulk density. Denitrification is a function of soil nitrate concentration, labile carbon availability, O_2 availability, soil water content, and soil physical properties that influence gas diffusivity.

4.3.3 Description of DayCent-MODFLOW Theory

This section describes the basic linkage between DayCent and MODFLOW, i.e. which information is passed between the two models, and when. Section 2.4 provides details regarding the Message Passing Interface (MPI) used to link the models without invasive code modification to either DayCent or MODFLOW. Section 2.5 describes an application of DayCent-MODFLOW to a waterlogged site in an agricultural area of northern Colorado, USA.

DayCent-MODFLOW is linked on a daily time step, with results from each model providing inputs and constraints on the other. Therefore, the linkage could be termed “tight linkage” or “tight coupling”. The linkage process through time steps of a simulation is shown in Figure 4.1. As DayCent is a 1D field-scale model, multiple DayCent models are included to represent the collection of cultivated fields overlying the unconfined aquifer. Therefore, multiple DayCent models are linked to a single MODFLOW model based on the geological locations. The simulation runs according to the following steps, repeated for each time step:

1. MODFLOW passes basic grid cell information to the set of DayCent models: surface elevation (top of MODFLOW grid cells), bottom elevation of MODFLOW grid cells, specific yield S_y of aquifer material, and saturated hydraulic conductivity K of top layer. The soil and aquifer properties are shared between DayCent and MODFLOW.

If the time step is the first of the simulation, MODFLOW also passes initial groundwater head values for each grid cell.

2. The received values are assigned to corresponding model variables for each DayCent model.
3. Each DayCent model is run for the time step.
4. The recharge rate calculated by each DayCent model is sent to corresponding MODFLOW grid cells within the Recharge package. MODFLOW then runs for the time step. MODFLOW groundwater head for each grid cell is passed to the corresponding DayCent model, in preparation for the next time step run.

This process is continued until the end of the simulation.

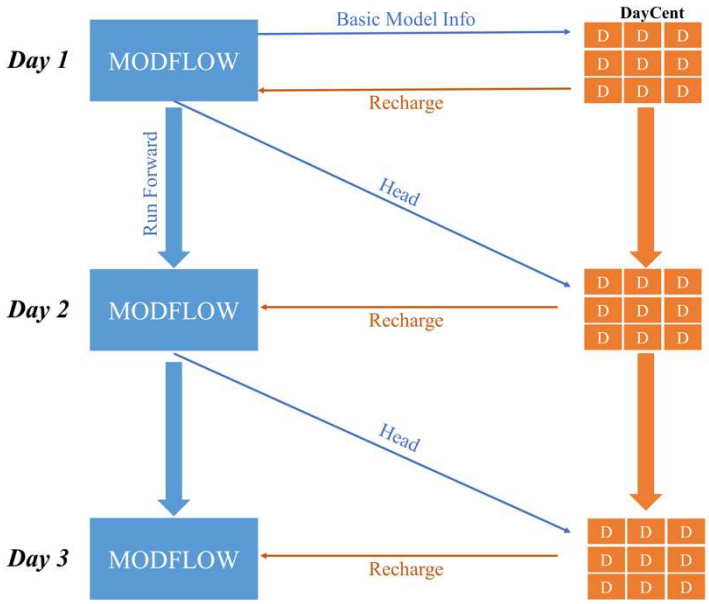

Figure 4.1. Flow chart of data passing in the coupled DayCent-MODFLOW model, showing a single MODFLOW model coupled with a set of field-based DayCent models.

DayCent has two modes of running, based on the received groundwater head from MODFLOW. The first mode is the normal running of DayCent, in which the water table is not present in the root zone. DayCent simulates unsaturated water flow, crop ET, and soil water

content in the root zone according to the weather and irrigation schedule. At the end of the time step, it outputs deep percolation from the bottom of the root zone and passes it as recharge to MODFLOW grid cells.

The second mode is when the groundwater head is above the bottom of the root zone, i.e. the water table is present in the root zone. This condition is shown in Figure 4.2, which shows the DayCent soil layers, the MODFLOW grid cells, and the water table located in the root zone. This requires an adaptation by DayCent to account for groundwater influence on hydrologic and chemical processes in the root zone, and a careful accounting of water mass within the root zone between the two models. To preserve the mass of water, we calculate the change of groundwater storage in MODFLOW grid cells and make the same amount of water change in DayCent. This is calculated as:

$$delta_{i,j} = sy_j \cdot (h_{i,j} - h_{i-1,j}) \qquad (5)$$

where i is the time step, j is the location. $delta_{i,j}$ is the water changed in MODFLOW at time step i and location j. sy_j is the specific yield at location j. $h_{i,j}$- $h_{i-1,j}$ is the head difference at the end of the day between consecutive time steps.

Depending on the change, DayCent either drains water from or injects water to the root zone layers to maintain the same condition as simulated by MODFLOW. After the time step simulation, DayCent either passes a positive or negative recharge to MODFLOW based on the change of saturated water level in the root zone (equation 6):

$$rech_{i,j} = swc_{i,j} - swc_{i-1,j} \qquad (6)$$

where $rech_{i,j}$ is the groundwater recharge generated by DayCent. $swc_{i,j}$- $swc_{i-1,j}$ is the soil water content between time steps.

If the simulated groundwater head by MODFLOW is above the ground surface, DayCent routes the ponded water as surface runoff and passes the same amount as negative recharge to MODFLOW (equation 7):

$$runoff_{i,j} = sy_j \cdot (h_{i,j} - elv_{surf}) \quad (7)$$

where $runoff_{i,j}$ is the runoff when the water table is above surface .

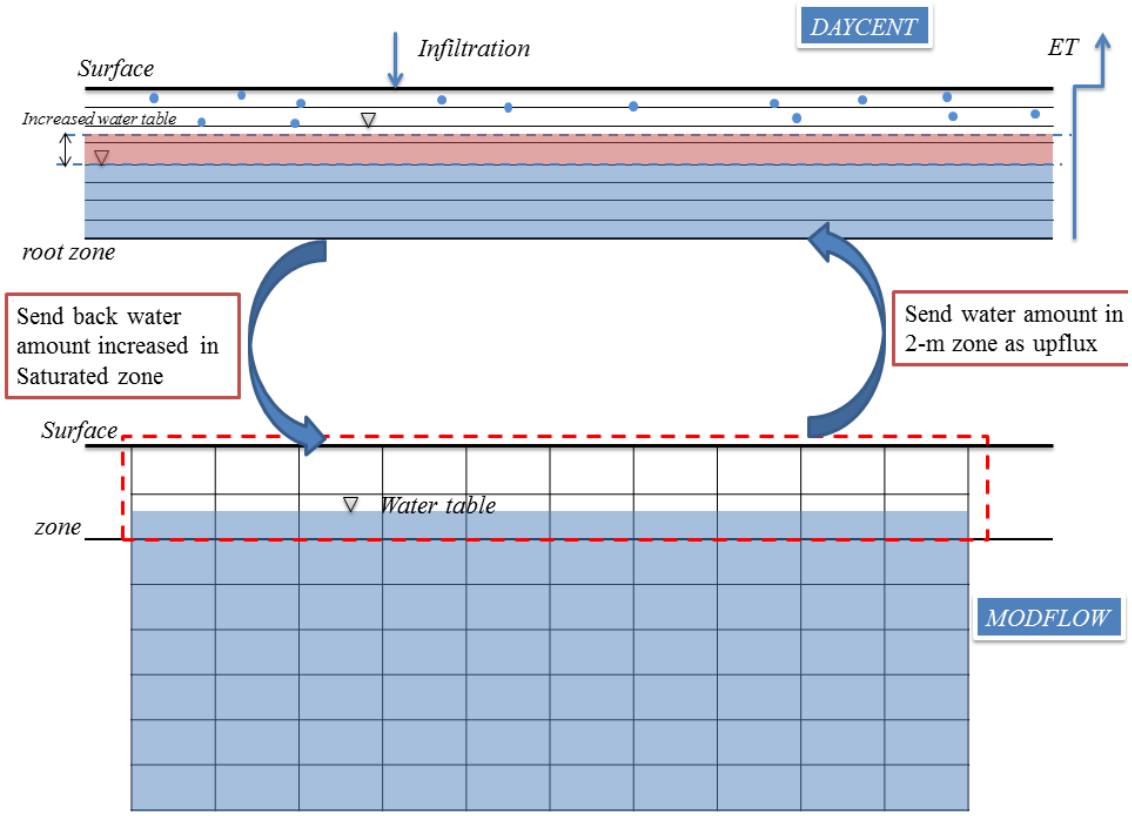

Figure 4.2: The interaction between DayCent and MODFLOW with respect to the water table and passing water between DayCent soil profile and MODFLOW grid cells.

4.3.4 Description of DayCent-MODFLOW Linkage using MPI

A key requirement of the DayCent-MODFLOW linkage is to limit model invasiveness, i.e. the need to change the code of either or both models. Model code modification, such as that performed by Bailey et al. (2016) to link SWAT and MODFLOW, requires code updating whenever new SWAT or MODFLOW codes are published. Model updates can be handled more

easily if linkage procedures are accomplished strictly via non-invasive procedures. In this study, therefore, DayCent is not integrated into MODFLOW, but instead they are linked using Message Passing Interface (Gropp et al., 1996), an inter-process communication technique.

All communication between MODFLOW and DayCent (see Figure 4.1) is achieved using MPI. MPI is a message passing library in parallel computation. MPI specifies the names, calling sequences, and results of subroutines to be called in Fortran or other languages. The program is still compiled with ordinary compilers but linked with the MPI library (Gropp et al., 1999). MPI has become the most popular message-passing library standard for parallel programming (Quinn, 2003). MPI assumes the underlying hardware is a collection of processors with its own local memory (Figure 4.3A). Each processor only has access to the instructions and its local memory. However, the interconnection work allows message-passing between processors through implicit channels. MPI serves as a communication function that enables processes to communicate with each other. MPI also supports synchronization between processors. One process cannot receive the message after another sends it.

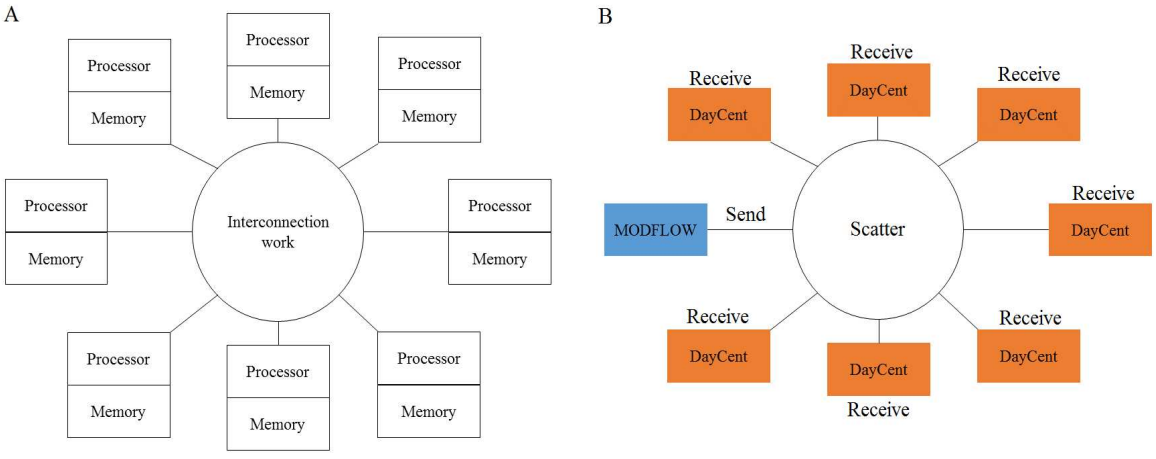

Figure 4.3: The message-passing model from the book of Parallel Programming in C with MPI and OpenMP (Quinn, 2003)

MPI has two principal advantages over other message-passing models: it runs well on MIMD (multiple instruction, multiple data) architectures, which are used in this study; and it is easier to debug than shared-variable programs since each processor has its own controls of memory (Quinn, 2003).

For linking DayCent and MODFLOW, the following four main functions are used: *MPI_Send*, *MPI_Recv*, *MPI_Scatter*, and *MPI_Gather*. *MPI_Send* and *MPI_Recv* are basic calls to send messages either as data points or as arrays of values from one processor to another processor. Each *MPI_Recv* must have a corresponding *MPI_Send* for the program to continue. *MPI_Scatter* and *MPI_Gather* are one-to-multiple and multiple-to-one processes. The message in the source processor is scattered to other processors. Each processor receives a part of the copy from the original message. This is often used for array scatter. Each processor receives a portion of the array. *MPI_Gather* gathers different messages from other processors into one message and saves it in the source processor. *MPI_Scatter* and *MPI_Recv* are vital when coupling 1D and 2D models such as with DayCent and MODFLOW.

The recharge rates sent from the DayCent field-scale models to the single MODFLOW model is applied to the top cells of the MODFLOW grid. The water table elevation (i.e. groundwater head) sent from the MODFLOW grid cells to the DayCent models is applied to the soil profiles of each individual DayCent simulation. Hence, the MPI process is a set of 1D models (DayCent) communicating with a 2D model (MODFLOW), and vice versa (see Figure 4.3B). Since there is only one MODFLOW model in the coupled system, there is just one processor for MODFLOW. All other processors are used for DayCent.

After splitting, the processors in each group are assigned a new rank number as their ID. There are also two communicators: one is for communicating between MODFLOW and

DayCent; the second is for communicating between the multiple DayCent models. As multiple DayCent simulations start, the source processor ("rank 0") reads an "Info array" from the "*Soil and Crop*" file which contains the information of the cells' soil physical properties, crop type, and their corresponding locations in MODFLOW. The information passed from MODFLOW to the DayCent simulations are added to the "Info array" by matching their locations. This information is then scattered to all other DayCent processors. By doing so, each DayCent simulation is linked to a unique MODFLOW grid cell location with a unique rank and run with unique information, such as crop type and associated crop scheduling. Figure 4.3B shows the forward step with *MPI_Scatter*. After DayCent simulations run for a time step, recharge values are gathered using *MPI_Gather* and sent to corresponding MODFLOW grid cells, which is the reverse step of Figure 4.3B. This finishes the entire MPI process.

In this study, Open MPI library is employed using the Linux system. DayCent and MODFLOW are run separately using the command "*mpirun*". All MPI processes are coded in modules using Fortran to make minimum modifications to the original code. Generally, the number of DayCent simulations is much more than the number of processors contained in a typical desktop computer. One common feature of computer operating systems is multitasking which allows more than one task to run in one processor (Reilly, 2004). Multitasking is not a parallel execution as it allows time sharing and scheduling of CPUs (Oracle, 2016). One of the disadvantages of MPI is that all processes start at the same time, resulting in intensive memory allocation.

The input file for DayCent-MODFLOW is the same input file format for original DayCent and MODFLOW simulations, except for the additional "*Soil and Crop*" file. In MODFLOW, any recharge values listed in the Recharge package input file are eliminated from the simulation, as

recharge arrays will be populated by DayCent deep percolation values. In MODFLOW, the water budget now includes recharge received from DayCent. The water balance from DayCent consists of irrigation and precipitation infiltration, runoff, evaporation and transpiration, upflux or drainage caused by the change of water table in MODFLOW, deep percolation, and the change in soil water content.

4.3.5 Application of DayCent-MODFLOW

A highly irrigated area in the South Platte River Basin in northern Colorado (Figure 4.4A and B) is selected as our study area for application of the DayCent-MODFLOW modeling system. The study area is approximately 4.7 km x 4.7 km (Figure 4.4C), with 83% of the area covered by crops. Main crop types include alfalfa, corn, grass pasture, wheat, and sugar beets. Soils are mainly sandy, but there are pockets of clay accumulation. Due to semi-arid climate and low annual rainfall rates (< 35 cm/yr), irrigation is used to satisfy crop ET. Irrigation water is supplied during the growing season (April-October) either by groundwater pumping from the underlying unconfined aquifer or by canals that divert water from the South Platte River. There are 40 pumping wells and 4 canals in the study area (see Figure 4.4C). Model application for this site was chosen due to the prevailing high groundwater levels in the region. Waterlogging due to high groundwater levels has been a problem for landowners for many years. Groundwater typically is within 4.5 m of the ground surface. High groundwater levels are caused by a combination of canal seepage, high rates of deep percolation from irrigation events, and decrease in pumping over the previous 15 decades due to water right issues (Deng and Bailey, 2020).

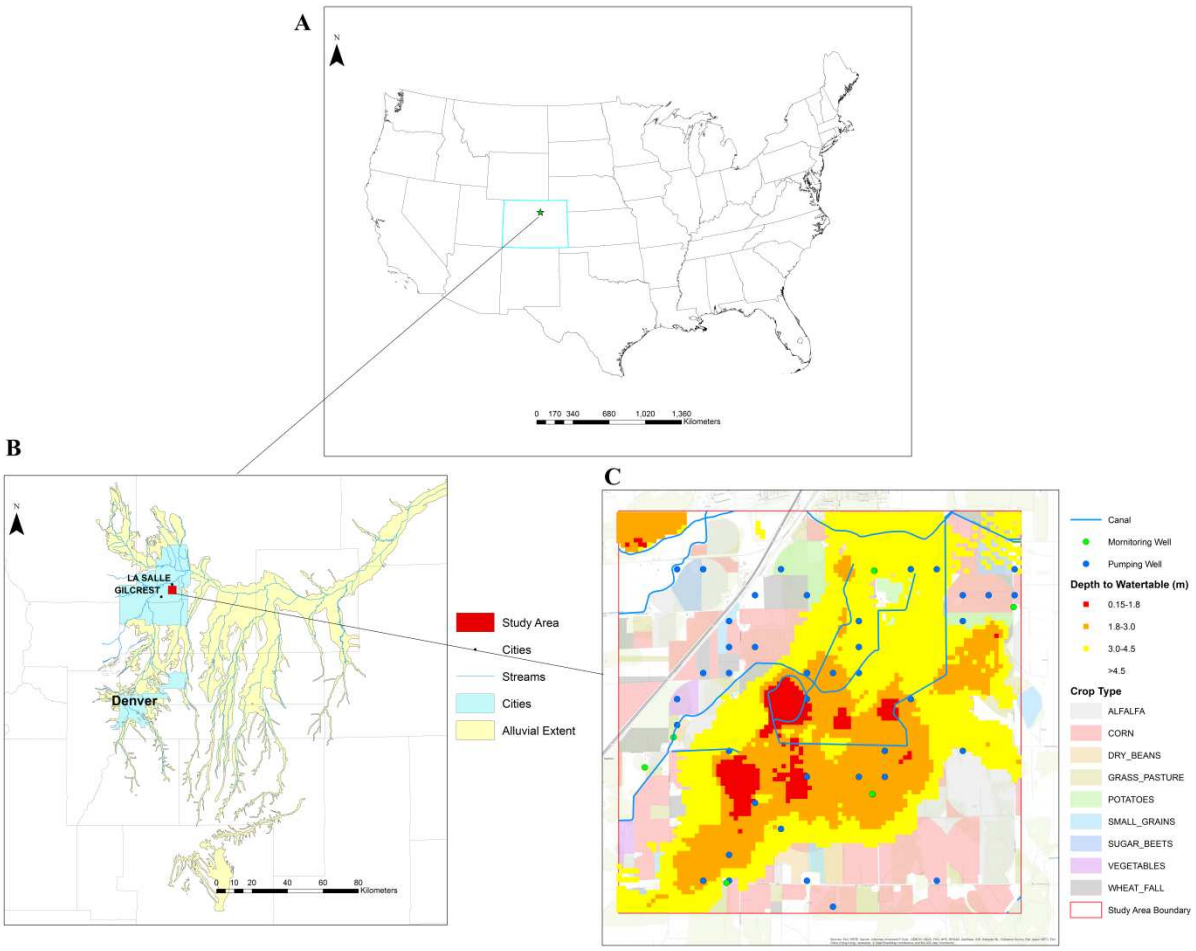

Figure 4.4: Study area of the DayCent-MODFLOW application, located in the South Platte River Basin, Colorado (Figure A). The South Platte River Basin is shown in B. Figure C shows the distribution of crop type and an interpolated map of observed groundwater depth, based on results from a regional assessment of monitoring well data from the Colorado Geological Survey (CGS, 2014).

The MODFLOW model grid consists of 31 rows and 31 columns (Figure 4.5A), with each cell 152 m x 152 m (500 ft x 500 ft), and 10 vertical layers that represent the unconfined aquifer from the ground surface to the shale bedrock. The thickness of the aquifer ranges from 4.7 m to 36.1 m. The values for the grid cells are obtained from a larger MODFLOW model of the study region, calibrated and tested against groundwater levels (Deng and Bailey, 2020). A 3D hydraulic conductivity (K) map (Figure 4.5B) was developed by interpolating data from over 400 boreholes using a 3D Kriging method and then mapping to the grid cells (Deng and Bailey, 2020). For this study, aquifer source/sink fluxes for MODFLOW include canal seepage and

groundwater pumping, with recharge provided by DayCent within the coupled system. Time-variant specified-head boundary conditions are applied for each grid cell along the perimeter of the model domain, using results from the larger regional model.

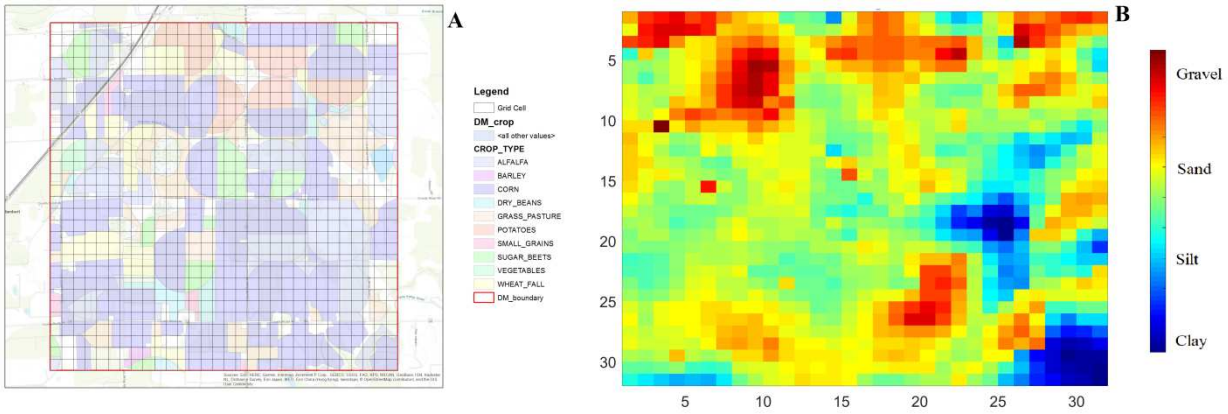

Figure 4.5: Figure A is the MODFLOW grid cells in the model top layer. Figure B is the hydraulic conductivity map in the model top layer.

The soil physical property data is obtained from SSURGO. Irrigation parcel data were obtained from Colorado's Decision Support System (CDSS) for the region. Crop rotation data were obtained from the Cropland Data Layer (CDL) of NASS (National Agricultural Statistics Service). Management schedules were set up for nine crops in DayCent. For each DayCent simulation, the root zone is divided uniformly into 14 layers for a total thickness of 210 cm. Parameters for each crop type were based on values from other studies in the South Platte River Basin (Dozier et al., 2017; Zhang, et al., 2020). Crop management data including planting dates, harvest dates, and fertilizer rates were obtained from NASS (USDA, NASS, 2003, 2010). Each MODFLOW cell that has a crop covered in the top layer is corresponding to one DayCent model, resulting in 806 models (Figure 4.5A).

The coupled model was simulated for the 2000-2012 period, using monthly stress periods for MODFLOW and daily time steps for both models. The model was run on an Amazon AWS Linux server with 96 CPUs and 384 GB ram, with the maximum number of open files changing

from 1024 to 1 million. The model took 9 hours to run. Model results are compared to 100 observed groundwater head values from five monitoring wells (see Figure 4.4C) and reference ET from the various crop types. Simulated results of emitted N_20 and CH_4 are shown to demonstrate possible uses of the model.

4.4. RESULTS AND DISCUSSION

4.4.1 MODFLOW head results (head comparison, depth to water table map)

Simulated groundwater levels are compared to observed levels in Figures 4.6 and 4.7. Figure 4.6A shows the 1:1 plot of measured groundwater head vs. simulated groundwater head for the simulation period. The Mean Absolute Error (MAE) is 0.98 m and the Root Mean Square Error (RMSE) is 0.78 m. The histogram of residuals (difference between measured and simulated) is shown in Figure 4.6B, showing that most of the residuals are < 1 m, with an average residual (mean of errors) of 0.48 m. Knowing that the average aquifer thickness in this region is 5-36 m, the residuals between simulated and measured head values indicate that the MODFLOW model simulates the groundwater system in a reasonable manner. Figure 4.7 shows an interpolated spatial map of observed groundwater depth (ground surface to the water table) (Figure 4.7A) for spring 2012 compared to an interpolated map of simulated groundwater depth values from the MODFLOW cells (Figure 4.7B). The areas marked in red indicate waterlogging (water table < 2 m from the ground surface, and hence in the root zone of the crops). In general, the simulated results capture the principal patterns in the system, with most waterlogging happening in the areas centered in the irrigation area. The shallow groundwater levels in the northwest portion of the study region is due to thinness of the aquifer near the South Platte River.

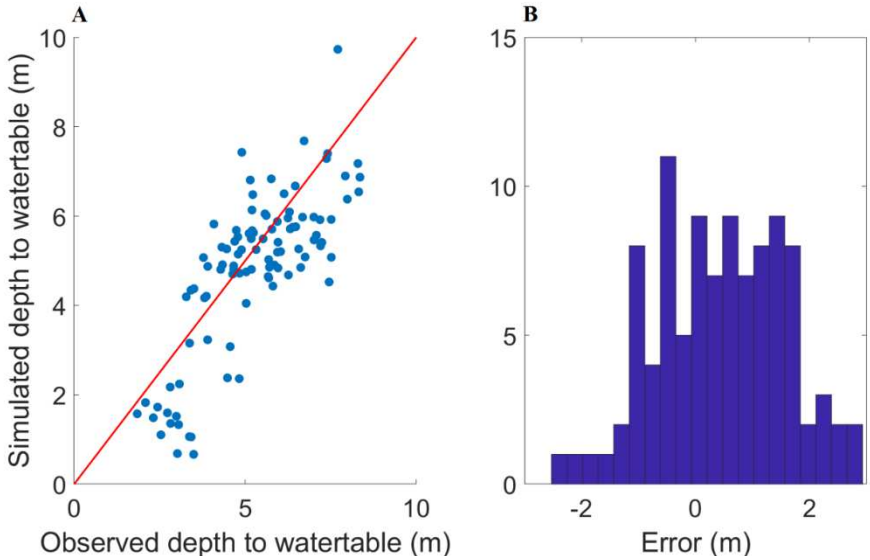

Figure 4.6: (A) 1:1 plot of measured groundwater head vs. simulated groundwater head; (B) histogram of the head errors.

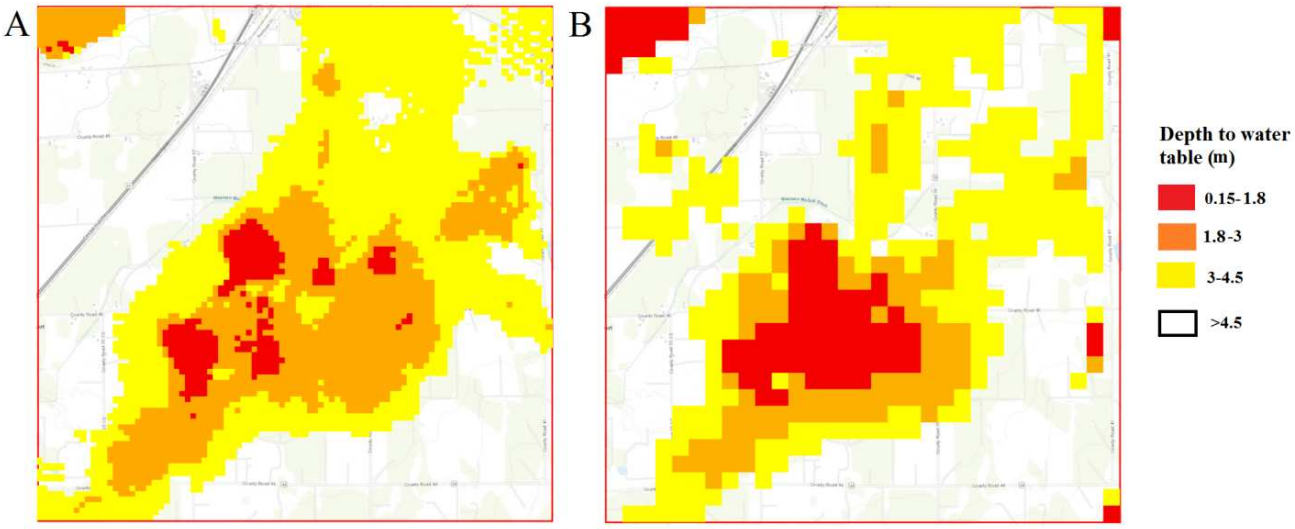

Figure 4.7: Comparison between interpolated maps of groundwater depth (m) for (A) observed values and (B) simulated values.

Figure 4.8A shows the cross-section of ground surface, water table elevation, and bedrock elevation through a west-east transect of the study area for spring 2012, showing a high water table in the west-central portion of the region (see Figure 4.7). Figure 4.8B shows the percent of area waterlogged, defining waterlogging as groundwater within the root zone (< 2 m from the ground surface). Average percent area between 2000 and 2012 is 8%, with more area

waterlogged during the initial and latter years of the period. The increase in waterlogging during the 2008-2012 period is likely due to an overall decrease in groundwater pumping and increase in surface water irrigation in the region due to water right considerations (Deng and Bailey, 2020).

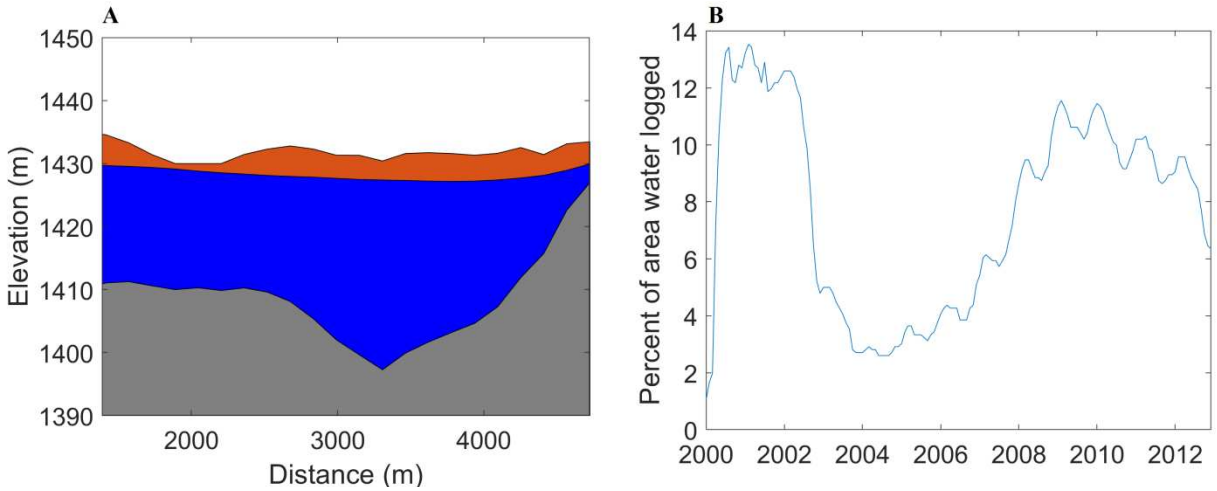

Figure 4.8: Figure A, the time series of average percent of waterlogging area. Figure B, the west to east cross section of middle of the Study Area. Grey is the bedrock, blue is the groundwater, and orange is the soil.

4.4.2 ET results from DayCent (ET for each crop comparison, ET map to crop type)

The daily average crop ET over the entire study area is plotted in Figure 4.9A, showing high values during the irrigation season and regular fluctuations from year to year. The average daily ET is 1.2 mm and high values of ET are approximately 4 mm/day. The average daily ET during the irrigation season (May-September) is about 2.2 mm. A plot of ET simulated for each DayCent model for a single day in June 2010 is shown in Figure 4.9B. The average ET is 4 mm and the highest ET is 5.5 mm.

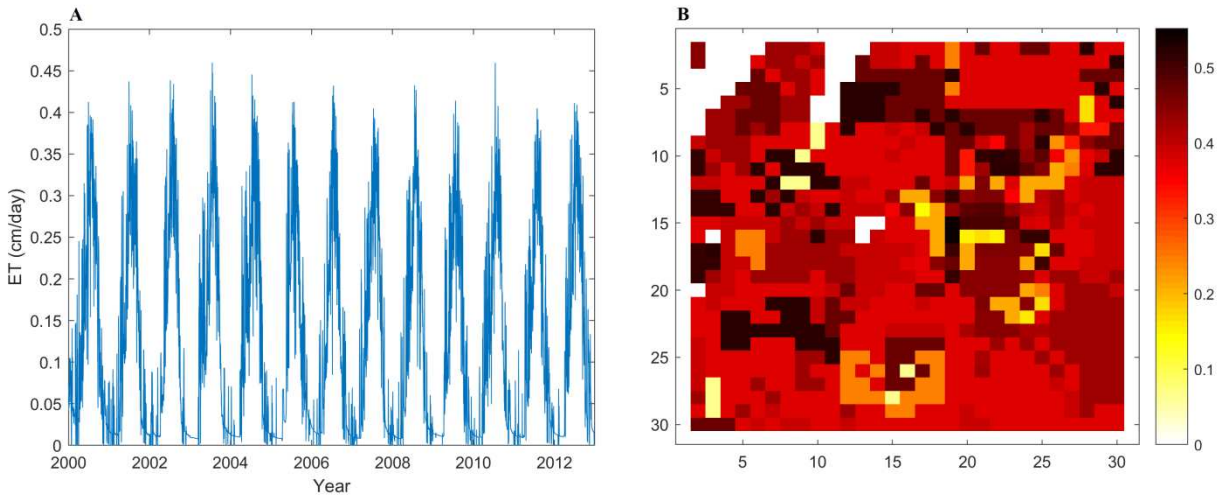

Figure 4.9. (A) shows the time series of average crop ET over the study area; (B) shows the distribution of simulated ET for a single day in June 2010.

The spatial distribution of ET is compared to crop type in Figure 4.10. Figure 4.10A shows the crop type for each field, and Figure 4.10B shows the simulated ET for a selected day in June 2010, with results color-coded to match the crop type in Figure 4.10A that generates the specific range of ET values. Results show the high correlation between the crop type and the resulting ET. For example, the areas with corn (red) correspond to a specific range of ET depths that are generated from fields with corn. The result demonstrates the correct spatial mapping between the MODFLOW grid and the DayCent models. Some areas do not match due to the same crop type having different ET depths in different locations because of different soil water conditions. Also, each MODFLOW cell simulates only a single crop, and often there are multiple crop types for a single cell.

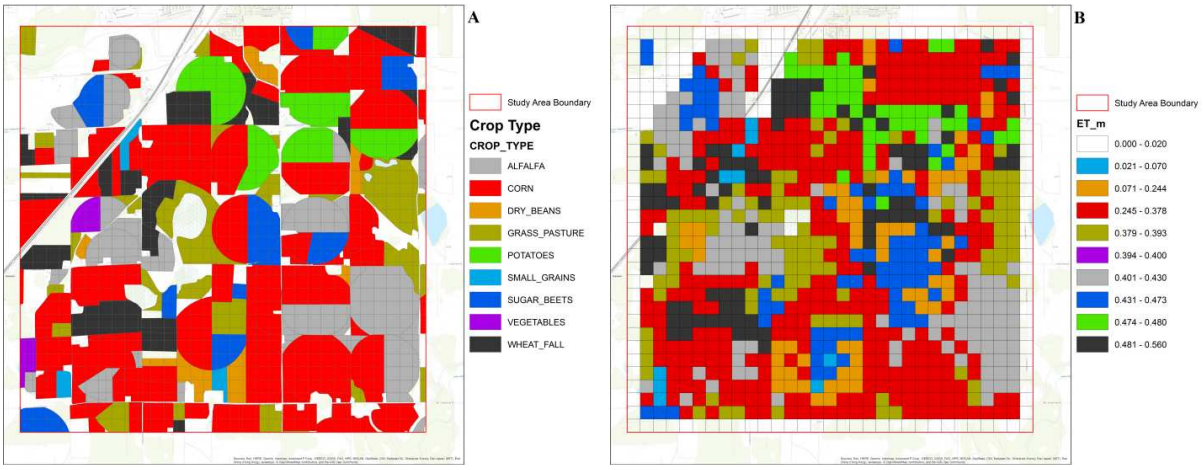

Figure 4.10: (A) crop type for each field in the study area; (B) simulated ET (cm) for a single day in June 2010.

The estimated reference ET for each crop type is used to test simulation results, as there are no field-based ET measurements in the study area. References ET values were collected from the CoAgMet (Colorado Agricultural Meteorological Network) data at LaSalle, Colorado, just north of the study area and calculated using the ASCE standardized method. Figure 4.11 shows a time series of daily ET (cm) for both reference ET and the model for 7 crop types during 2012. The majority of ET occurs during the irrigation season between days 100 and 300 (April - September). The reference and simulated ET rates for alfalfa, corn, grass hay, and small grain match well with a mean error of approximately 0.02 cm. ET for small grain is slightly underestimated with a mean error of -0.04 cm. ET for sugar beets and potatoes are slightly estimated, although generally simulated ET rates match reference ET rates quite well for each crop type.

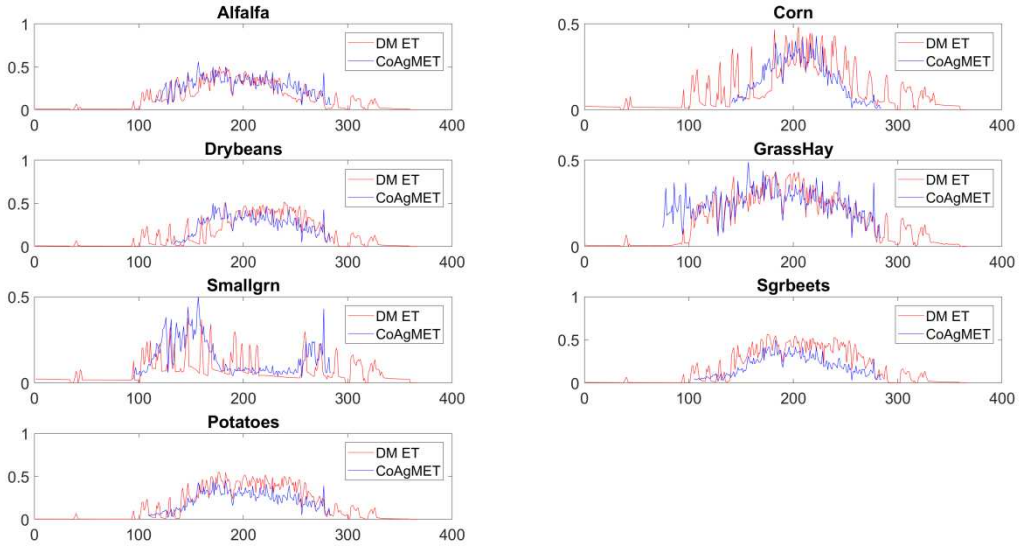

Figure 4.11: Time series of daily ET (cm) for reference ET and model-simulated ET during 2012 for 7 crop types (alfalfa, corn, dry beans, grass hay, small grain, sugar beets, and potatoes).

4.4.3 General DayCent-MODFLOW model outputs

The rates of water exchange between MODFLOW and DayCent are plotted in Figure 4.12 for each day during the 2000-2012 simulation period. Figure 4.12A shows the daily average water depth passed to DayCent from MODFLOW. Positive values indicate that the water table is present in the root zone after the MODFLOW daily simulation, and water is passed from MODFLOW to the DayCent models. Conversely, negative values indicate that water level dropped in the root zone after MOFLOW simulation and DayCent receive it as water loss. Results from Figure 4.12A demonstrate that many interactions are occurring in the root zone between DayCent and MODFLOW, particularly during the times of increased waterlogging during 2000-2003 and 2007-2012 (see Figure 4.8B). This can be also found in the chart of Figure 4.12B, showing the amount of water passed from DayCent to MODFLOW during the simulation period. There are no negative values because the time series is a monthly averaged depth.

Positive values indicate deep percolation or water storage increases in the root zone due to precipitation or irrigation, whereas negative values occur when there is more ET than infiltration.

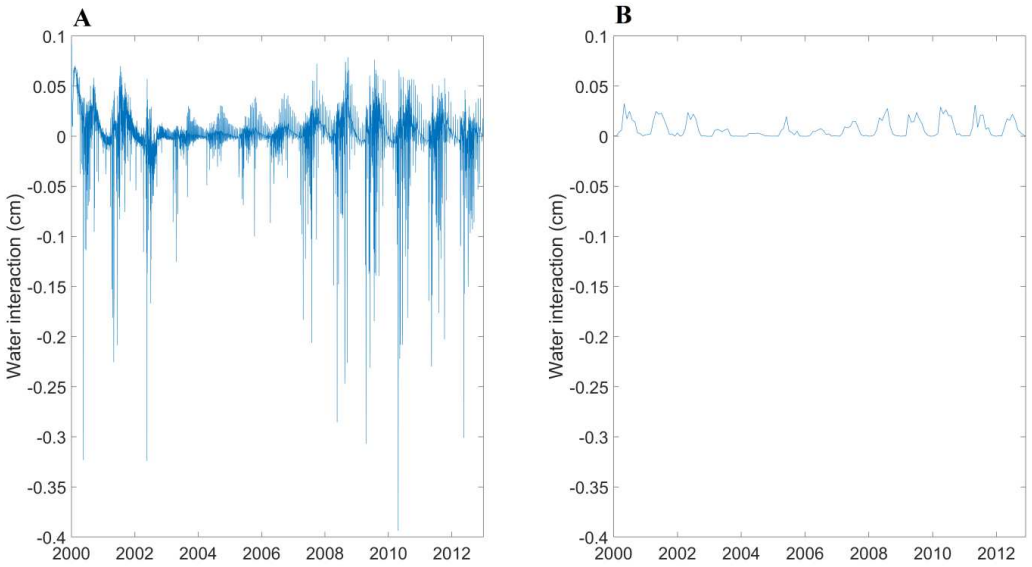

Figure 4.12: (A) daily water depth (cm) passed to DayCent from MODFLOW; (B) daily water depth (cm) passed to MODFLOW from DayCent.

4.4.4 Greenhouse Gas results (CH4 and N2O)

Greenhouse gas emissions varied with soil saturated conditions. The average gas emissions (kg/ha) for N_2O and CH_4 are shown in Figure 4.13. A study near Fort Collins, CO, approximately 60 km from the study area, estimated N_2O emissions between 0 and 246 kg N/ha for corn, with the maximum annual rates varying between 202 and 246 kg N/ha between 2002 and 2006 (Halvorson et al., 2009). In our study, due to waterlogging conditions, the simulated N_2O emission is much lower than the normal conditions, with an annual average of 1.2 kg N/ha, with lower values occurring during the increased waterlogging activity of 2000-2002 and 2007-2012. However, even during times of non-waterlogging, the emission rates are much lower than what is observed in Halvorson et al. (2009). Therefore, we note that the model has not been calibrated to field-estimated emission rates. These results are provided as a proof-of-concept, to demonstrate that emission rates are decreased under waterlogged conditions. Regarding CH_4

emission, well drained agriculture soil without waterlogging is usually a sink of CH_4 (Powlson et al., 1997). Under waterlogging conditions, soil becomes a source and the amount of CH_4 emission depends on various factors such as crop type, water saturated periods, and soil temperature (Bartlett & Harriss, 1993). Average annual CH_4 emission simulated in the study area (Figure 4.13B) is 19350 kg C/ha.

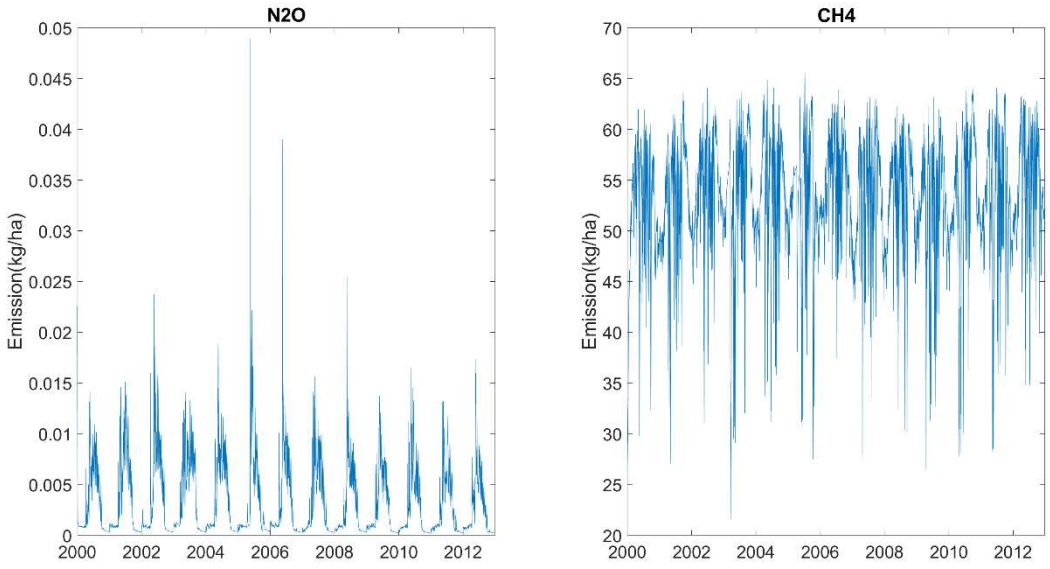

Figure 4.13: Estimation of Greenhouse Gas emissions in the Study Area under waterlogging conditions.

4.5. SUMMARY AND CONCLUSIONS

In this study, a new hydro-agronomic model is introduced by integrating the MODFLOW 3D groundwater flow model and the DayCent 1D agronomic hydrologic model to simulate water table elevation, crop ET, and greenhouse gas emissions in the root zone of waterlogged areas. The model can be applied to any agricultural areas, but coding has been aimed at ensuring correct representation of these processes in areas of shallow groundwater. The coupling between a single MODFLOW model and a suite of field-scale DayCent models is achieved by applying MPI (Message Passing Interface) parallel programming. DayCent passes recharge to

MODFLOW, whereas MODFLOW passes soil water to DayCent in the case of groundwater head rising to within the root zone of simulated crops.

There are several advantages of using DayCent-MODFLOW over other linked agronomic-groundwater models:

1. groundwater recharge is calculated by DayCent, an agroecosystem model aimed at field-scale processes;
2. groundwater recharge is calculated within the root zone under waterlogged conditions, considering daily interactions between the two models;
3. DayCent crop growth and ET algorithms are constrained by the presence of shallow groundwater, under waterlogging conditions;
4. the models are simulated separately but simultaneously using the MPI infrastructure, minimizing code invasiveness for either model;
5. the parallel process greatly decreases overall run time.

The coupled DayCent-MODFLOW model is applied to a waterlogged irrigated area near LaSalle, Colorado, within the semi-arid South Platte River Basin. Model results are compared against observed groundwater levels and reference ET for 7 crop types, demonstrating accuracy in simulating these system-response variables. Stimulated emission rates (kg/ha) for N_20 and CH_4 are loosely compared to annual emission rates from the region. The model can be used to assess crop growth, recharge, and gas emissions under deep and shallow water table conditions in agricultural areas.

Acknowledgements

This study was performed through grants from the Colorado Water Conservation Board, State of Colorado Department of Natural Resources, grant No. 201900000014.

REFERENCES

Allen, R. G., Pereira, L. S., Raes, D., & Smith, M. (Eds.). (1998). *Crop evapotranspiration: Guidelines for computing crop water requirements*. Food and Agriculture Organization of the United Nations.

Alley, W. M., Healy, R. W., LaBaugh, J. W., & Reilly, T. E. (2002). *Flow and Storage in Groundwater Systems*. *296*, 7.

Arnold, J. G., Srinivasan, R., Muttiah, R. S., & Williams, J. R. (1998). Large area hydrologic modeling and assessment part I: Model development 1. *JAWRA Journal of the American Water Resources Association*, *34*(1), 73–89.

Bailey, R. T., Wible, T. C., Arabi, M., Records, R. M., & Ditty, J. (2016). Assessing regional-scale spatio-temporal patterns of groundwater–surface water interactions using a coupled SWAT-MODFLOW model. *Hydrological Processes*, *30*(23), 4420–4433.

Bartlett, K. B., & Harriss, R. C. (1993). Review and assessment of methane emissions from wetlands. *Chemosphere*, *26*(1–4), 261–320.

Bedekar, V., Niswonger, R. G., Kipp, K., Panday, S., & Tonkin, M. (2012). Approaches to the Simulation of Unconfined Flow and Perched Groundwater Flow in MODFLOW. *Ground Water*, *50*(2), 187–198. https://doi.org/10.1111/j.1745-6584.2011.00829.x

Cannell, R. Q., Belford, R. K., Gales, K., Dennis, C. W., & Prew, R. D. (1980). Effects of waterlogging at different stages of development on the growth and yield of winter wheat. *Journal of the Science of Food and Agriculture*, *31*(2), 117–132. https://doi.org/10.1002/jsfa.2740310203

Cavazza, L., & Pisa, P. R. (1988). Effect of watertable depth and waterlogging on crop yield. *Agricultural Water Management*, *14*(1–4), 29–34. https://doi.org/10.1016/0378-3774(88)90057-1

Cheng, K., Ogle, S. M., Parton, W. J., & Pan, G. (2014). Simulating greenhouse gas mitigation potentials for Chinese Croplands using the DAYCENT ecosystem model. *Global Change Biology*, *20*(3), 948–962.

Collaku, A., & Harrison, S. A. (n.d.). Losses in wheat due to waterlogging. *Crop Science*, *42*(2), 444–450.

Del Grosso, S. J., Halvorson, A. D., & Parton, W. J. (2008). Testing DAYCENT model simulations of corn yields and nitrous oxide emissions in irrigated tillage systems in Colorado. *Journal of Environmental Quality*, *37*(4), 1383–1389.

Del Grosso, Stephen J., Parton, W. J., Mosier, A. R., Walsh, M. K., Ojima, D. S., & Thornton, P. E. (2006). DAYCENT national-scale simulations of nitrous oxide emissions from cropped soils in the United States. *Journal of Environmental Quality*, *35*(4), 1451–1460.

Gautam, S., Mishra, U., Scown, C. D., & Zhang, Y. (2020). Sorghum biomass production in the continental United States and its potential impacts on soil organic carbon and nitrous oxide emissions. *GCB Bioenergy*, *12*(10), 878–890.

Gropp, W., Gropp, W. D., Lusk, E., Skjellum, A., & Lusk, A. D. F. E. E. (1999). *Using MPI: Portable Parallel Programming with the Message-passing Interface*. MIT Press.

Gropp, W., Lusk, E., Doss, N., & Skjellum, A. (1996). A high-performance, portable implementation of the MPI message passing interface standard. *Parallel Computing*, *22*(6), 789–828.

Harbaugh, A. W., Banta, E. R., Hill, M. C., & McDonald, M. G. (2000). Modflow-2000, the u. S. Geological survey modular ground-water model-user guide to modularization concepts and the ground-water flow process. *Open-File Report. U. S. Geological Survey*, *92*, 134.

Harbaugh, A. W., & McDonald, M. G. (1996). *Programmer's documentation for MODFLOW-96, an update to the US Geological Survey modular finite-difference ground-water flow model*. US Geological Survey; Branch of Information Services [distributor],.

Hargreaves, G. H., & Allen, R. G. (2003). History and Evaluation of Hargreaves Evapotranspiration Equation. *Journal of Irrigation and Drainage Engineering*, *129*(1), 53–63. https://doi.org/10.1061/(ASCE)0733-9437(2003)129:1(53)

Healy, R. W. (2008). Simulating water, solute, and heat transport in the subsurface with the VS2DI software package. *Vadose Zone Journal*, *7*(2), 632–639.

Houk, E., Frasier, M., & Schuck, E. (2006). The agricultural impacts of irrigation induced waterlogging and soil salinity in the Arkansas Basin. *Agricultural Water Management*, 9.

Jones, J. W., Hoogenboom, G., Porter, C. H., Boote, K. J., Batchelor, W. D., Hunt, L. A., Wilkens, P. W., Singh, U., Gijsman, A. J., & Ritchie, J. T. (2003). The DSSAT cropping system model. *European Journal of Agronomy*, *18*(3–4), 235–265.

Kaur, G., Zurweller, B. A., Nelson, K. A., Motavalli, P. P., & Dudenhoeffer, C. J. (2017). Soil Waterlogging and Nitrogen Fertilizer Management Effects on Corn and Soybean Yields. *Agronomy Journal*, *109*(1), 97–106. https://doi.org/10.2134/agronj2016.07.0411

Kroes, J. G., Dam, J. C. van, Groenendijk, P., Hendriks, R. F. A., & Jacobs, C. M. J. (2009). *SWAP Version 3.2. Theory description and user manual* (1649(02); p.). Alterra. https://library.wur.nl/WebQuery/wurpubs/400886

Langevin, C. D., Hughes, J. D., Banta, E. R., Niswonger, R. G., Panday, S., & Provost, A. M. (2017). *Documentation for the MODFLOW 6 groundwater flow model*. US Geological Survey.

Lee, J., Pedroso, G., Linquist, B. A., Putnam, D., Kessel, C. van, & Six, J. (2012). Simulating switchgrass biomass production across ecoregions using the DAYCENT model. *GCB Bioenergy*, *4*(5), 521–533. https://doi.org/10.1111/j.1757-1707.2011.01140.x

McDonald, M. G., & Harbaugh, A. W. (1988). *A modular three-dimensional finite-difference ground-water flow model*. US Geological Survey.

Meurant, G., & Riker, A. J. (2014). *Flooding and Plant Growth*. Elsevier Science.

Monsi, M., & Saeki, T. (1953). The light factor in plant communities and its significance for dry matter production. *Japanese Journal of Botany*, *14*(1), 22–52.

Niswonger, R. G., Panday, S., & Ibaraki, M. (2011). MODFLOW-NWT, a Newton formulation for MODFLOW-2005. *US Geological Survey Techniques and Methods*, *6*(A37), 44.

Oracle. (2016). *Concurrency vs Parallelism, Concurrent Programming vs Parallel Programming*. https://web.archive.org/web/20160407121734/https://blogs.oracle.com/yuanlin/entry/concurrency_vs_parallelism_concurrent_programming

Panday, S., & Huyakorn, P. S. (2008). MODFLOW SURFACT: A State-of-the-Art Use of Vadose Zone Flow and Transport Equations and Numerical Techniques for Environmental Evaluations. *Vadose Zone Journal*, *7*(2), 610–631. https://doi.org/10.2136/vzj2007.0052

Parton, W. J., Holland, E. A., Del Grosso, S. J., Hartman, M. D., Martin, R. E., Mosier, A. R., Ojima, D. S., & Schimel, D. S. (2001). Generalized model for NO x and N2O emissions from soils. *Journal of Geophysical Research: Atmospheres*, *106*(D15), 17403–17419.

Parton, William J., Hartman, M., Ojima, D., & Schimel, D. (1998). DAYCENT and its land surface submodel: Description and testing. *Global and Planetary Change*, *19*(1–4), 35–48.

Ploschuk, R. A., Danlel Jullo, M., & Timothy David, C. (2018). Waterlogging of Winter Crops at Early and Late Stages: Impacts on Leaf Physiology, Growth and Yield. *Frontiers in Plant Science*, *9*, 15.

Powlson, D. S., Goulding, K. W. T., Willison, T. W., Webster, C. P., & Hütsch, B. W. (1997). The effect of agriculture on methane oxidation in soil. *Nutrient Cycling in Agroecosystems*, *49*(1), 59–70. https://doi.org/10.1023/A:1009704226554

Pruess, K., Oldenburg, C. M., & Moridis, G. J. (1999). *TOUGH2 user's guide version 2*. Lawrence Berkeley National Lab.(LBNL), Berkeley, CA (United States).

Quinn, M. J. (2003). *Parallel programming*. TMH CSE, 526.

Reilly, E. D. (2004). *Concise Encyclopedia of Computer Science*. John Wiley & Sons.

Richards, L. A. (1931). Capillary conduction of liquids through porous mediums. *Physics*, *1*(5), 318–333. https://doi.org/10.1063/1.1745010

Robertson, A. D., Zhang, Y., Sherrod, L. A., Rosenzweig, S. T., Ma, L., Ahuja, L., & Schipanski, M. E. (2018). Climate change impacts on yields and soil carbon in row crop dryland agriculture. *Journal of Environmental Quality*, *47*(4), 684–694.

SELLERS, P. J. (1985). Canopy reflectance, photosynthesis and transpiration. *International Journal of Remote Sensing*, *6*(8), 1335–1372. https://doi.org/10.1080/01431168508948283

Šimůnek, J., Van Genuchten, M. T., & Šejna, M. (2012). The HYDRUS software package for simulating the two-and three-dimensional movement of water, heat, and multiple solutes in variably-saturated porous media. *Technical Manual*.

Stehfest, E., Heistermann, M., Priess, J. A., Ojima, D. S., & Alcamo, J. (2007). Simulation of global crop production with the ecosystem model DayCent. *Ecological Modelling*, *209*(2), 203–219. https://doi.org/10.1016/j.ecolmodel.2007.06.028

Therrien, R., McLaren, R. G., Sudicky, E. A., & Panday, S. M. (2010). HydroGeoSphere: A three-dimensional numerical model describing fully-integrated subsurface and surface flow and solute transport. *Groundwater Simulations Group, University of Waterloo, Waterloo, ON*.

Thoms, R. B., Johnson, R. L., & Healy, R. W. (2006). *User's guide to the variably saturated flow (VSF) process to MODFLOW*.

United Nations, U. N. F. C. on C. C. (1992). *United Nations framework convention on climate change*. UNFCCC.

USDA, NASS. (2003). Agricultural Chemical Usage: 2002 Field Crops Summary. *National Agricultural Statistics Service*.

USDA, NASS. (2010). Field Crops: Usual Planting and Harvesting Dates. *National Agricultural Statistics Service*.

USEPA. (2016). *Inventory of US greenhouse gas emissions and sinks: 1990-2014.(No. EPA 430-R-16-002)*. US Environmental Protection Agency Washington, DC.

White, M. D., & Oostrom, M. (2003). *STOMP subsurface transport over multiple phases version 3.0 User's guide*. Pacific Northwest National Lab., Richland, WA (US).

Xiang, Z., Bailey, R. T., Nozari, S., Husain, Z., Kisekka, I., Sharda, V., & Gowda, P. (2020). DSSAT-MODFLOW: A new modeling framework for exploring groundwater conservation strategies in irrigated areas. *Agricultural Water Management*, *232*, 106033.

Zhang, Y., Arabi, M., & Paustian, K. (2020). Analysis of parameter uncertainty in model simulations of irrigated and rainfed agroecosystems. *Environmental Modelling & Software*, *126*, 104642. https://doi.org/10.1016/j.envsoft.2020.104642

Zhang, Y., Gurung, R., Marx, E., Williams, S., Ogle, S. M., & Paustian, K. (2020). DayCent Model Predictions of NPP and Grain Yields for Agricultural Lands in the Contiguous U.S. *Journal of Geophysical Research: Biogeosciences*, *125*(7), e2020JG005750. https://doi.org/10.1029/2020JG005750

Zhang, Y., Hansen, N., Trout, T., Nielsen, D., & Paustian, K. (2018). Modeling Deficit Irrigation of Maize with the DayCent Model. *Agronomy Journal*, *110*(5), 1754–1764. https://doi.org/10.2134/agronj2017.10.0585

Zhang, Y., Marx, E., Williams, S., Gurung, R., Ogle, S., Horton, R., Bader, D., & Paustian, K. (2020). Adaptation in U.S. Corn Belt increases resistance to soil carbon loss with climate change. *Scientific Reports*, *10*(1), 13799. https://doi.org/10.1038/s41598-020-70819-z

Zhang, Y., Qian, Y., Bremer, D. J., & Kaye, J. P. (2013). Simulation of nitrous oxide emissions and estimation of global warming potential in turfgrass systems using the DAYCENT model. *Journal of Environmental Quality*, *42*(4), 1100–1108.

Zhang, Y., Suyker, A., & Paustian, K. (2018). Improved crop canopy and water balance dynamics for agroecosystem modeling using DayCent. *Agronomy Journal*, *110*(2), 511–524.

CHAPTER 5. SUMMARY AND FUTURE WORK

The research presented in this dissertation summarizes efforts to quantify effects of management-driven groundwater sources and sinks (irrigation recharge, canal seepage, groundwater pumping, recharge pond seepage) on groundwater levels and groundwater-surface interactions in a regional-scale, irrigated stream-aquifer system. These efforts contained first, presenting a new method to assess the impact of groundwater stresses on water table elevation in waterlogged agricultural areas; building a numerical groundwater flow model is constructed and used to simulate groundwater head and groundwater flow, with results compared against measured groundwater levels; applying global sensitivity analysis (GSA) methods to rank and quantify temporally and spatially the influence of each groundwater stress on water table elevation; identifying management practices from the GSA results and run with the groundwater flow model to quantify spatio-temporal effects on water table elevation; second, assessing the impact of recharge ponds in the Study Area using a new loose coupled model with MODFLOW groundwater flow model and the DayCent agronomic hydrologic model; simulating different management scenarios to evaluate the impact of recharge ponds on groundwater level and return flow to the river; third, introducing a new hydro-agronomic model by integrating the MODFLOW 3D groundwater flow model and the DayCent 1D agronomic hydrologic model to simulate water table elevation, crop ET, and greenhouse gas emissions in the root zone of waterlogged areas; applying MPI (Message Passing Interface) parallel programing to link a single MODFLOW model and a suite of field-scale DayCent models; applying the mode on a sub-area of the Study Area. The methods and results of this dissertation can be applied to other waterlogged agricultural regions worldwide.

The major conclusions for the development of MODFLOW, GSA, a loosely coupled DayCent-MODFLOW model, and a tightly coupled DayCent-MODFLOW are contained in Chapter 2-4. Possible areas of future work are:

- The use of DayCent-MODFLOW to forecast streamflow depletions caused by expected groundwater pumping and related streamflow accretions caused by recharge ponds. In this manner, the model could be used as part of a decision support system to assist water district managers in determining necessary volumes and timing of recharge pond applications.
- The use of DayCent-MODFLOW to explore plant-soil-water dynamics and associated greenhouse gas emissions at the regional scale. This should be accompanied by thorough field measurements of gas emissions, to provide verification data for the model. The model could then be used to explore the impact of land use and climate change on greenhouse gas emissions in irrigated agricultural areas.
- Coupling DayCent-MODFLOW with a groundwater reactive transport model (e.g. RT3D, MT3D) to assess transport of carbon and nitrogen species in the soil-aquifer system.